Inaugural-Dissertation

zur
Erlangung der Doktorwürde
der
Naturwissenschaftlich-Mathematischen Gesamtfakultät
der
Ruprecht-Karls-Universität
Heidelberg

vorgelegt von
Diplom-Biologin Caroline Gähler
aus München

Tag der mündlichen Prüfung:……

Association of Hepatitis B Virus derived lipopeptides to serum factors and model membranes

Caroline Gähler

2011

Referees: Prof. Dr. Stephan Urban
Prof. Dr. Valerie Bosch

Table of contents

Table of contents ..... **III**

Abbreviations ..... **VI**

Zusammenfassung ..... **IX**

Summary ..... **X**

1. Introduction **1**

1.1 Viral Hepatitis B *1*
1.1.1 Transmission routes of HBV 2
1.1.2 Epidemiology and pathogenesis 3
1.1.3 Prophylaxis and therapy 3

1.2 Hepadnaviridae *4*
1.2.1 HBV genotypes 6
1.2.2 Viral particles 6
1.2.3 The viral genome 7
1.2.4 The viral surface proteins 9
1.2.5 Topology of the surface proteins 10
1.2.6 HBV entry 11
1.2.6.1 Animal models and cell culture systems 11
1.2.6.2 Early steps of HBV infection 11
1.2.7 The viral replication cycle 12

1.3. HBV preS1-derived lipopeptides as entry inhibitors *15*

1.4. Membrane fusion *16*
1.4.1. Viral membrane fusion 17
1.4.2 viral fusion peptides 19
1.4.3 Membrane fusion by hepatitis B viruses 20

1.5. Hepatitis Delta Virus *21*
1.5.1. History and pathogenesis 21
1.5.2. Morphology and viral proteins 21
1.5.3 HDV entry 23
1.5.4 The HDV genome and its replication 23

1.6. Transport of fatty acid esters and fatty acids in the blood *25*
1.6.1. Lipoproteins 25
1.6.2 Serum albumin as transporter molecule and its role in hepatic uptake of fatty acids 26
1.6.3 Drug transport by HSA 27

2. Material and Methods **29**

2.1 Material *29*
2.1.1 cell culture 29
2.1.2 Equipment and consumables 29
2.1.3 Chemicals 32
2.1.4 Protein Markers for SDS-PAGE 35
2.1.5 Antibodies 35
2.1.5.1 primary antibodies 35
2.1.5.2 Secondary antibodies 35

2.2 Methods *37*
2.2.1 Cell culture 37

2.2.1.1 HepAD38 cells 37
2.2.1.2 HepaRG 37
2.2.1.3 Isolation and cultivation of primary hepatocytes 37
2.2.1.4 Primary Human Hepatocytes (PHH) 38
2.2.1.5 PEG-precipitation of virus from HepAd38 supernatant 39
2.2.1.6 HBV infection of HepaRG and primary hepatocytes 39
2.2.1.7 HDV /WHDV infection of HepaRG and primary hepatocytes 39
2.2.1.8 Binding assay with radiolabeled preS-peptide on PMH 39
2.2.2 Analysis of infections 40
2.2.2.1 Immunofluorescence of HBV/ HDV infected cells 40
2.2.3 Biochemical methods 40
2.2.3.1 Peptide synthesis 40
2.2.3.2 Serum preparation 41
2.2.3.3 Purification of high density Lipoproteins from human serum 41
2.2.3.4 Size exclusion chromatography (SEC) of peptide-albumin /-serum complexes 42
2.2.3.5 Fishing of binding partners for HBVpreS/2-48^{myristoyl} in Serum 42
2.2.3.6 Fishing of binding partners for HBVpreS/2-48^{myristoyl} on primary hepatocytes 42
2.2.3.7 Mass spectrometry 43
2.2.4 Assay for membrane activity analysis 43
2.2.4.1 Liposome production 43
2.2.4.2 membrane activity assay of HBV preS derived lipopeptides on liposomes 44
2.2.4.3 flotation assay with HBV preS-derived lipopeptides on liposomes 44
2.2.4.4 Electron microscopy of liposomes and peptides 45
2.2.5 Analysis methods 45
2.2.5.1 SDS-PAGE 45
2.2.5.2 Transfer of proteins separated by SDS-PAGE onto a nitrocellulose membrane (Western blot) and immunodetection 46
2.2.5.3 Silver staining of SDS-PAGE gels 47

3. Results 48

3.1 Binding of HBV preS1 derived lipopeptides to serum factors 49
3.1.1. Identification of preS-binding partners 50
3.1.1.1 HBV preS/2-48^{myristoyl} showed a size shift in SEC when preincubated with serum 50
3.1.1.2 Functional peptides carrying a crosslinker moiety for identification of binding partners 51
3.1.1.3 Human Serum Albumin and Apolipoprotein A1 bind to preS-peptides 53
3.1.2 The peptide - HSA interaction 54
3.1.2.1 HBV preS peptides bound HSA in the SEC-assay 54
3.1.2.2 The peptide-HSA binding depends on the length of the N-terminal acylation 55
3.1.2.3 The peptide-HSA binding *in vivo* 57
3.1.2.4 The dissociation constant (K_D) for the peptide-HSA binding was found to be in the micromolar range 58
Fig. 3.9: Binding curves for the peptide-HSA interaction. A: Increasing amounts of either C12-, C14- or C18- 60
3.1.3 PreS-peptides bound to Serum components from other species 61
3.1.4 Binding of HBV preS-peptides to high density lipoproteins 62
3.1.4.1 HDLs were purified from human serum 62
3.1.4.2 HDL bound HBV preS derived lipopeptides depending on their N-terminal moiety 64
3.1.5 Neither HDL nor HSA influenced peptide binding to primary hepatocytes 66
3.1.6 Liver tropism was not impaired in a ApoA1-deficient mouse 67
3.1.7 Addition of HSA or HDL did not influence HBV infection 67

3.2 Attempts to identify a cellular interaction partner for HBV preS-peptides 68

3.3 Membrane activity of HBV preS-derived peptides 72
3.3.1 The liposome-based membrane activity assay 72
3.3.1.1 The wildtype PreS-peptide showed a concentration-dependent membrane activity 73
3.3.1.2 Membrane activity of preS depended on the integrity of the essential site 74
3.3.1.3 Deletions of the N-terminal amino acids were tolerated up to amino acid 7 75

3.3.1.4 The N-terminal acylation required a minimal length for membrane activity 75
3.3.2 After coincubation, preS-peptides showed coflotation with liposomes 77
3.3.3 HBV preS-peptides caused structural alterations in liposomes 78

3.4 Analysis of HBV and HDV infection on Hepatocytes from different rodent species 79
3.4.1 HBV infection 80
3.4.1.1 HBV preferentially infected differentiated HepaRG cells 80
3.4.1.2 Primary hepatocytes from rat and rabbit were not susceptible to HBV infection 80
3.4.1.3 Primary hepatocytes from hamster and guinea pig showed susceptibility to HBV 82
3.4.2 HDV infection 83
3.4.2.1 Infection of HepaRG with HDV led to typical nuclear staining 83
3.4.2.2 Primary rat hepatocytes are not susceptible to HDV but to WHDV 84
3.4.2.3 Primary rabbit hepatocytes could be infected with HDV at a low rate 85
3.4.2.4 Primary hamster hepatocytes and primary guinea pig hepatocytes were not susceptible to HDV but could be infected with WHDV 86

4. Discussion 88

4.1. Binding partners for HBV preS-peptides in serum 88
4.1.1 PreS-peptides bind serum factors in an acylation-dependent manner 88
4.1.2 Identification of albumin and apolipoprotein A1 as binding partners for preS-peptides 88
4.1.3 The affinity for HSA increases with the fatty acid chain length 90
4.1.4 PreS-peptide binding to albumin takes place *in vivo* 91
4.1.5 Does the albumin binding influence liver tropism or binding to hepatocytes? 91
4.1.6 Apolipoprotein A1 was identified as binding partner for HBV preS-derived peptides 94
4.1.7 Apolipoproteins, HCV and HBV 95
4.1.8 Does the peptide-HDL interaction play a role in liver tropism or peptide binding to hepatocytes? ... 96

4.2 Attempts to identify cellular interaction partners for HBV preS-peptides 97

4.3 Membrane activity of HBV preS-derived peptides 97

4.4 Primary hepatocytes from other species are susceptible to HBV and HDV 99

5. References 103

6. Acknowledgements 116

Abbreviations

abbreviation	full word(s)
%	percent
(k)Da	(kilo) dalton
×g	times
°C	degree celsius
µg	microgram
µM	micromolar
µm	micrometer
Å	Ångström
aa	amino acids
ADAR-1	adenosine deaminase acting on RNA 1
AU	arbitrary units
bp	base pairs
BSA	bovine serum albumin
C/N-term.	carboxy- / amino-terminally
cccDNA	covalently closed circular DNA
cDNA	copy DNA
cm^2	square centimetres
CO_2	carbon dioxide
cpm	counts per minute
D-aa	D- aminoacids
DHBV	duck hepatitis B virus
DM	dodecyl maltoside
DNA	Desoxyribonucleic acid
DPX	*p*-xylene-bis-puridinium bromide
ELISA	enzyme linked immunoabsorbance assay
EM	electron microscopy
ER	endoplasmatic reticulum
FA	fatty acid
FCS	fetal calf serum
FITC	fluorescein isothiocyanate
g	gram
×g	fold of gravitational acceleration
G	Gauge
GE	genome equivalents
h	hour(s)
H_2O_{dd}	water, double destilled
HBcAg	Hepatitis B core antigen
HBeAg	Hepatitis B early antigen
HBsAg	Hepatitis B surface antigen
HBV	hepatitis B virus
HCC	hepatocellular carcinoma
HCV	hepatitis C virus
HDAg	hepatitis delta antigen
HDL	high density lipoprotein
HDlAg	hepatitis delta large antigen
HDsAg	hepatitis delta small antigen
HDV	hepatitis delta virus
HPLC	high performance liquid chromatography

HPTS	Hydroxypyrene-1,3,6-trisulfonic acid
HR	high resolution
HSA	human serum albumin
HSPG	heparan sulfate proteoglycans
IC_{50}	inhibitory concentration 50%
IF	immunofluorescence
IU/ml	international units per milliliter
kb	kilo-basepairs
K_d	dissociation constant
kDa	kilodalton
krpm	kilo rotations per minute
LDL	low density lipoproteins
M	mol
mg	milligram
min	minute
ml	milliliter
mM	millimolar
mm	millimeter
MOI	multplicity of infection
mRNA	messenger RNA
mut	mutant
MW	molecular weight
nm	nanometer
nt	nucleotide
OG	octyl glucoside
ORF	open reading frame
p.i.	post infection
PBS	phosphate buffer saline
PC	phosphatidylcholine
PFA	paraformaldehyde
PGH	primary guineapig hepatocytes
pgRNA	pregenomic RNA
pH	negative logarithm (base 10) of the molar concentration of dissolved hydronium ions
PHaH	primary hamster hepatocyte
PHH	primary human hepatocyte
PMH	primary mouse hepatocyte
pmol	picomol
PRH	primary rat hepatocyte
PS	phosphatidylserine
RNA	ribonucleic acid
RNA-Pol II	RNA-polymerase II
rpm	rotations per minute
RSA	rat serum albumin
rt	room temperature
RT	reverse transcriptase
S/CO	signal over cutoff
SDS-PAGE	sodium dodecyl sulfate polyacrylamid gelelectrophoresis
SEC	size exclusion chromatography
SN	supernatant
SVP	subviral particle
TM	transmembrane

TNF-α	tumor necrosis factor alpha
U	units
uPA	
UV	ultraviolet [1]
V	volt
V_0	void volume
V_e	elution volume
VLDL	very low density lipoproteins
w/	with
w/o	without
wb	western blot
WHDV	woodchuck hepatitis delta virus
WHV	woodchuck hepatitis virus
wt	wildtype

Zusammenfassung

Das Hepatitis B Virus (HBV) ist ein umhülltes hepatotropes Virus mit ausgeprägter Wirtsspezifizität. Zur Infektion von Hepatozyten benötigt es den N-terminalen Teil des großen Hüllproteins (Large-surface protein, L-Protein), besonders die essentielle Domäne (Aminosäuren 9-15) und die N-terminale Myristoylierung.

Die HBV-Infektion kann durch Zugabe von geringen Mengen an acylierten Peptiden, welche dem N-Terminus des L-Proteins entsprechen (HBV präS/2-48^{myristoyl}), effizient inhibiert werden (IC_{50}: 400 pmol). Hierfür sind wieder die Korrektheit der essentiellen Domäne und die N-terminale Fettsäure von Bedeutung. Werden diese Peptide Mäusen injiziert, so ist ein ausgeprägter Lebertropismus zu beobachten. Eine Mutation in der essentiellen Domäne führt zum Verlust des Lebertropismus, das entfernen der Acylierung verursacht eine rasche Ausscheidung des Peptids. Dies deutet auf eine Fettsäure-abhängige Bindung des Peptides an einen Serumfaktor hin. In dieser Arbeit wurden zunächst solche Faktoren identifiziert und die Interaktion charakterisiert; im zweiten Abschnitt wurde die Membranaktivität dieser Peptide untersucht. Der dritte Teil beschäftigt sich mit der hepadnaviralen Infektion verschiedener Spezies.

Serum Albumin und Apolipoprotein A1 wurden als acylierungs-abhängige, sequenzunabhängige Bindepartner für HBV präS1-Peptide identifiziert. Das myristoylierte Peptid band Albumin mit geringer Affinität (K_D =17µM), die Bindung an beide Faktoren stieg mit der Hydrophobizität des Peptids. Die Albuminbindung konnte *in vivo* bestätigt werden. Keiner der Faktoren hatte einen starken Einfluss auf die Bindung des Peptides an Hepatozyten, auf die HBV-Infektion oder auf die Infektionsinhibition. Diese Interaktionen stabilisieren also das Peptid im Serum, sie sind jedoch für weitere Schritte nicht relevant.

Versuche, zelluläre Interaktionspartner für präS-peptide zu identifizieren, waren erfolglos.

Im zweiten Teil dieser Arbeit wurde die Rolle der präS1-Domäne im viralen Zelleintritt untersucht. Da HBV ein umhülltes Virus ist, muss es während des Eintritts in die Wirtszelle sein Nukleokapsid freisetzen; die erste Transmembran-Domäne (TM-I), die den drei Oberflächenproteinen des Virus gemeinsam ist, wurde als virales Fusionspeptid beschrieben. Hier wurde die Membranaktivität des HBV präS1-Peptids analysiert. Es konnte gezeigt werden, dass dieses Peptid Modellmembranen in Abhängigkeit der essentiellen Domäne und der N-terminalen Acylierung destabilisiert. Koflotations-Versuche zeigten eine acylierungsabhängige Bindung an Liposomen. Dies deutet auf eine Rolle der präS1-Domäne im Zelleintritt hin.

Der dritte Teil behandelt die Infektion von Hepatozyten verschiedener Spezies mit HBV, Hepatitis Delta Virus [2], ein Viroid, welches vermutlich den gleichen Zelleintrittsmechanismus verwendet wie HBV und Waldmurmeltier-HDV (Woodchuck-HDV, WHDV); letzteres ist ein Hepatitis Delta Virus, welches die Oberflächenproteine des Woodchuck-Hepatitis Virus trägt. Hierfür wurden primäre Hepatozyten von Ratte, Kaninchen, Hamster und Meerschweinchen isoliert und mit HBV, HDV oder WHDV infiziert. Ratten-Hepatozyten konnten weder mit HBV noch mit HDV infiziert werden. Kaninchen-Hepatozyten waren suszeptibel für HDV, jedoch nicht für HBV. Sowohl in Hamster- als auch in Meerschweinchen-Hepatozyten war eine HBV-Infektion, jedoch keine HDV-Infektion detektierbar. Alle getesteten Hepatozyten waren suszeptibel für eine WHDV-Infektion.

Diese Daten weisen darauf hin, dass der HBV-Rezeptor auch in anderen Spezies vorhanden ist. Die Restriktion der verschiedenen Infektionnen findet vermutlich an einem späteren Schritt statt und ist für HDV und HBV verschieden.

Summary

Hepatitis B Virus (HBV) is an enveloped, hepatotropic virus with a restricted host range. Infection of hepatocytes has been shown to require the N-terminal part of the large envelope protein (L-protein); intactness of the essential site (amino acids 9-15) is crucial, the N-terminal myristoylation is mandatory.
HBV infection is efficiently inhibited by lipopeptides corresponding to the N-terminus of the L-protein (HBV preS/2-48^{myristoyl}). Equally requiring the essential site and the N-terminal acylation, these peptides prevent HBV infection already at picomolar concentrations (IC_{50}: 400 pmol).
These features are also important for a marked liver tropism that is observed when preS-peptides are injected into mice. While a non-acylated peptide gets rapidly excreted from the body, a mutant acylated peptide is retained but loses its liver specificity, arguing for an acylation-dependent serum factor binding.
In this work, serum factor binding and membrane activity of these peptides were analyzed; a third part addressed hepadnaviral infection of different species.
First, serum albumin and apolipoprotein A1 have been identified as acylation-dependent, sequence-independent interaction partners for HBV preS-derived lipopeptides. The myristoylated peptide bound albumin with relatively low affinity (K_D =17µM), binding to both serum factors was found to increase with hydrophobicity. Albumin binding was confirmed *in vivo*. None of the identified factors had a marked effect on peptide-binding to hepatocytes, HBV infection or infection inhibition. It was therefore concluded that these interactions stabilize the peptide in the serum but are not required for further steps. Attempts to identify protein binding partners for preS-peptides on hepatocytes were unsuccessful.
In the second part, the focus turned towards viral entry. Being an enveloped virus, HBV has to release its nucleocapsid during viral entry; the first transmembrane-domain (TM-I), common to the three surface proteins, has been proposed as viral fusion peptide. Here, a possible role of the N-terminal part of the L-protein during this step was studied by analyzing the membrane activity of preS-derived peptides. They could be shown to destabilize model membranes depending again on the essential site and the acylation; coflotation assays demonstrated acylation-dependent association to liposomes. This indicates a possible involvement of the L-protein N-terminus in viral fusion.
In the third part, it was assessed whether other hepatocytes from small animals belonging to different orders show susceptibility to HBV, to hepatitis delta virus [2], a viroid thought to share a common entry pathway with HBV, or to woodchuck hepatitis delta virus (WHDV), an HDV-virus containing the envelope proteins from woodchuck hepatitis virus. Primary hepatocytes from rat, rabbit, hamster and guinea pig were therefore isolated and infected with HBV, HDV or WHDV. Rat hepatocytes could not be infected, neither with HBV nor with HDV. Rabbit hepatocytes showed susceptibility to HDV, but not to HBV. In both hamster and guinea pig hepatocytes, HBV infection but no HDV infection was observed. All primary hepatocytes were susceptible to WHDV.
These findings indicate that the receptor for HBV is also present in other species; restriction of infection probably occurs at a post-entry step and affects HDV and HBV separately.

1. Introduction

1.1 Viral Hepatitis B

An infection with the Hepatitis B Virus (HBV) is one of the most frequent causes for an inflammation of the liver (hepatitis) and represents a major health issue. Today, about two billion people carry markers of an HBV infection, 350 million are currently chronically infected [3].

The term hepatitis B dates back to 1947, when MacCallum described jaundice development after measles-vaccinations with inoculates from measles-patients [4]. He suggested the differentiation between epidemic infectious hepatitis, termed hepatitis A, and a "homologous serum hepatitis", termed hepatitis B. The causative agent for the latter was not identified until the mid sixties. Blumberg and coworkers described an antigen in the serum of an aboriginal patient that reacted with antibodies from a hemophilia patient and was later found to be involved in the development of hepatitis [5]. Prince and colleagues performed immunofluorescence staining on liver sections [6] and immunodiffusion tests in serum of multiply transfused patients [7]. Both times, they detected an antigen that they brought into connection with viral hepatitis B.

The consequences of an HBV-infection range from transient hepatitis to chronic infection. The latter can lead to liver cirrhosis, liver failure or hepatocellular carcinoma (HCC), which account for HBV being among the ten most important causes of death worldwide. HCC, a non-HBV specific disease, causes 300.000 to 500.000 deaths every year. More than 4 million acute cases of HBV are registered annually, and one quarter of the infected die of chronic active hepatitis, cirrhosis or primary liver cancer [3].

High endemic areas for HBV are South East Asia, the Pacific region (without Japan, Australia and New Zealand), sub-Saharan Africa, the Amazon basin, parts of the Middle East, central Asia and some countries of Eastern Europe (fig. 1.1). In these regions, which are inhabited by about 45% of the world population, 70-90% of all people get infected with HBV before reaching the age of 40; 20% are chronically HBV-infected.

In northern America, Western and Northern Europe, Australia and parts of South America, HBV occurs only sporadically. Less than 2% of the population are chronically infected, the infection rate is at ~20% [3]. With 0,4 - 0,8% chronically infected patients and 5 - 8% infection rate, Germany can be classified as low endemic country (fig.1.1).

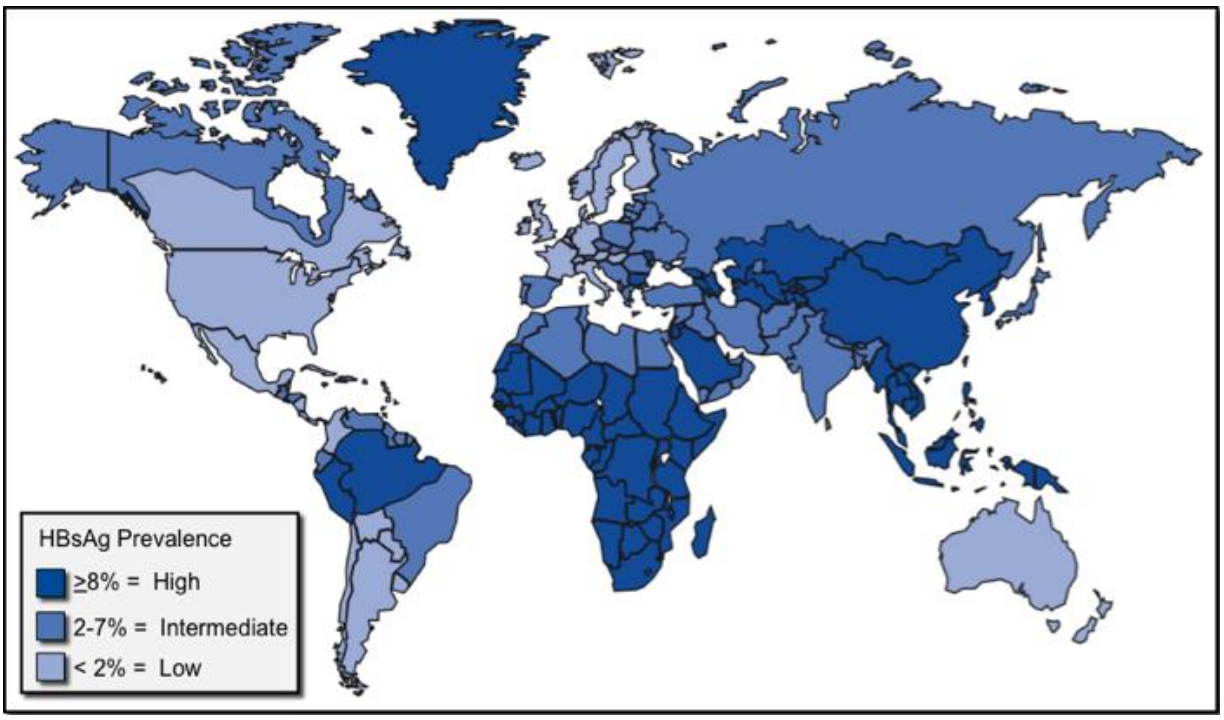

Fig.1.1 HBV seroprevalence in the world. This world map shows prevalence of hepatitis B Virus surface antigen (HBsAg) which is commonly used as marker for HBV infection. Countries with high prevalence are marked in dark blue, countries with intermediate prevalence in blue and countries with low prevalence in light blue. [8]

1.1.1 Transmission routes of HBV

HBV is transmitted parenteral via blood, blood products and other body fluids, such as sudor or lacrimal fluid. While the human body is the only reservoir of the virus, HBV stays infectious outside of the body for a certain time; yet, the most common ways of transmission are direct contact with injured skin or mucosa. In highly endemic areas, infection occurs usually perinatally (during birth) or in early childhood. In low and medium endemic regions, this route is rare; horizontal transfer of the virus by unprotected sexual contact or use of contaminated needles for drug consumption is observed more frequently. Medical personnel that often has contact with virus-containing blood is also at an increased risk of infection [9].

1.1.2 Epidemiology and pathogenesis

After entering the host, HBV reaches the liver via the blood system where it infects hepatocytes, the liver parenchymal cells. Here, replication of the virus is not causing cell death; as there is no immediate immune answer, 70-100% of the hepatocytes usually get infected [10].

It is only when a strong T-cell answer, directed against HBV-derived peptides being presented on the surface of infected hepatocytes, causes secretion of cytokines (e.g., TNF-α), free radicals and proteases that hepatocytes undergo cell death [11].

65% of all infections in adults proceed without apparent symptoms; 35% develop the immunopathologically caused acute hepatitis whose most prominent symptom is the icterus (jaundice) [12]. 1% of all acute infections develop into a fulminant hepatitis. If liver transplantation does not take place, this leads to rapid decay of the liver and to the patient's death. In 90 - 95% of infections, however, the disease passes with complete elimination of the virus from the liver, without causing any liver damage. Viral antigens are no longer detectable, antibodies against the HBV S-antigen (HBsAg) conferring life-long immunity are found in the serum. The remaining 5 - 10% of infected patients develop a chronic HBV infection that progresses with or without symptoms. The virus continuously replicates, causing a constant immune reaction against hepatocytes without clearance of infection [11]. Up to 90% of perinatal infections become chronic due to the immature immune system in infants.

Chronic infection is defined by persistence of the viral small surface antigen (HBsAg) in the serum of infected patients for more than six months [12]. It is thought to be caused by a weak or absent immune reaction. Patients with a chronic HBV infection have a 100 fold increased risk of developing liver cancer; 10-25% die of HCC or liver cirrhosis [12]. It is assumed that 60-80% of primary liver cancer are caused by HBV [13].

1.1.3 Prophylaxis and therapy

Since 1981, a safe and efficient vaccine from purified HBsAg is available. Being formerly purified from plasma of HBV infected patients, it is nowadays produced mainly by usage of genetically modified yeast cells. Vaccination with this HBsAg confers immunity against HBV for approximately 10 years [12].

For HBV infected patients, there is no drug that reliably eliminates the virus. All therapies target suppression of viral replication, aiming to avoid liver failure by cirrhosis or HCC. Besides immunomodulatory treatment with interferon α, nucleoside- and nucleotide analogues such as Lamivudine, Adefovir, Entecavir, Telbivudine, Clevudine and Tenofovir are employed [14]. Treatment with these drugs, however, favors the emergence of escape mutations in the HBV DNA polymerase, leading to formation of resistant viruses. For example, 80% of all patients under Lamivudine-treatment develop resistant mutants within 4 years [15].

Several new nucleoside/nucleotide analogues with improved antiviral action are currently being developed, and the inhibition of viral replication by targeting other viral proteins is under investigation [14].

1.2 Hepadnaviridae

The HBV virus is the prototype of the Hepadnaviridae, a family of small enveloped viruses with a partially double stranded DNA-genome that can cause a sometimes chronic form of liver inflammation (**Hepa**totropic **DNA** Viruses). This family can be divided into two genera: orthohepadnaviruses infect mammals while avihepadnaviruses target birds. Both genera have certain features in common:

- A 3 - 3,3kb relaxed circular DNA (rcDNA)
- A virus-associated polymerase that can fill the gap in the partially double stranded genome
- The production of a large excess of subviral particles
- A marked host specificity with strong liver tropism.

The family of orthohepadnaviruses includes several viruses isolated from different primates, squirrels or woodchucks that show differing sequence-homology with HBV. Isolates from primates are very close to human HBV and are therefore considered as genotypes (table 1.1).

Avihepadnaviruses (table 1.2) share only ~40% of their sequence with HBV. Their genomes are smaller and code for only two surface proteins (orthohepadnaviruses: three surface proteins). Also, they do not code for the X-protein, a non-structural protein with unclear function. Given the rather easy access to peking ducks, whose hepatocytes are susceptible to

duck hepatitis B virus (DHBV) infection, these animals have been frequently used as animal model in HBV research.

Table 1.1.: Representative members of the orthohepadnaviruses (from: [16]) Gorilla HBV shows only 5% divergence from chimpanzee HBV, these viruses are therefore classified as one genotype.

Virus	host	abbreviation
Hepatitis B Virus	human *Homo sapiens*	HBV
Chimpanzee-Hepatitis B Virus	Chimpanzee *Pan troglodytes*	HBV_{cpz}
Gibbon-Hepatitis B Virus	White-handed Gibbon *Hylobates lar*	HBV_{gbn}
Orang Utan-Hepatitis B Virus	Orang Utan *Pongo pygmaeus*	HBV_{oru}
Gorilla Hepatitis B Virus	Gorilla *Gorilla gorilla*	HBV_{cpz}
Woolly Monkey Hepatitis B Virus	Woolly Monkey *Lagothrix lagotricha*	WMHBV
Woodchuck Hepatitis B Virus	Woodchuck *Marmota monax*	WHV
Ground squirrel Hepatitis B Virus	Ground squirrel *Spermophilus beecheyi*	GSHV
Arctic squirrel Hepatitis B Virus	Arctic squirrel *Spermophilus parryi*	ASHV

Table 1.2.: Representative members of the avihepadnaviruses (from: [16])

Virus	host	abbreviation
Duck Hepatitis B Virus	Peking Duck *Anas domesticus*	DHBV
Grey Teal Hepatitis B Virus	Grey Teal *Anas gibberifrons gracilis*	GTHBV
Heron Hepatitis B Virus	Heron *Ardea cinerea*	HHBV
Maned Duck Hepatitis B Virus	Maned Duck *Chenonetta jubata*	MDHBV
Ross Goose Hepatitis B Virus	Ross Goose *Anser rossi*	RGHV
Snow goose Hepatitis B Virus	Snow Goose *Anser caerulescens*	SGHBV
Stork Hepatitis B Virus	Stork *Ciconia ciconia*	STHBV

1.2.1 HBV genotypes

Due to a high replication rate and the high error rate of the viral reverse transcriptase, the hepatitis B virus is capable of quickly adapting to changes in environmental conditions. This led to the emergence of the eight different genotypes HBV-A to HBV-H (criteria: sequence homology < 92%). Furthermore, these genotypes can be further divided into subgenotypes that differ in their geographic prevalence. These are defined by two pairs of determinants of the HBsAg that behave mainly allelic und mutually exclude each other: d,y and r,w.

Table 1.3.: HBV-Genotypes. Given are length of genome, differences in the ORFs and geographic prevalence. (from [16]).

Genotype	Length of the genome (in bp)	ORF-differences	Geographic prevalence
A	3221	Insertion of aa 153 and 154 in HBc	Africa Europe
B	3215		Asia
C	3215		Asia, Australia
D	3182	Deletion of aa 1-11 in preS1	Mongolia, Europe, India, Southern Africa, Australia
E	3212	Deletion of aa 11 in preS1	Central Africa
F	3215		Southern and central America
G	3248	Insertion of 12 aa in HBc Deletion of aa 11 in preS1	Central America
H	3215		Central America

1.2.2 Viral particles

The infectious agent of HBV is a spherical particle with a diameter of 42 - 47 nm, called Dane-Particle after its discoverer [17] (fig. 1.2). It contains an icosahedral capsid built of 240 units of the core-protein (also called Hepatitis B core Antigen, HBcAg). This capsid has a diameter of 22-25 nm and contains the 3,2 kb-viral genome and the viral polymerase. It is enveloped by a membrane that consists mainly of viral envelope proteins and to ~25% of host-derived lipids (mainly phospholipids, cholesteryl-esters and triglycerides) [18]. The small envelope protein (S-protein) is the main component; due to its antigenicity, it is also called Hepatitis B surface Antigen. The membrane also contains the middle protein (M-protein), whose function is unknown, and the large protein (L-protein), which is responsible for virus envelopment during morphogenesis [19] and for receptor binding during virus entry [20].

Cells infected with HBV produce not only Dane-particles but also subviral particles (SVPs). SVPs consist of non infectious empty membrane material that does not contain capsids (fig. 1.2). They exist either as spherical particles with a diameter of ~22 nm or as filamentous particles of 22nm in diameter, reaching up to 200nm in length. SVPs are found in the serum of infected patients in a 10^4-10^6 – fold excess over the Dane-particles. The distribution of the surface proteins differs between the three viral particles; while Dane-particles have a S:M:L-ratio of 4:1:1, this ratio is 100:5:1 in spherical SVPs. Filamentous particles have a slightly larger amount of L-protein compared to spherical SVPs.

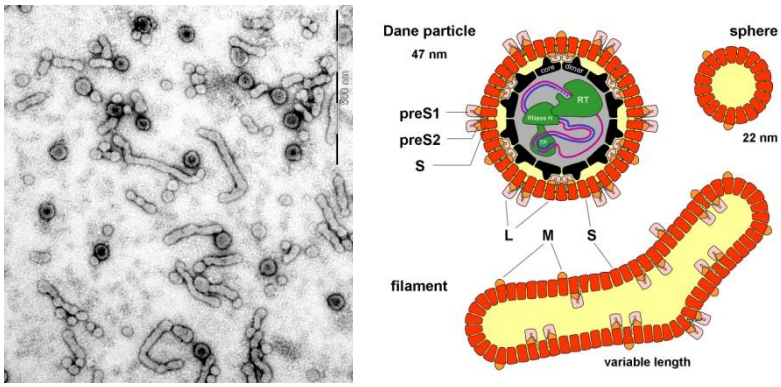

Fig.1.2. Left panel: Electron micrograph of negative-stained HBV-particles. Right panel: Schematic representation of the composition of Dane-particles, spherical and filamentous subviral particles. S, M, L: small, middle and large surface protein, respectively. **RT**: reverse transcriptase. **TP**: terminal protein. **preS1/2:** N-terminal extensions of the surface protein**s.** Courtesy of S. Seitz.

1.2.3 The viral genome

Inside the capsid, the viral DNA is found as partially double stranded, ~3200 base pairs (bp) relaxed circular DNA (rcDNA). The negative strand is of one unit length (3100-3300 bp, differing by subtype); it has the terminal protein [21] bound 5´-terminally. The positive strand is shorter (1700-2800 nt) and has a 17-19 nt oligoribonucleotide on its 5´-end. Both strands contain direct repeats (DR) of 11 nucleotides; the one on the negative strand is called DR1, the other DR2 (fig. 1.3).

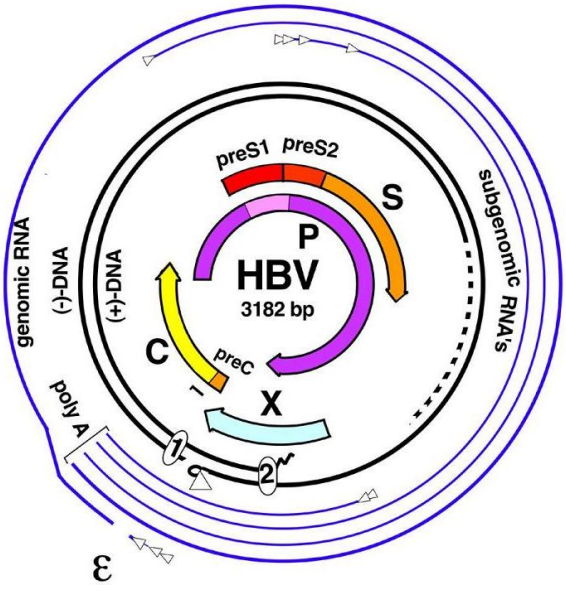

Fig. 1.3: Organization of the HBV-genome. Inner black circle: rcDNA, positive strand. **Outer black circle:** rcDNA, negative strand with associated reverse transcriptase (triangle). positions of the direct repeats 1 and 2 are indicated (white circles). On the inside, positions of the open reading frames (ORFs) are given, coding for either surface proteins (preS1/ preS2/ S), the viral polymerase (P) the precore/core (preC/C) or the X-protein (X). The outer blue circles depict either subgenomic RNAs with their different initiation points (white triangles) and polyA-tails on the 3´-end or the genomic RNA with its encapsidation signal ε. From: [22]

The HBV genome is tightly organized; every nucleotide is in a coding region, over 50% of the sequence are part of an open reading frame (ORF). It contains a total of four ORFs (tab. 1.4):

- The preS-S (presurface-surface) ORF encodes the three viral surface proteins; it has three in frame-start codons that allow a differential initiation of translation.
- The preCore/ Core ORF codes for the Hepatitis B core-antigen (HBcAg) and the Hepatitis B early-Antigen (HBeAg), a soluble factor with unknown function. Initiation of translation on an internal AUG leads to the production of the 21 kDa core protein; initiation on an upstream start codon causes synthesis of the 24 kDa precore protein, the e-antigen. The precore-sequence contains a signal-sequence directing the nascent protein to the secretory pathway. During its passage through the Golgi-apparatus, it is cleaved by cellular proteases, giving rise to the 16 kDa HBeAg that is secreted into the blood stream.
- The viral polymerase is responsible for DNA-synthesis and for packaging of the viral genome into newly formed capsids; it is encoded by the polymerase-ORF (P-ORF).
- The X-ORF contains the sequence for the X-protein, a factor that is able to modulate the host cell signal transduction as well as the gene expression of viral and host-genes. Its exact function is unknown, but it has been shown to be necessary for viral replication.

Table 1.4: HBV proteins. Name, molecular weight, modifications and function are indicated.

Protein	Name	Molecular weight and modifications	Function
HBsAg	S-protein	24 kD 27 kD glycosylated	surface protein induction of neutralizing antibodies formation of particles
preS2-HBsAg	M-protein	33 kD 36 kD glycosylated	surface protein binding to Serum albumin
preS1-HBsAg	L-protein	39 kD acylated 42 kD acylated, glycosylated	surface protein receptor binding capsid binding in morphogenesis
HBcAg	Core-protein	22 kD phosphorylated	capsid protein binding the genome at envelopment
HBeAg	e-antigen	16 kD	secreted protein, correlates with HBV replication
HBx	X-protein	17 kD	transactivator for viral and cellular promotors exact function unknown
P	polymerase	90 kD	DNA-and RNA-dependent Polymerase (reverse Transcriptase), RNAse H, terminal protein for initiation of replication

1.2.4 The viral surface proteins

The membrane of HBV contains three type II transmembrane glycoproteins that are all encoded by a single ORF (fig. 1.4): the small (S), the middle (M) and the large (L) surface protein [23]. The S-protein is the main membrane component of all HBV particles. It has a length of 226 aa and a glycosylation site on Asn146; since this site is modified in only a part of all S-proteins, there is an unglycosylated (24kDa) and a glycosylated form (27kDa) [24]. It possesses four transmembrane domains and forms the membrane anchor of all three surface proteins (fig. 1.4).

Initiation of transcription 165 nucleotides upstream leads to the synthesis of the M-protein. It is characterized by 55 additional amino acids (aa) on the N-terminus. This so-called preS2-domain is partially glycosylated on Asn4 and has a molecular weight of 33 kDa and 36 kDa, respectively. The M-protein is N-terminally acylated and accounts for 5-15% of all HBsAg [25].

The start codon for the L-protein lies 489 nucleotides upstream of the S-start codon; translation of the corresponding mRNA gives rise to a 334-345 aa protein (depending on the genotype). The L-protein is therefore characterized by its preS1-domain of 108-119 aa and carries a N-terminal signal for myristoylation on Gly2 [26]. The attachment of this C14 fatty acid is performed cotranslationally by cellular N-myristyl transferases [27]. It has been shown to play no role during viral assembly, yet it is indispensable for viral infectivity [28]. The L-protein, which accounts for 1-2% of all HBV surface proteins, is also partially glycosylated in the S-domain and occurs therefore in two isoforms, p39 and gp42.

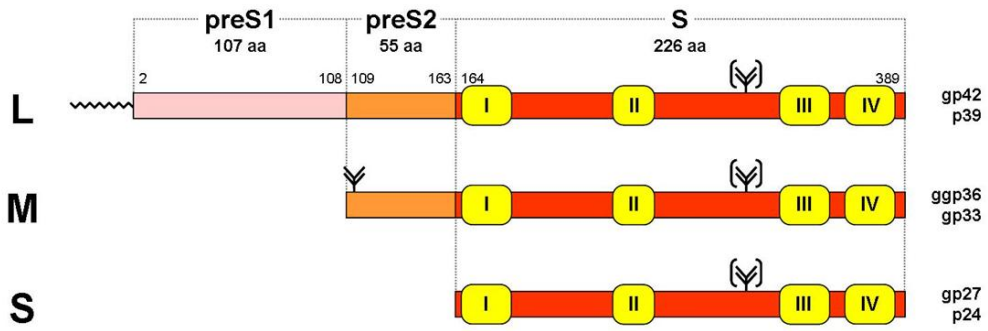

Fig. 1.4: schematic representation of the domain structure of the Large (L), the middle (M) and the small (S) HBV surface proteins. Red: S domain. **Orange:** preS2-domain. **pink:** preS1-domain. **yellow:** transmembrane domains. glycosylation. myristoylation. Numbers indicate amino acids. p:protein gp: glycoprotein; ggp: double glycosylated protein. Courtesy of S. Seitz.

1.2.5 Topology of the surface proteins

Since the HBV surface proteins are membrane proteins, they are synthesized and inserted cotranslationally on the membrane of the endoplasmatic reticulum (ER), where they adopt their complex membrane topology [29] (fig. 1.5).

The insertion of the S-protein into the ER-membrane is initiated by a N-terminal signal sequence (aa 8-22), which will not be cleaved by a host protease but composes the first transmembrane domain (TM-I). A second signal at aa 80-98 leads to the translocation of the downstream polypeptide through the ER-membrane and into the ER-lumen; the upstream sequence stays in the cytosol, the signal itself becomes the transmembrane domain II (TM-II) [30]. The C-terminal 57 hydrophobic aa of the S-protein also get embedded into the ER-membrane and form the TM-III and TM-IV (fig. 1.5). The C-terminus of the S-protein faces the ER-lumen, aa 23-79 form a cytosolic loop, aa 99-169 face again the ER-lumen and form a large loop, the so called a-determinant, which carries the main epitope of the HBV surface antigen (HBsAg) (fig. 1.5). After particle secretion, cytosolic parts will be located on the inside of the particle, while ER-luminal parts will be exposed on the outside of the particle.

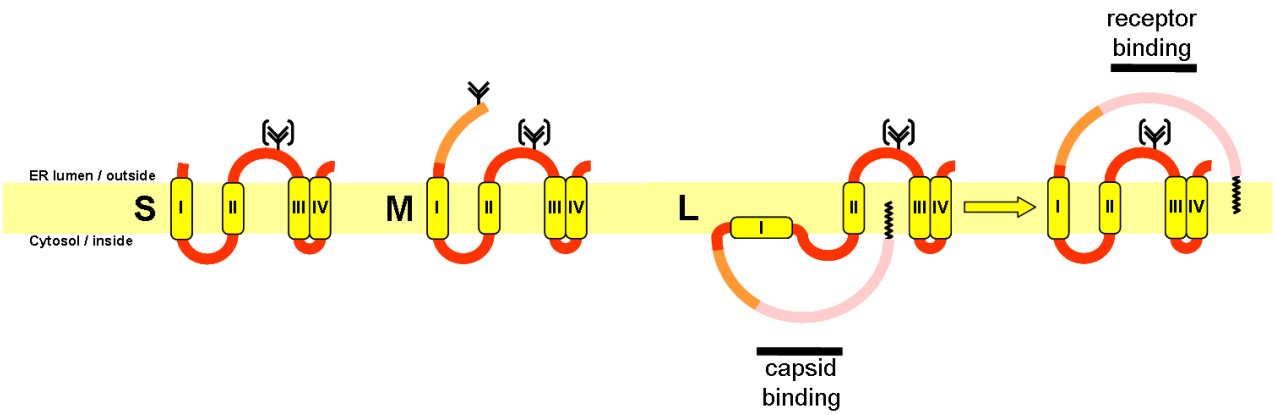

Fig.1.5: Schematic representation of the transmembrane topology of the three HBV glycoproteins. Red: S-domain. **Orange:** preS2-domain. **pink:** preS1-domain. **yellow:** transmembrane domains. : glycosylation : myristoylation. The N-terminus of the S-protein and the preS2-domain of the M-protein are directed towards the ER-lumen, the preS-domain of the L-protein adopts a dual topology: when oriented towards the inside of the particle, it binds the viral capsid, when oriented towards the outside, it mediates receptor recognition. Courtesy of S. Seitz.

The M-protein is synthesized in the same manner as the S-protein; thus, the preS2 domain is positioned towards the ER-lumen and on the particle surface after secretion [31].

The L-protein has to fulfill a dual role, its topology is therefore subjected to changes. Since HBV has no defined matrix protein, this function is fulfilled by the preS-domain of the L-protein. During its synthesis, the preS-domain is oriented towards the cytosol. Here, it

ensures binding of the capsid and therefore formation of enveloped viral particles [32]. After translation, 50% of the preS-domains get translocated to the outside if the viral particle (fig. 1.5).[33;34]. Recent data indicate a maturation process of viral particles involving a translocation of all L-proteins (S. Seitz, unpublished data). This translocation is necessary for receptor interaction, which has also been mapped to the preS1-domain [20]. The time point and the mechanism of this preS-translocation are under debate.

1.2.6 HBV entry

1.2.6.1 Animal models and cell culture systems

The first steps of a viral infection are often composed of a low-affinity, energy independent and reversible interaction of the virus with a cell surface structure, followed by a high-affinity binding to a specific receptor that mediates endocytosis. Thereafter, enveloped viruses have to uncoat their capsid by fusion of the viral membrane with a cellular membrane (plasma membrane or endosomal membrane). These initial events are only poorly understood in the case of HBV, since until recently, there have been only few *in vivo* or *in vitro* systems available. Due to the restricted host range of HBV, only primates (mainly chimpanzees) have been used [35]. These use of these animals, however, has been abandoned for ethical and financial reasons. The discovery that the tree shrew *Tupaia belangeri* can be infected with HBV [36;37] led to the first small animal model for HBV. Primary human hepatocytes (PHH) have been employed as an *in vitro* model, but these cells are obtainable only by surgical excision of liver parts from patients. Furthermore, PHH are problematic in cultivation, cannot be passaged and show high variance in their susceptibility.

Only recently, Gripon and colleagues described the hepatoma cell line HepaRG that is derived from a female patient suffering from chronic Hepatitis C Virus infection [38]. These cells can be passaged and, when treated with dimethylsulfoxid (DMSO), undergo a differentiation process that leads to susceptibility for HBV infection.

1.2.6.2 Early steps of HBV infection

Infection of hepatocytes is initiated by low affinity binding of the virus to cell surface Heparan Sulfate Proteoglycans (HSPGs) in a L-protein dependent manner [39]. This initial attachment step is followed by binding to an unknown cellular receptor and endocytosis. While the M-protein was shown to play no role in HBV infection[40], the S- and the L-protein are necessary for this step. The part of preS being essential for HBV infection was shown to

be in the preS1-sequence (aa 3-77); here, only a small deletion of aa 78-87 is tolerated [20]. Further deletions of the preS2-sequence do not influence viral infectivity [41]. The myristoylation at the N-terminus of the preS1 was shown to be necessary for infectivity [42; 28], yet its exact function is unknown.

On the cellular side, no receptor molecule for HBV has reliably been identified. Several molecules have so far been proposed, among which Interleukin 6 [43], the human squamous cell carcinoma antigen 1 (SCCA1) [44] or the asialoglycoprotein receptor [45]. Direct proof as an entry receptor has been given for none of these molecules.

The cellular receptor for the duck hepatitis B Virus (DHBV) has been found to be the duck caboxypeptidase D (dCPD) [46]. This is a trans-Golgi network protein that binds the primary binding sequence of the dHBV L-protein, aa 86-115. This part of the dHBV L-protein is a largely unstructured domain that binds at first with relatively low affinity to the dCPD, passing into a stronger interaction that is thought to finally mediate the fusion between the viral and the cellular membrane [46; 47]. For human HBV, however, this mechanism seems to play no role, since the human version of carboxypeptidase D does not bind the HBV L-protein.

1.2.7 The viral replication cycle

After receptor-mediated endocytosis, the viral capsid gets uncoated and is transported towards the nucleus where it delivers the viral genome. The core protein possesses a nuclear localization signal which facilitates the nuclear import [48]. The release of the viral genome occurs within the nuclear pore, where the capsid dissociates [49]. Once in the nucleus, the positive strand of the HBV DNA gets completed and its ends get ligated, leading to the formation of episomal covalently closed circular DNA (cccDNA) [50].

The cccDNA now serves as a template for the formation of viral RNAs by the cellular RNA polymerase II, which transcribes the cccDNA into three subgenomic RNAs (two for the surface proteins, one for the X-protein) and one pregenomic RNA (pgRNA). All formed RNAs have the same polyadenylation signal close to the core-ORF. While the subgenomic RNAs serve only as mRNAs, the pgRNA has two functions: it is the template for the synthesis of the viral DNA and also the mRNA for the translation of the preCore-, the Core-protein and the viral polymerase.

Following the export of the viral RNAs into the cytoplasm, the membrane proteins are synthesized on the ER-membrane and the Core-protein, the e-antigen and the viral polymerase are synthesized in the cytoplasm. The pgRNA has a hairpin secondary structure called ε close to its 5´-end; this is recognized and covalently bound by the N-terminus of the viral polymerase [51; 52]. The ε-structure serves as primer for the synthesis of the first four nucleotides of the negative strand [53]. After initiation, the entire complex is transferred to homologous sequences on the 3´-end and serves now as primer for the synthesis of the negative strand. Simultaneously, the RNA-template gets degraded by the RNAse H activity on the C-terminus of the polymerase [54]. At the end of the negative strand synthesis, a oligoribonucleotide remains on the 3´-end; it now serves as primer for the synthesis of the positive strand [55].

The ε-signal of the pgRNA also functions as a packaging signal; therefore, it is already during reverse transcription that the complex of pgRNA and polymerase gets bound by core protein and packaged into immature capsids. Maturation of the capsid before the end of positive strand synthesis leads to the characteristic partially double stranded genome.

The mature capsid can now pursue one of two ways: it either gets reimported into the nucleus, where the formation of new cccDNA increases this pool until 20 or more of these molecules are present and serve as templates for transcription [56]. This way is predominant during early time points of the infection and allows accumulation of cccDNA. When the amount of surface proteins increases, the capsids bind preferentially to the N-terminus of the L-protein and get translocated through the ER-membrane [57; 58]. After passage through the Golgi-complex, the virions get secreted into the blood.

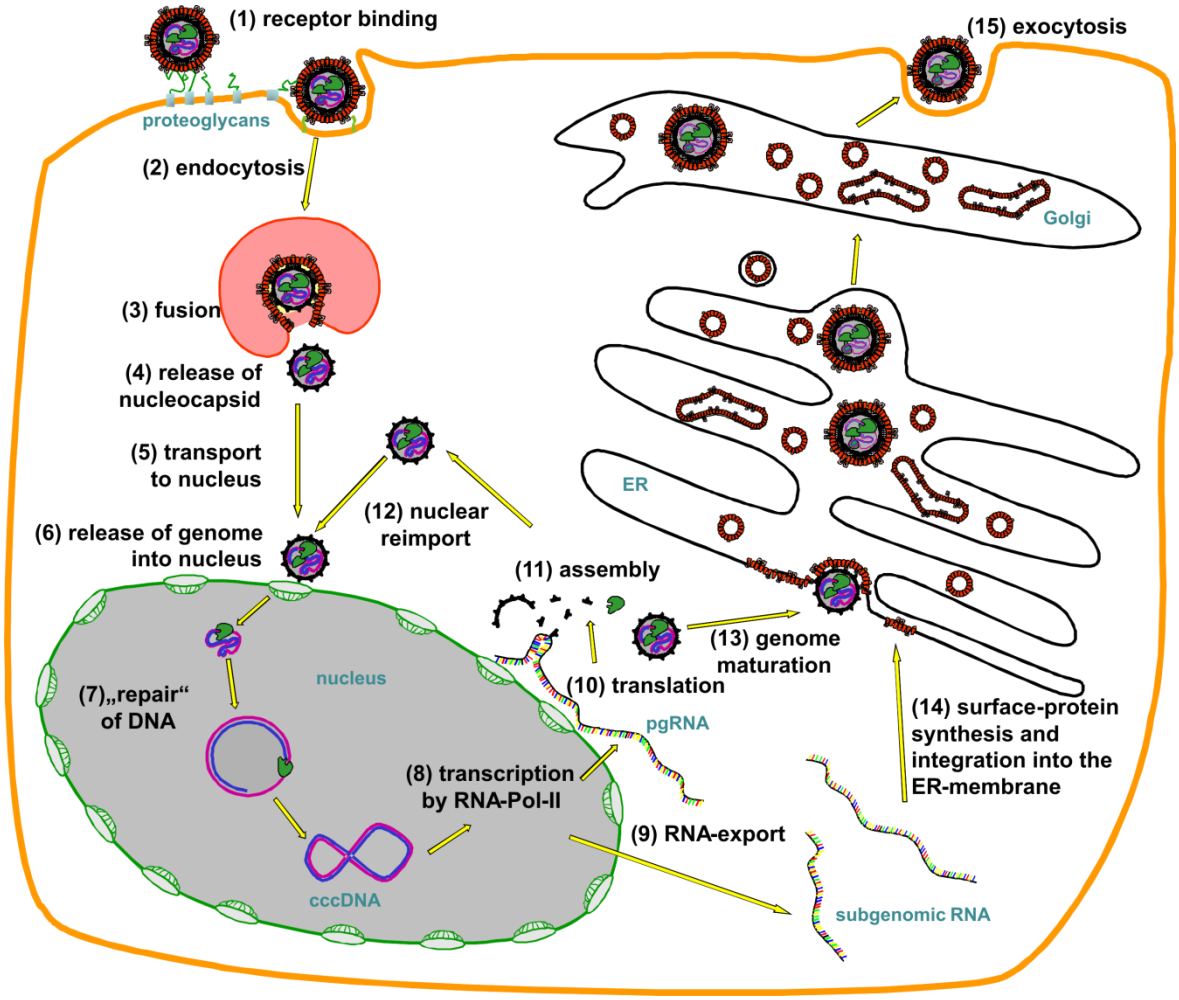

Fig. 1.6: The HBV replication cycle. HBV enters hepatocytes by binding to an yet unknown receptor molecule (1). After endocytosis (2), fusion of the viral membrane with a cellular membrane (3) leads to release of the nucleocapsid (4) that then gets transported to the nucleus (5). The viral genome is then released into the nucleus (6) where the positive strand gets completed and ligated (7); cccDNA is formed. Transcription of cccDNA by RNA-Pol-II (8) leads to formation of the mRNAs for surface proteins (9) and formation of the pregenomic RNA (pgRNA), which serves as mRNA for the core-protein (10) and as template for reverse transcription into viral DNA. Immature genomes get packaged into assembling nucleocapsids. These either get reimported into the nucleus or get enveloped at the ER-membrane where translation of viral surface proteins takes place (14). These viral particles then leave the cells by passage through the ER and the Golgi (15).

1.3. HBV preS1-derived lipopeptides as entry inhibitors

In 2005, Gripon and colleagues described lipopeptides derived from the L-protein preS1 N-terminus as potent inhibitors of HBV entry. Using HepaRG cells and primary human hepatocytes, they demonstrated that the first 47 amino acids (aa 2-48) are essential for infection inhibition and that the N-terminal acylation strongly enhances the inhibitory effect, postulating an IC_{50} of 8nM [59]. These findings were later confirmed on primary hepatocytes from *Tupaia belangeri* [60] and in *in vivo* studies on immunnodeficient whose livers were repopulated with primary *Tupaia belangeri* hepatocytes. In these *in vivo* studies from Petersen and colleagues, the ability to inhibit infection could be shown to be sequence dependent; it was furthermore observed that these peptides exhibit a strong liver tropism that is independent of the cells´ susceptibility to HBV, since accumulation of the preS-peptides was also observed in murine hepatocytes [61].

More detailed analysis of the peptides regarding their sequence requirements for infection inhibition and liver tropism in mice [62; 63]) revealed that both features strongly correlate. An intact amino acid sequence, concerning especially the essential site of aa 9-15, and the presence of a N-terminal acylation are both required for infection inhibition and for liver tropism (fig. 1.7). Mutations in the essential site, such as a G12E-mutation or a replacement of aa 11 and 13 by their respective D-enantiomer strongly reduced the HBV infection inhibition and abolished liver tropism, leading to equal distribution of these peptides throughout the body of the mice. A non-acylated version of the peptide was excreted from the body within four hours after injection (fig. 1.7).

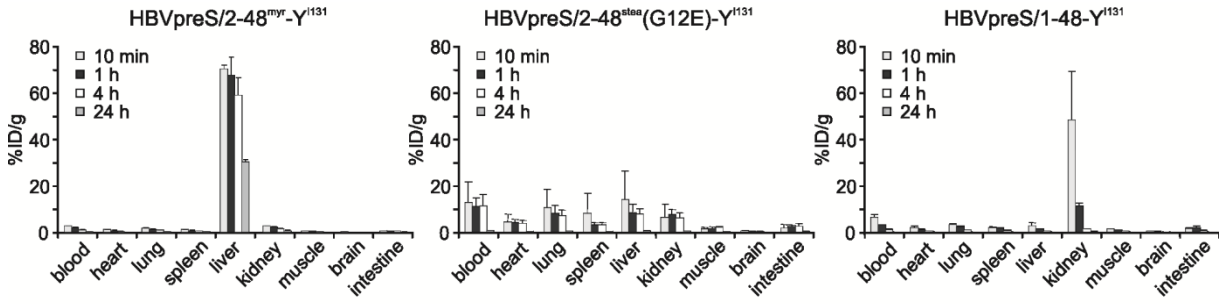

Fig. 1.7: Liver tropism of ^{131}I-labeled HBV preS1-derived peptides in mice. NMRI mice were intravenously injected with radioactively labeled HBV preS1-derived peptides. A myristoylated wildtype version (left panel), a stearoylated peptide carrying the G12E-mutation (middle panel) or a non-acylated wildtype version (right panel). At the indicated time points, organs were harvested and radioactivity was measured in a γ-counter. Three animals were used for each time point.(Data from:[63]).

Further studies of the preS1-peptide binding to different primary hepatocytes and HepaRG cells showed that this binding takes place on a variety of primary hepatocytes (such as rabbit, rat or dog hepatocytes, fig. 1.8), is dependent on the differentiation state of the cell and is most likely mediated by a cytoskeleton-linked proteinacious component of the plasma membrane [64].

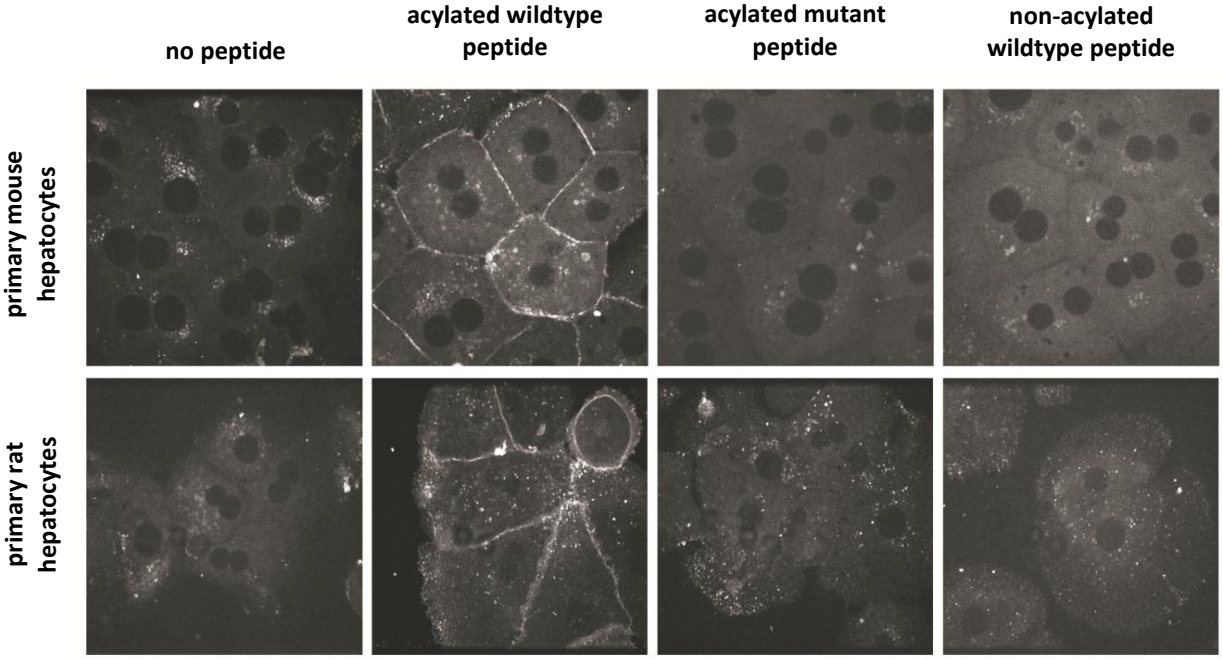

Fig. 1.8: Binding of FITC-labeled HBV preS-derived peptides to primary hepatocytes from mouse and rat. Primary hepatocytes from mouse (PMH) and rat (PRH), cultured on cover slips, were incubated without or with 200 nM fluorescein-isothiocyanate (FITC)-labeled acylated wildtype, acylated mutant or non-acylated wildtype peptide, respectively, washed and fixed. Plasma membrane-bound fluorescence was documented by spinning disk confocal microscopy with a 600x magnification. Autofluorescence is shown on the left (without peptide). Modified from A. Meier [64].

1.4. Membrane fusion

The fusion of two membranes is a tightly regulated process during which two lipid bilayers merge into one. This generally requires the presence of specialized proteins that bring these two membranes into close proximity and cause a local disturbance in the bilayers. This process plays a role in cell-cell communication (e.g., in neuronal exocytosis), intracellular transport (e.g., ER/golgi-shutteling), protein degradation by lysosomes, and is necessary for cell entry of enveloped viruses [65]. It is generally believed to occur via a hemifusion intermediate where, after having been brought into close contact, the adjacent monolayers fuse first, followed by fusion of the distant monolayers (fig. 1.9).

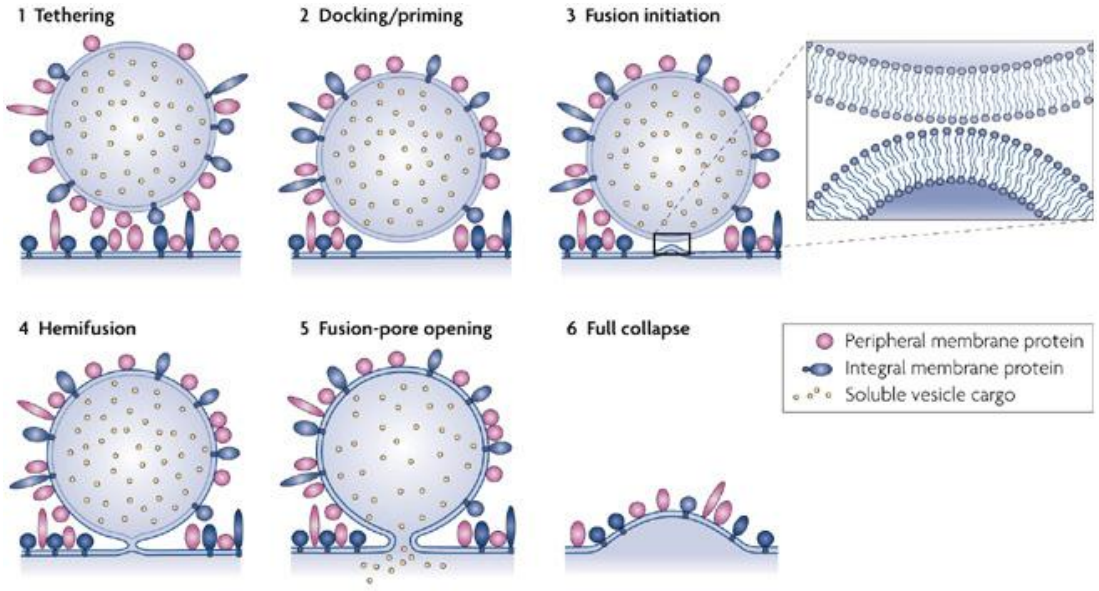

Fig. 1.9: Model of membrane fusion via the hemifusion intermediate. An example for a vesicle containing a soluble cargo fusing with a target membrane is depicted. After protein-mediated tethering (1), the vesicle is bound closely to the target membrane, an eventual priming of the fusion machinery takes place (2). Fusion is initiated by induction of membrane curvature (3). This leads to fusion of the adjacent outer membrane bilayers, the so-called hemifusion (4). Fusion of the inner bilayers induces full formation of the fusion pore (5), followed by full collapse and release of the cargo (6). (taken from: [65]).

1.4.1. Viral membrane fusion

In order to enter cells, viruses bind cell surface proteins and induce membrane fusion by specialized viral fusion proteins. In this process, insertion of viral fusion peptides into target membranes usually catalyzes the fusion process by destabilizing the membrane and reducing the required activation energy. This happens either at neutral pH at the plasma membrane or after endocytosis.

Viral fusion proteins, typically type I transmembrane proteins, are today divided into two classes [66]. Type I viral fusion proteins are characterized by an alpha-helical core structure. They are usually synthesized as single chain precursors that assemble into trimers and undergo proteolytic cleavage by host cell proteases soon after their synthesis, leading to formation of a metastable state. Upon activation during viral entry, refolding of the protein into a trimeric coiled coil takes place and exposes the viral fusion peptide that will be inserted into the target membrane. The Influenza haemagglutinin (HA) protein is a typical example for a type I fusion protein. The envelope proteins of flaviviruses are known examples of type II fusion proteins. These proteins, consisting most often of β-sheets, do not require proteolytic activation, but possess an internal fusion peptide. Often, the cleavage of another surface protein is required for the activation of the fusion protein itself [66]. During

the last years, a third class of viral fusion proteins has been proposed [67]. Their fusion proteins consist of five distinct domains and trimerize through their ectodomains, forming rod-like molecules of varying size. Fusion peptides of class III fusion proteins are less conserved than in the other two classes.

The influenza HA is synthesized as fusion-incompetent precursor (HA0) which is proteolytically cleaved into two subunits[68;69]: HA1 stays covalently attached to the transmembrane subdomain, HA2 is attached by a disulfide bond [70]. In the prefusion state, HA forms homotrimers that have their three fusion peptides buried within the molecule. Upon binding of HA1 to its receptor, the sialic acid, the virus is endocytosed [71]. In the low pH of the endosome, the HA2 fusion peptide is exposed and inserted into one layer of the target membrane, where it induces curvature and bends it towards the viral membrane [72] (fig. 1.10). During this process, one part of the HA2 changes from an extended loop conformation into a coiled coil, propeling the fusion peptide towards the host cell membrane. It is believed that the prefusogenic structure is primed for a conformational change that leads to fusion. It could be demonstrated that the HA2 fusion peptide adopts a boomerang-shaped structure that inserts it into the lipid bilayer [73] and lies in the target membrane inclined by ~45° [74] (fig. 1.10). The C-terminal domain of HA2 then folds back and forms a hairpin-like structure, thereby bringing the two membranes into close proximity. This induces curvature of the target membrane , the so-called nipple-formation, that will ultimately lead to membrane fusion.

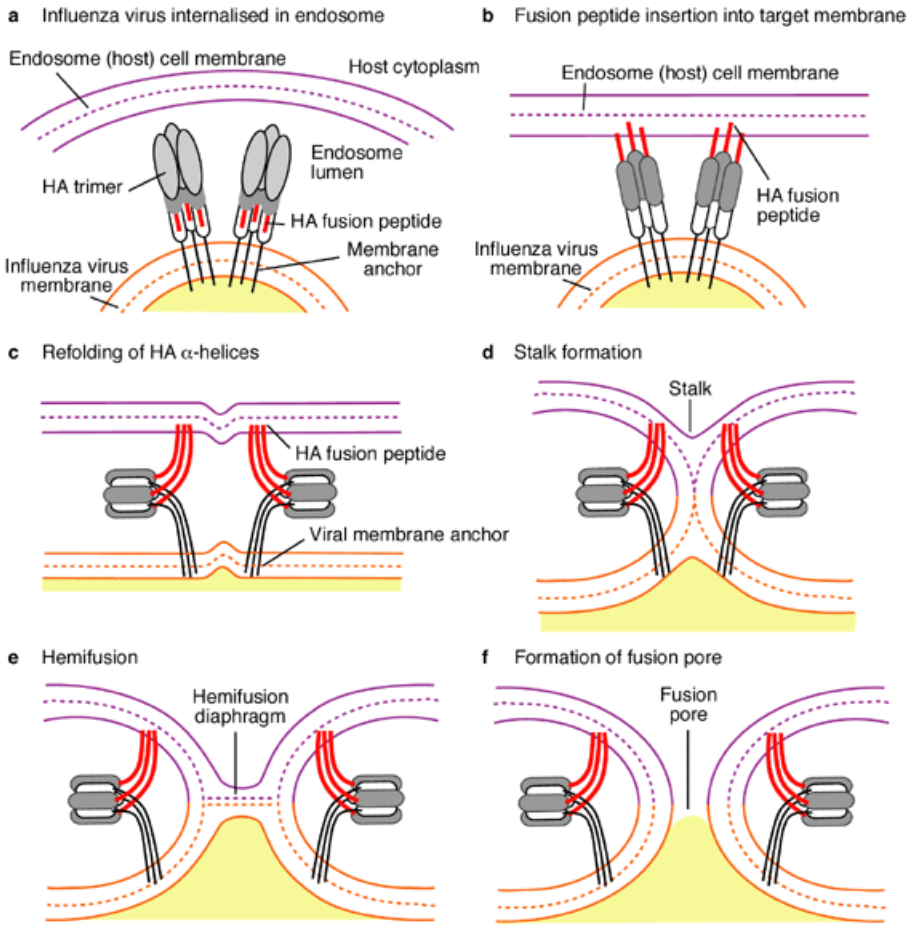

Fig. 1.10: The Influenza virus fusion pore formation. After endocytosis (a), the low pH of the endosome leads to a conformational change in the HA-protein and to exposure of the viral fusion peptide that gets inserted into the endosomal membrane (b). The C-terminal domain of the HA-protein then folds back into a coiled coil (c) which induces curvature in the viral and in the endosomal membrane. This induces stress on the membranes which is released by fusion of the outer membranes (d), leading to the hemifusion state (e). Ultimately, the inner membranes fuse, the fusion pore opens (f). Taken from [75].

1.4.2 Viral fusion peptides

The fusion peptide, which is often rich in hydrophobic and glycine residues, always interacts with the host cell membrane at an early stage of membrane fusion. Inclination is a feature often observed for viral fusion peptides that are therefore sometimes referred to as "tilted peptides". These are generally short protein fragments with an asymmetric distribution of hydrophobic residues that leads to inclined insertion into a membrane. In 1988, the fusion peptide of Newcastle disease virus was shown to have a 55° inclination in a phospholipid monolayer [76]. These membrane destabilizing peptides have several common features, such

as an overall hydrophobicity, a prevalence of small residues and show a gradient of hydrophobicity when helical.

Some viral fusion peptides do not insert themselves into the target membrane but merely associate with the surface of the membrane by interaction with phospholipids. This has been described for peptides from the HIV gp41 N-terminus [77] that is thought to interact with negatively charged phospholipids and thereby gets inserted laterally into the host cell membrane, inducing curvature.

Interaction with phospholipids can induce formation of structures in viral proteins; Galdiero and coworkers reported such behaviour for Herpes simplex virus type I glycoprotein-derived peptides performing circular dichroism measurements of liposomes [78]. An extensive study on structural properties of viral fusion properties compared peptides from several viruses, including Influenza [79], HIV (class I) or tick-borne encephalitis virus [79] and also compared these to cellular fusion proteins such as syntaxin [80]. Formation of secondary structures upon exposure to trifluoroethanol (TFE), which is known to stabilize secondary structures, was studied by circular dichroism spectroscopy. for all studied peptides, an increase in secondary structure was observed when TFE-concentrations increased; the need for structural flexibility in fusion peptides was proposed. Hofmann and coworkers designed unnatural peptides with fusogenic activity. They postulated that the ratio of α-helix promoting leucine to β-sheet promoting valine is crucial, and that secondary-structure destabilizing prolines and glycines in the hydrophobic core act as enhancers [81].

1.4.3 Membrane fusion by hepatitis B viruses

HBV does not encode a classical fusion protein requiring proteolytic cleavage for successful entry. Lu and coworkers described HBV infection of otherwise non-susceptible HepG2 cells after protease treatment of viral particles, claiming the exposure of a fusion sequence between the pres2- and the S-domain [82].

For the duck hepatitis B virus (DHBV), the first transmembrane domain (TM-I) of the large surface protein has been proposed as fusion peptide that is necessary for DHBV entry [83, 84]. It is thought that acidification leads to exposure of the TM-I on the viral surface, a step which would be required for membrane fusion.

Interaction of HBV preS-domains with phospholipid vesicles has been described [85]; In these studies, however, recombinantly expressed preS-peptides without N-terminal acylations and no mutant controls were used. These results therefore should be interpreted with caution.

1.5. Hepatitis Delta Virus

1.5.1. History and pathogenesis

Four decades ago, Rizzetto and coworkers described a new antigen in hepatocytes and serum of chronically HBV infected patients [86], using immunofluorescence. Assuming that this new antigen was another antigen produced by the HBV infection, it was termed Hepatitis Delta Antigen (HDAg). It was not until 1980 that this antigen was assigned to a single strand RNA-genome virus, then called Hepatitis Delta Virus [2; 87]. HDV was then classified into a new genus, the deltaviridae.

Today, 8 HDV genotypes are known; genotypes 2-7 are specific for certain geographic areas [88]. HDV can either co-infect with HBV [89], leading to ~5% chronicity, whereas superinfection leads to a chronic infection in up to 80% of all cases. Interestingly, HBV replication is usually suppressed in chronically HDV infected patients [90].

HDV infection usually induces severe hepatitis within 37 weeks post infection, fulminant hepatitis being recorded more often than in HBV infection alone. The resulting massive necrosis of hepatocytes leads to liver failure and death in 80% of all cases, liver transplantation often being the only remedy.

Coding only for the delta antigen, HDV depends on the surface proteins of HBV for the production of new viral particles and can therefore spread only in the livers of patients infected with HBV; it is therefore termed a satellite virus.

1.5.2. Morphology and viral proteins

HDV forms spherical, 36-43 nm particles containing a ribonucleic core-like structure with a diameter of 19 nm. A lipid shell containing the HBV surface proteins envelops one genomic RNA of 1700 nt which is complexed with ~70 molecules of the large and small Delta antigen (fg. 1.11) (HDLAg and HDSAg, respectively). These are synthesized from one ORF and differ only by 19 additional amino acids on the C-terminus of the HDLAg [91].

The Delta Antigen consists of dimers of an antiparallel coiled coil structure leading to oligomerisation into octamers and thereby form ringlike structures of 50 Å diameter; it is not

exposed on the viral surface (fig. 1.11). HDAg contains a nuclear localization signal (NLS) that allows targeting of the ribonucleoprotein (RNP) to the nucleus [92]. A domain comprising amino acids 35-65 allows binding to the nucleolus-protein nucleolin [93]. Three arginine-rich domains are thought to be responsible for binding to the HDV RNA [94]. Furthermore, HDLAg contains a nuclear export signal (NES) [95] and a farnisoylation motif on its C-terminus [96]. The viral envelope contains all three HBV surface proteins in a L:M:S-ratio of 95:5:1, being more similar to subviral spheres than to HBV particles (fig. 1.11).

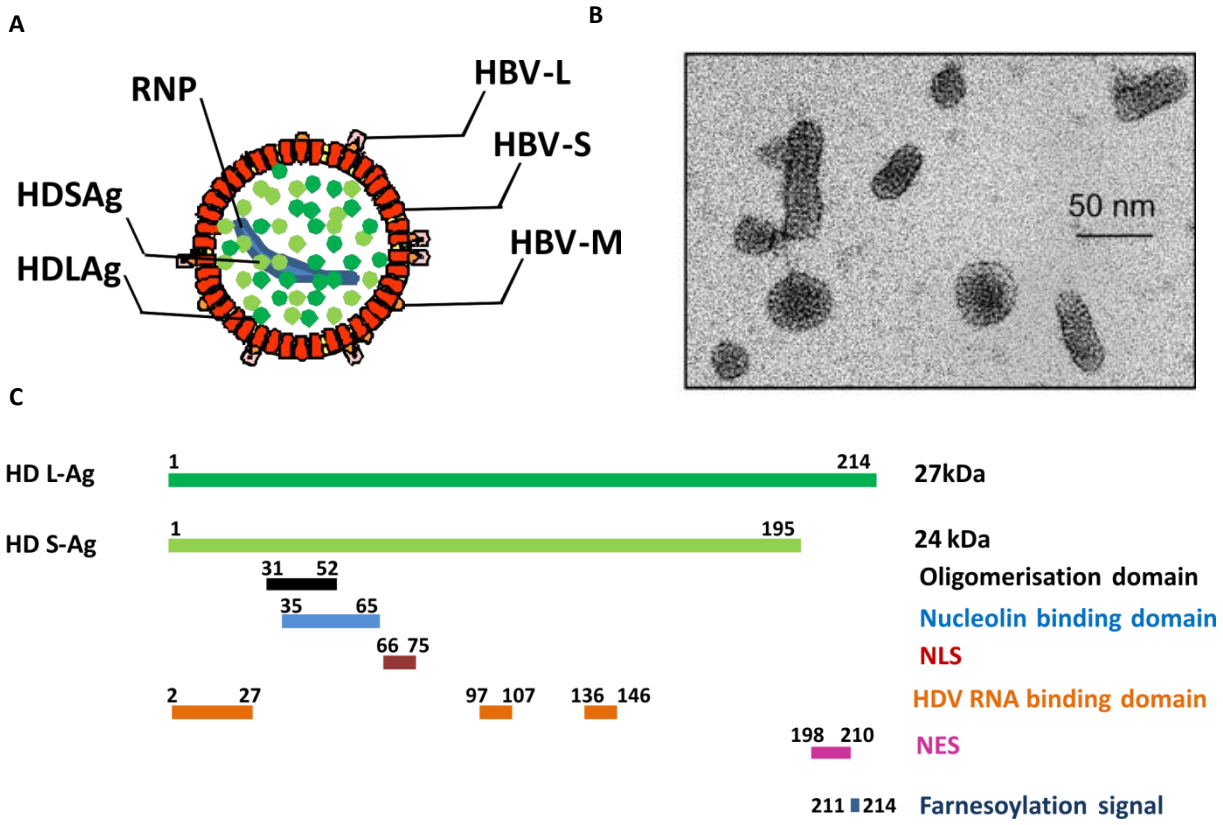

Fig.1.11: Schematic representation of the HDV particle, the Delta antigens and their functional domains.
A: The HDV particle. RNP: ribonucleoprotein. HDSAg: small hepatitis delta antigen. HDLAg: large hepatitis delta antigen. HBV-L/M/S: large, middle and small hepatitis B virus surface protein, respectively.
B: Electron micrograph of affinity purified HDV-particles. From: Gudima et al., 2007.
C: The large (HDLAg) and small (HDSAg) HDV proteins and their functional domains. NLS: nuclear localization signal. NES: nuclear export signal.

1.5.3 HDV entry

As for HBV, the entry process of HDV into hepatocytes is largely unknown. There are, however, many similarities between HDV and HBV entry, pointing towards a common mechanism. It has been shown that, as for HBV, the L-protein is crucial for HDV infectivity [97], especially the residues 1-75 [98], requiring the presence of the N-terminal myristoylation [99]. Strongly hinting towards a common entry receptor is the fact that HDV infection, as well, can be inhibited by acylated preS1-derived lipopeptides [100]. In contrast to HBV, HDV does not require the glycosylation of the surface proteins for efficient infection [101]. As for HBV, the antigenic loop (AGL) in the S-domain is also needed, since virions containing deletions in this domain have been shown to lose infectivity [102]; its function in viral entry has been reported to be independent from that of the preS1-domain [103].

1.5.4 The HDV genome and its replication

HDV particles contain a circular, negative single strand RNA [104] of 1672-1679 nt in length [105; 106]. It shows 74% internal base pairing and therefore folds as unbranched, double stranded rod like structure [104]. The nucleotides 680-780 form a ribozyme domain that allows autocleavage and ligation [107; 108; 104] and a putative promotor site for the HDAg RNA.

Replication of HDV (fig. 1.12) takes place without DNA intermediates and leads to the occurrence of three forms of RNA: in an infected cell, the genome, the antigenome, and the mRNA for the Delta-Antigen are present in a ratio of ~ 500:50:1 [104]. This is performed exclusively by the RNA-Polymerase II [109].

Following entry, the HDV genome is localized to the nucleus where RNA-Pol-II transcribes it into the 800 nt mRNA that encodes the HDSAg. The small antigen is required for replication of the genome by binding to RNA-Pol-II and inhibiting binding of the negative elongation factor (NELF). Replication itself occurs via the rolling circle mechanism. This leads to the formation of the multiple concatemers of the antigenome, which are autocatalytically cleaved by its ribozyme activity, ligated by cellular ligases and thus form a new template for synthesis of the genome [110; 111]. This is then either packaged into viral particles or serves again as template for antigenome synthesis.

Early in infection, formation of HDSAg is predominant, ensuring a highly active replication of the genome. The HDLAg is synthesized only later, when the enzyme adenosine deaminase

acting on RNA-1 (ADAR-1) edits the antigenome post-transcriptionally, leading to deamination of Adenosine 105 into Inosine [112]. Thereby, the stop-codon UAG becomes an UIG, now coding for tryptophane, allowing synthesis of the large antigen. HDLAg then acts as dominant negative inhibitor on the replication, a property which is enhanced by the N-teminal isoprenylation [113]. When no HBsAg is present in the cell, a nuclear localization signal (NLS, aa 66-75) localizes HDLAg and HDSAg to the nucleus; only in the presence of HBsAg do they relocalize to the cytoplasm, where the isoprenylated HDLAg mediates binding to the HBV surface proteins [114; 115].

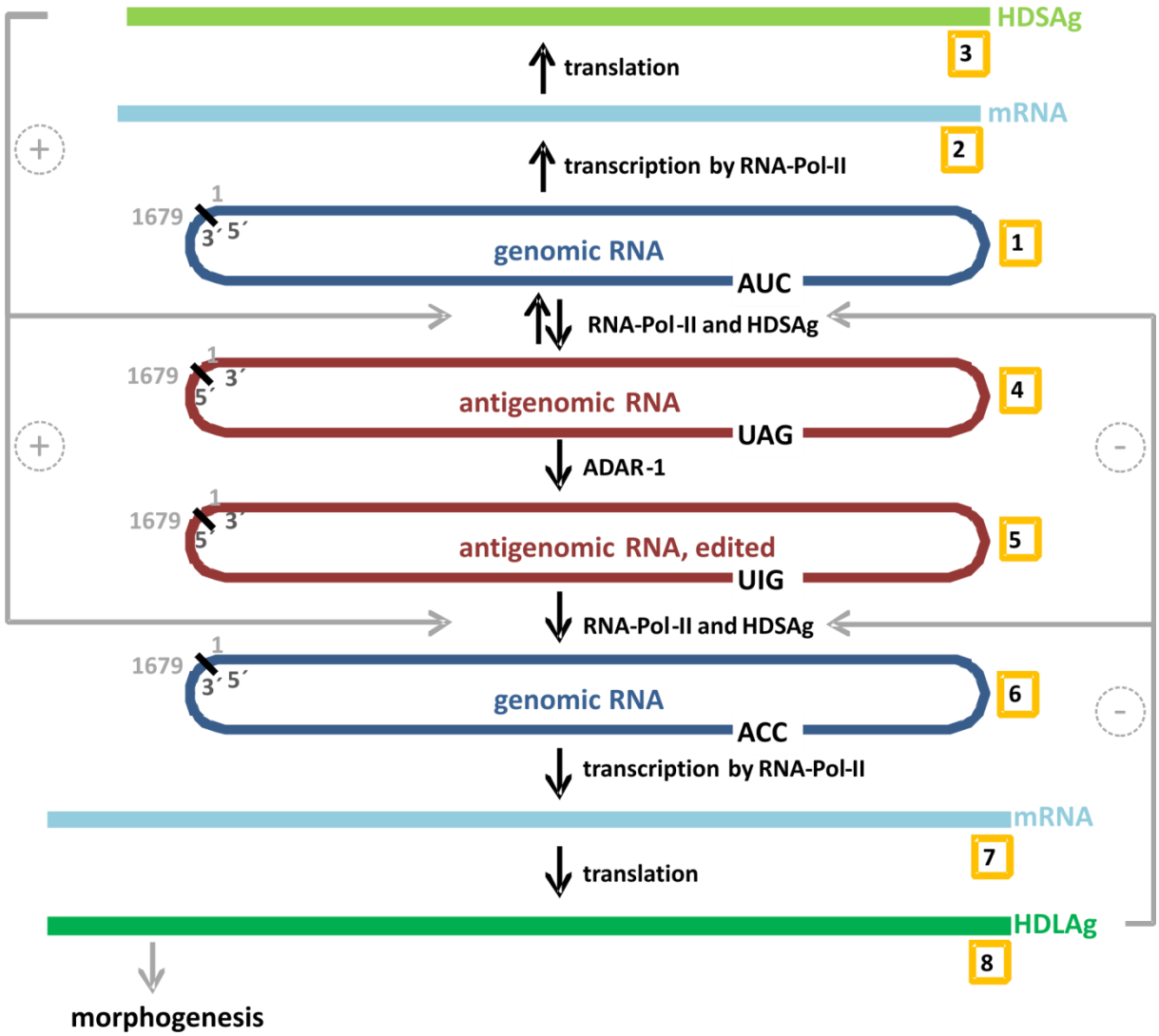

Fig. 1.12: The HDV replication cycle. Genomic RNA (1) is transcribed into mRNA for HDSAg (2), which is then translated into HDsAg (3). HDsAg then cooperates with RNA-Pol-II to form complementary antigenomic RNA (4) that serves as template for the formation of new genomic RNA. The action of ADAR-1 on this antigenomic RNA leads to the formation of edited antigenomic RNA (5). This is again translated into genomic RNA (6) which is transcribed by RNA-Pol-II into mRNA for HDLAg (7). From this mRNA, HDLAg is translated which represses replication of the genome and is therefore important for morphogenesis of HDV virions. Modified after [116].

1.6. Transport of fatty acid esters and fatty acids in the blood

1.6.1. Lipoproteins

The human body requires substantial amounts of lipids, especially phospholipids, for membrane synthesis, cholesterol for membrane modification and as raw material for certain hormones as well as fats as energy reservoir. These molecules are either synthesized by the liver or enter the body as dietary fat through the gut. Independent of their origin, redistribution of fats and fatty acids in the body is necessary in order to meet every organs´ needs. Since these molecules are very hydrophobic but are transported in the blood - a hydrophilic environment - special transport mechanisms are required. This task is fulfilled by lipoproteins which are large aggregates of triglycerides, phospholipids and cholesterol wrapped in a layer of specialized proteins, the so called apolipoproteins. Blood contains a variety of lipoproteins that are responsible for different transport ways and vary in their plasma levels according to the dietary status of a person. Since lipoproteins differ in their content of lipids and fats, they show characteristic differences in their density which led to their classification. An overview of lipoproteins in human plasma is given in table 1.5.

Table 1.5: Main lipoproteins in plasma and their characteristics. from [117]

Lipoprotein	Chylomicron	Very low density lipoprotein [118]	Low density lipoprotein [118]	High density lipoprotein (HDL)
apolipoproteins	apoA-IV, apoB-48, apoC-II, apoC-III, apoE	apoB-100. apoC-I, apoC-II, apoC-III, apoE	apoB-100	apoA-I, apoA-II, apoA-IV, apoC-I-III, apoD, apoE
transport way	intestine to liver	liver to periphery	periphery	periphery to liver
density (g/ml)	<1,0006	0,95-1,0006	1,0006-1,063	1,063-1,210
transported fats	triglycerides, cholesterol	triglycerides, phospholipids, cholesterol	phospholipids, cholesterol	cholesterol

Triacylglycerides are the main form of storage fat in the body, where they are stocked in adipocytes. When hormones signalize the need for these fats, they are mobilized from the adipose tissue, the fatty acid ester bonds are enzymatically dissolved and free fatty acids are released. Those enter into the bloodstream, where they bind to the abundant transporter molecule serum albumin and get transported to the site of need (heart, sceletal muscles, cortex of the kidneys).

1.6.2 Serum albumin as transporter molecule and its role in hepatic uptake of fatty acids

Serum albumin is the most abundant protein in plasma; this 62 kDa protein is found at a concentration of 42 mg/ml (640 µM) and thus constitutes around 50% of all serum proteins.
Its fatty acid binding was described first by Kendall in 1941 who observed that after cristallization, albumin still showed a yellowish colour. He ascribed this to the association of fatty acids [119]. It is known today that albumin binds 0,1-2 mol of fatty acids (up to 10 in certain disease states) per mol HSA in a non-covalent way [120; 121] and thus assures their transport in the blood. Albumin has a half life of ~20 days and is produced in the liver of a normal healthy adult at a rate of ~15 grams per day.
Human serum albumin (HSA) is a 585 amino acid protein that comprises three homologous domains (I-III) consisting of two subdomains (A and B) each, the whole protein being stabilized by a total of 17 disulfide bonds. Albumin has been shown to undergo structural changes upon alterations in pH, calcium concentration and fatty acid binding and is thought to be stabilized by binding to fatty acids. In 1975, Sudlow and colleagues reported two distinct binding sites on HSA that were identified by displacement studies on fluorescently labeled drugs [122]. These binding sites have since then been termed Sudlow site I and II; three subdomains for site I have been described more recently [123]. Site I is relatively large since large molecules such as bilirubin bind here and several reports of two different compounds binding to this site simultaneously have been made [124]. Due to its broad ligand spectrum, this site is thought to be relatively flexible in its structure.
Sudlow site II is probably smaller since it does not bind larger substances; it is not subdivided into more domains; binding is often strongly stereoselective, typical ligands are aromatic carboxylic acids [125].
Fatty acids are bound to HSA with a relatively high affinity, varying with their length; dissociation constants (K_D) of 460 nM for the interaction between human Serum Albumin (HSA) and myristic acid [120] and 14 nM for the HSA-stearic acid (C18) binding [126] have been reported. Binding of fatty acids leads to structural changes in the HSA molecule; binding to Sudlow Site I has been shown to lead to a rearrangement of the hydrogen bond network in this site, increasing the volume of this pocket and altering its polarity by opening up a solvent channel in this site [127]. A recent study on the binding of phospholipids has reported K_D values of, e.g., ~5 µM for binding of Lysophosphatidylethanolamine [128].Many endogenous

substances such as bilirubin, hemin or thyroxine bind to different sites on HSA; these are mainly acidic, lipophilic substances getting transported in the blood in this complex [129]. Svenson et al. performed a study on the binding of short cationic antimicrobial peptides using isothermal titration calorimetry and reported a K_D in the range of 4-22 µM [130].

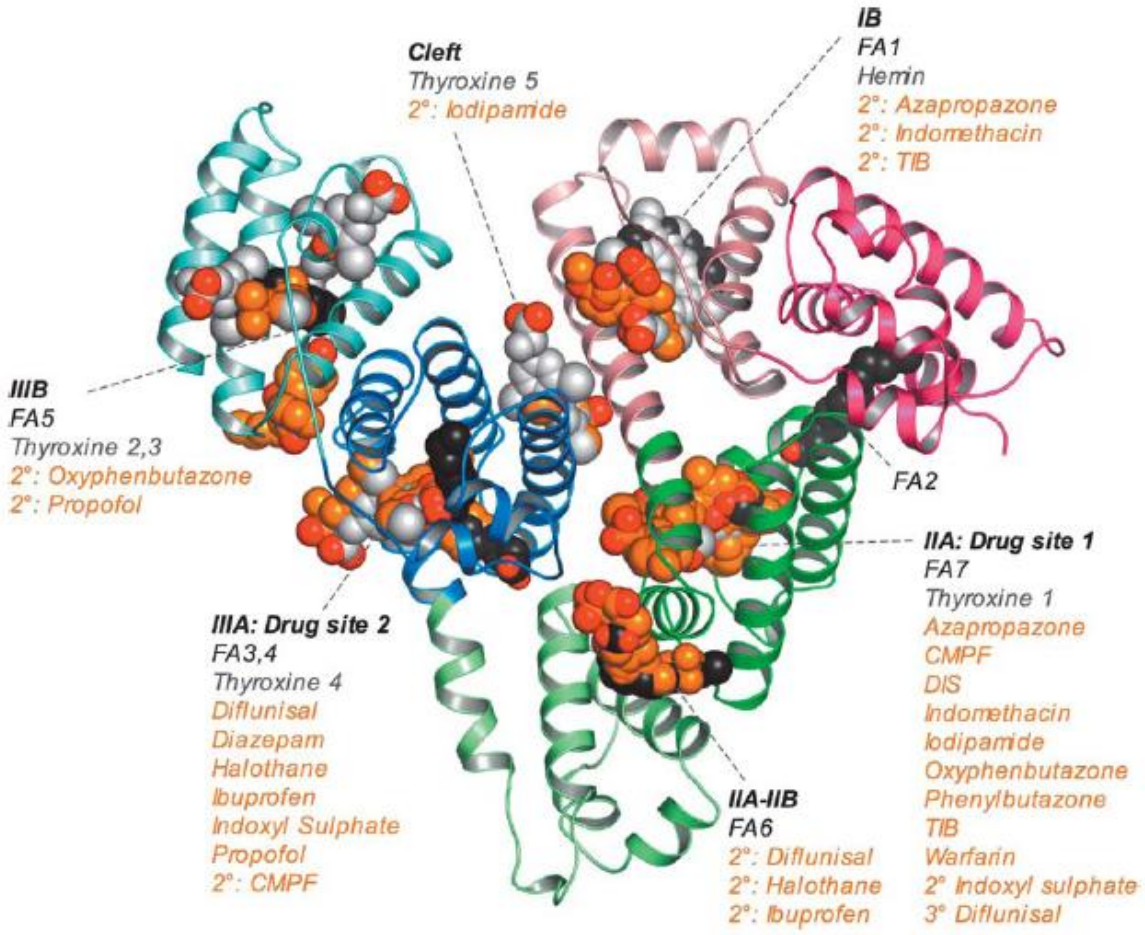

Fig. 1.13: Crystal structure of HSA and its ligand binding sites. Ligands are depicted in space filling representation; oxygen atoms are colored red; all other atoms in fatty acids or endogenous ligands are colored dark grey, light grey and orange, respectively. IB- IIIA: subdomains A and B of the homologous domains i-III. FA: fatty acid binding site. black: natural ligands. orange: drugs binding to the respective sites. from: [127].

1.6.3 Drug transport by HSA

Apart from natural ligands, albumin is an important interaction partner for different drugs, strongly affecting their adsorption, metabolism, elimination and solubility. This is mainly the case for acidic or electronegative compounds such as Diazepam or Ibuprofen, usually binding at subdomains IIA or IIIA (fig. 1.13) [131]. While this binding often helps solubilizing those molecules, drugs that bind with high affinity to HSA (>95% bound) usually show a slower distribution, require higher doses and may not be efficiently eliminated from the body.

Drugs bind mainly to Sudlow site I or Sudlow site II. In site I, they occupy partially overlapping binding compartments; for some cases, interactions between drugs and endogenous ligands, especially fatty acids, have been reported [132], competition or cooperation between both playing a role.

2. Material and Methods

2.1 Material

2.1.1 Cell culture

eucaryotic cell lines	
HepaRG	Human hepatoma cell line, isolated from a patient with HCC and chronic HCV infection (Gripon 2002)
HepAD 38	derived from a human hepatoma cell line (HepG2); stably transfected with a plasmid that contains HBV-cDNA under control of a tetracycline-regulated promotor

cell culture media	
HepaRG	**cultivating medium:** Williams Medium E, 10% FCS (heat inactivated), 50U/ml penicillin, 50µg/ml streptomycin, 50µM hydrocortisone-hemisuccinate, 5µg/ml insulin **differentiating medium:** as cultivating medium; addition of 2% DMSO
HepAD38	**cultivating medium:** DMEM/F-12, 10% FCS (not heat inactivated), 50U/ml penicillin, 50µg/ml streptomycin, 400µg/ml G418, 50µM Hydrocortisone-hemisuccinate, 5µg/ml Insulin, 0,3µg/ml Tetracyclin **Medium for virus-production:** as cultivating medium, without tetracyclin
primary hepatocytes	**isolation medium:** Williams Medium E without additives **cultivating medium** (until 4h after isolation): Williams Medium E, 10% FCS, 50U/ml penicillin, 50µg/ml streptomycin, 73µg/ml L-glutamin **cultivating medium** (4h after isolation): Williams Medium E, 50U/ml penicillin, 50µg/ml streptomycin, 73µg/ml L-glutamin

2.1.2 Equipment and consumables

Rotors		
SW-28-Rotor		Beckman
SW-60 Rotor		Beckman
TH 660-Rotor		Sorvall
TH 641-Rotor		Sorvall
TLA 120-Rotor		Beckman

Chromatography system

Component	**name**	**manufacturer**
Äkta Purifier 10		GE Healthcare, Sweden
pH/ conductivity sensor	pH/C 900	GE Healthcare, Sweden

UV-monitor	UV 900	GE Healthcare, Sweden
system pump	P 900	GE Healthcare, Sweden
sample pump	P 960	GE Healthcare, Sweden
fraction collector	Frac 950	GE Healthcare, Sweden
control unit	CU 950	GE Healthcare, Sweden
injection valve	INV 907	GE Healthcare, Sweden
position valve	PV 908	GE Healthcare, Sweden
Mixer	M925	GE Healthcare, Sweden
Unicorn 5.1 Software		GE Healthcare, Sweden

consumables

Product		**Manufacturer**
cannulae	22G, 0,55×25mm	B. Braun
cannulae	27G, 0,4×19mm	B. Braun
Cell culture bottle	75cm^2	Corning
Cell culture dish	100mm	Corning
Cell culture 12/24 well plate		Corning
Cell strainer	100nm	Beckton Dickinson
Centrifuge tubes, quickseal	8×35mm, polyallomer	Beckman
Centrifuge tubes	25×89mm, polyallomer	Beckman
Centrifuge tubes	14×95mm, polyclear	Seton
Chromatography paper, 3MM Chr		Whatman
Corning Polystyrol Cellstack		Corning
Cotton swabs	Sterile packed	Noba
Coverslips, ø 18mm		Marienfeld GmbH
Diaper inlay	Molinea	Hartmann
dissecting instruments		Aesculap /others
Filter 0,2 µm (for syringes)		Sartorius
Filter 0,45 µm (for syringes)		Roth
Filtrating membrane Nitrocellulose 0,45µm		Millipore
folded filter ø 185mm		Sartorius
Glass bottles	250ml, 500ml, 1000ml 2000ml	Schott
Glass graduated cylinder	50ml, 100ml, 250 ml, 1000ml, 2000ml	Brand
Glass micropipettes	2µl-100µl	Drummond scientific
Glass pipettes	5ml, 10ml, 20ml, 25ml	Hirschmann
Glass tubes for liposome preparation	12 ml volume	Schott Duran
Microwell 96 well plate	Luminunc, white	VWR
Nitrocellulose membrane, 0,45µm		Schleicher & Schuell

Nylon membrane, positively charged		Roche Applied Science
Parafilm		American Can Company
Pasteur pipettes, 230mm		WU Mainz
Petri dish, 100mm×15mm		Greiner Bio-One
Perfusion tubing	Silicone, ø 2mm	Amersham
Perfusion tubing	Silicone, ø 7,5mm	Masterflex
Pipet	2-20µl, 20-200µl, 200-1000µl	HTL lab solutions
Pipet tips, with filter		Starlab
Pipet tips, without filter		Starlab
Pipet boy	Accujet Pro	Brand
Quick seal centrifuge tubes		Beckman
Reaction tubes	0,5ml, 1,5ml, 2ml	Sarstedt
Reaction tubes	15ml, 50ml	Greiner Bio one
sample tubes for AxSYM	2ml	Sarsted
Scalpels		B. Braun
Serologic Pipets	5ml, 10ml, 25ml	Corning
Serum collection tubes	8ml serum monovette	Sarstedt
Syringes	1ml, 5ml, 10ml; luer-lock	B. Braun
Syringes	50ml, luer-lock	Becton-Dickinson
three-way stopcocks	luer-Lock, 10cm	Becton Dickinson
Vacuum-filter, Bottle-top, 0,45µm		Corning
Venous catheter	22G, 0,9mm×25mm	B. Braun
Venous catheter	24G, 0,5mm×19mm	Abbocath

Equipment	**type**	**manufacturer**
95°C-Oven		Heraeus
Autoclave	EL V 5050	Tuttnauer Systec
Cell counting chamber		ASSISTENT
Cell counter		Ivo
Centrifuge, small (0,5-2ml-tubes)	Biofuge Pico	Heraeus
Centrifuge, large (15/50ml-tubes)	Multifuge 3S-R	Heraeus
CO_2-Incubator		Heraeus
Dot-Blot-chamber	Minifold	Schleicher & Schuell
Fractionator		Beckman
Freezer -20°C	Premium NoFrost	Liebherr
Freezer -80°C	NapCOIL UF 600	Napco
Gel pouring chamber		Hoefer
Gel running chamber for SDS-PAGE	Mighty small basic unit	Amersham Pharmacia
Grids for electron microscopy	300-mesh	Plano GmbH
Heating block 95°C	Ori-Block OB-3	Techne

Ice machine	AF200	Scotsman
Laboratory scales	770	Kern
Li-Cor Scanner		Licor
Magnetic stirrer	Combimag RCO	Ika Labortechnik
Microscope	HC CTR MIC	Leica
Microwave oven	KOR-63D7	Daewoo
Perfusion pump, small	P1	GE Healthcare
Perfusion pump, large	Masterflex	Cole-Parmer
pH-Meter	632	Metrohm
Phosphoimager	FX	Biorad
Power supply for electro blotting (Western Blot)	PS-3030D	Monacor
Power supply for Gel electrophoresis		Pharmacia
Refrigerator 4°C	Premium	Liebherr
Rotating shaker	RM-2M	Neolab
Shaker for 1,5 ml reaction tubes		Eppendorf
Table top ultracentrifuge	Optima MAX	Beckman Coulter
Teetering shaker	DRS-12	Neolab
Transfer chamber for western blot	SD transfer cell	Biorad
Ultracentrifuge	Sorvall discovery 90 SE	Sorvall, Thermo scientific
Vacuum pump	BVC21	Vacuubrand
Vacuum membrane pump	CVC 3000	Vacuubrand
Vortexer		Cenco
Water purification system	TKA GenPure	TKA
Water bath	W6	B. Braun

2.1.3 Chemicals

Chemical		**manufacturer**
Acetic acid		Merck
Acrylamid/Bisacrylamid (29:1), 30% (w/v)		Serva Electrophoresis
Ammoniac		J.T. Baker
Ammonium peroxide sulphate	APS	Grüssing
Ampicillin		Sigma-Aldrich
Bovine Serum Albumin, Fraction V	BSA	Carl Roth
Brilliant Blue R		Chroma-Gesellschaft
Bromphenol blue		Chroma
Caesium chloride		Invitrogen/Gibco
Calcium chloride dihydrate		Merck

Cholesterol		Avanti Polar Lipids
^{32}P-dCTP		Amersham bioscience
Collagenase		Sigma-Aldrich
DAPI		Roche Applied Science
Dimethyl sulfoxide	DMSO	Merck
1,2-Dioleoyl-sn-Glycero-3-(Phospjo-L-Serine) (sodium salt)	DOPS	Avanti polar lipids
Di-sodium hydrogen phosphate-dihydrate		Grüssing
Dithiothreitol	DTT	Fermentas
D-MEM/F12		Invitrogen
n-Dodecyl-β-D Maltoside		neoLab
Easycoll	1,124g/ml	Biochrom
Embedding medium for microscopy	Vectashield	Vector laboratories
Ethanol absolute		Sigma-Aldrich
Ethanol denatured 1% Petroleum ether		central supply
Ethylenediaminetetraacetic acid (EDTA)		Carl Roth
Ethylene glycol-bis(2-aminoethylether)-N,N,N´,N´-tetraacetic acid (EGTA)		Sigma-Aldrich
Fetal Calf Serum	FCS	various sources
Formaldehyde solution 37% p.a.		J.T. Baker
G418	Geneticin	Invitrogen
Gelfiltration standard		BioRad
Glucose D+		Merck
Glutamine, L-		Invitrogen
Glycerine (99,5%)		Sigma-Aldrich
Glycine		Applichem
Guanidinium hydrochloride		Applichem
HEPES		Roth
Human Serum Albumin, 96-99%	HSA	Sigma-Aldrich
Hydrochloric acid 37%		J.T. Baker
Hydrocortisone hemisuccinate		Sigma-Aldrich
Hydrogen peroxide (30%)		Merck
Imidazol		Merck
Insulin		Sigma-Aldrich
Isopropyl alcohol		Applichem
Milk powder, fat-free		Roth
Magnesium chloride		Merck
Methanol		J.T. Baker

Octyl glucoside		Roth
Nycodenz		Axis Shield
Orange G		Sigma-Aldrich
1-Palmitoyl-2-Oleoyl-sn-Glycero-3-Phosphocholine	POPC	Avanti Polar Lipids
1-Palmitoyl-2-Oleoyl-sn-Glycero-3-Phosphoethanolamine	POPE	Avanti Polar Lipids
Paraformaldehyde	PFA	Sigma-Aldrich
PBS, 10× for cell culture		Invitrogen
Penicillin/ Streptomycin	5000U/ml / 5000µg/ml	Invitrogen
L-α-Phosphatidylinositol-4-Phosphate (Brain, Porcine Diammonium salt)	PIP	Avanti Polar Lipids
Polyethylene glycol 8000	PEG	Sigma-Aldrich
Polysorbate 20	Tween-20	Roth
Polysorbate 80	Tween-80	Roth
Potassium chloride		Merck
Potassium dihydrogen phosphate		Applichem
Potassium hydrogen phosphate		Merck
Protease inhibitor-cocktail, EDTA-free	PFA	Roche applied science
Rat Serum Albumin	RSA	Sigma-Aldrich
Saccharose, D(+)		Carl Roth
Silver nitrate		Grüssing
Sodium acetate		J.T. Baker
Sodium azide		Riedel-de-Haën
Sodium carbonate		Applichem
Sodium chloride		Applichem
Sodium dihydrogen phosphate-monohydrate		Merck
Sodium dodecylsulfate	SDS	Serva
Sodium hydrogen carbonate		J.T. Baker
Sodium hydroxide		Applichem
Sodium thiosulfate		Grüssing
Trichloroacetic acid	TCA	J.T. Baker
Tetramethylethylendiamin	TEMED	Roth
Tetracycline		Sigma-Aldrich
Tricine		Sigma-Aldrich
Urea		Grüssing
Tris(hydroxymethyl)-aminomethan	Tris	Roth
Triton x-100		Sigma-Aldrich

Trypan Blue solution, 0,4%		Sigma-Aldrich
Trypsin (cell culture)	0,05% in PBS	PAA
Uranyl acetate		
Water (ad iniectabilia)		Braun
Williams Medium E		Invitrogen

2.1.4 Protein Markers for SDS-PAGE

Marker	size range	manufacturer
Novex sharp Pre-stained protein standard	3,5 – 260 kDa	Invitrogen
PageRuler unstained Protein Ladder	10 - 200 kDa	Fermentas

2.1.5 Antibodies

2.1.5.1 Primary antibodies

Antibody	Specificity	Dilution	Source/Manufacturer
Ma18/7 (Mouse)	Monoclonal antibody reacting against 20-DPAF-24 in the HBV preS1	1:20 (WB)	Heerman et al., 1984
H 863 (rabbit)	Polyclonal antibody reacting against HBV preS1/preS2	1:10.000 (WB)	S. Urban
H363 (rabbit)	Polyclonal antibody against HBV core	1:1.000 (IF)	H. Schaller
33633	Human serum, contains anti HDV-antibodies	1:1.000 (IF)	
HYB 069-01 (mouse)	Monoclonal antibody against human Apolipoprotein A1	1:1.000 (WB)	Dianova
GTA-7	Human serum, contains anti HDV-antibodies	1:1.000 (IF)	Raffaela Romeo, Italy
DOAE	Human serum, contains anti HDV-antibodies	1:1.000 (IF)	Raffaela Romeo, Italy
BTFZ	Human serum, contains anti HDV-antibodies	1:1.000 (IF)	

2.1.5.2 Secondary antibodies

Antibody	Dilution	manufacturer
Goat anti mouse, Alexa Fluor 488 coupled	1:1.000 (IF)	Invitrogen
Goat anti rabbit, Alexa Fluor 546 coupled	1:1.000 (IF)	Invitrogen
Goat anti Human, Alexa Fluor 555 coupled	1:1.000 (IF)	Invitrogen

Goat anti mouse, Alexa Fluor 680 coupled	1:20.000 (WB)	Molecular Probes
Goat anti rabbit, IR dye 800 coupled	1:20.000 (WB)	Invitrogen

2.2 Methods

2.2.1 Cell culture

All cell culture work was performed under sterile conditions on a laminar flow hood.

2.2.1.1 HepAD38 cells

For production of infectious HBV particles, HepAD38 cells were grown in 1- or 2-stacks and cultivated for two weeks in HepAD38 culture medium with tetracycline (100ml/ stack) at 37°C. The subsequent removal of tetracycline (tet off) led to the expression of the HBV genome and therefore to the secretion of capsids, Dane-particles and subviral particles. The supernatant (SN) from the first two weeks tef off was discarded, since during this time period, the cells produce mainly naked capsids and very little Dane-particles. Starting day 14 after tet off, SN was collected every four days, centrifuged at 10.000 rpm for 30 min and filtered sterile through a 45µm filter.

2.2.1.2 HepaRG

HepaRG cells were grown at a density of $1{,}25\times10^6$ cells / 12-well plate and cultured for two weeks in culture medium at 37°C, 5% CO_2. Afterwards, Medium exchange with differentiation medium was performed on day 1, 2, 5, 8 and 11. After a two week differentiation process, cells in the differentiated islands were susceptible for HBV.

2.2.1.3 Isolation and cultivation of primary hepatocytes

Here follows the general description of the method; since the employed materials and amounts of buffer vary with the species, these are given in a separate Table.

Mice were sacrificed by cervical dislocation, rats, hamsters and guinea pigs by a CO_2-overdose and rabbits by intravenous injection of Narcoren®. At death, the animal was fixed in supine, the abdomen was opened, the liver and surrounding blood vessels were exposed. A venous catheter was placed into the *Vena cava inferior* and the *Vena portae* was incised. The liver was flushed for at least five minutes with 42°C warmed EGTA-solution and subsequently perfused with 42° warm collagenase solution, until a swelling of the liver and detaching of the liver capsule indicated sufficient digestion. The organ was then removed from the abdominal cavity and transferred to the remaining collagenase solution. All further steps were performed in a laminar flow under sterile conditions.

In a 10cm cell culture dish, the liver capsule was carefully removed using forceps, the outflowing hepatocytes filtered through a 100µm cell strainer in order to remove remaining connective tissue and singularize cells. After centrifugation (28×g, 5min, 4°C), the cell pellet was resuspended in a percoll-solution with a density of 1,063g/ml, separation of vital hepatocytes from those undergoing cell death and non-parenchymal cells was achieved by centrifugation at 50×g, 10min, 4°C without break. After another washing step (spin at 28×g, 5min, 4°C), the cells were resuspended in isolation medium and assessed by the trypan blue method for viability and cell number.

For infection experiments, cells were diluted in PHep-I medium and seeded onto collagen coated 12 well dishes with a density of $8{,}8\times10^4$ cells /cm^2. 4h after plating, the medium was changed o PHep-II Medium, 24 h after plating to PHep-infection medium.

EGTA Perfusion buffer	2 mM L-Glutamine, 0.5 % Glucose, 25 mM HEPES, 2 mM EGTA, pH7.4
Collagenase buffer	2 mM L-Glutamine, 0.5 % Glucose, 25 mM HEPES, 3 mM $CaCl_2$, 3 mg/ ml Collagenase type IV, prepared in Williams E Medium

	Mouse *Mus musculus*	**Rat** *Rattus rattus*	**Hamster** *Mesocricetus auratus*	**Guinea pig** *Cavia porcellus*	**Rabbit** *Oryctolagus cuniculus*
Weight	Ca. 30g	Ca. 150g	ca. 80g	ca. 200g	Ca. 600g
Catheter	24G	20G	22G	20G	18G
EGTA-buffer	50ml	150ml	100ml	150ml	250ml
Collagenase-buffer	50ml	150ml	100ml	150ml	250ml
Ø Perfusion tubing	1,5mm	7,5mm	7,5mm	7,5mm	7,5mm
Flow rate	5ml/min	20ml/min	15ml/min	20ml/min	30ml/min

2.2.1.4 Primary Human Hepatocytes (PHH)

PHH were obtained from Thomas Weiss, University Clinics Regensburg. The cells were isolated and cultivated in serum free medium. Liver samples used for this procedure were obtained by hepatectomy on patients with metastatic liver tumors or colorectal tumors. All procedures were performed according to the guide lines of the Human Tissue and Cell Research (HTCR) foundation and with agreement of the patient.

The PHH were shipped on ice, resuspended upon arrival in cold PHH-I medium and assessed by the trypan blue method for viability and cell number. Cells were then seeded in 12-well plates at a density of of 4×10^6 cells /plate.

2.2.1.5 PEG-precipitation of virus from HepAd38 supernatant

18ml of a 40% PEG-solution were added per 100ml cell culture SN. The solution was shaken overnight at 4°C and centrifuged (JA-10 Rotor, 60min, 17.600×g, 4°C). The pellet was resuspended in 1% of the starting volume and again shaken over night at 4°C. After a short centrifugation, the SN was brought to 5% of the starting volume with PBS/10% FCS, aliquoted and stored at -80°C.

2.2.1.6 HBV infection of HepaRG and primary hepatocytes

All infection experiments were performed with an inoculum of 1×10^4 GE/ cell in HepaRG differentiation medium. For inhibition experiments, the cells were incubated for 30 min with 200nM or 500nM HBV preS/2-48^{myristoyl} before addition of the virus; the peptide was also present during virus inoculation. The cells were infected with PEG-precipitated stock virus in the presence of 4% PEG for ~16h at 37°C, 5% CO_2. The virus was then washed off thouroughly with 1×PBS, fresh medium was added. Supernatants of day 7-12 were harvested: As marker for infection, secreted HBsAg was measured in a commercial AXSYM-ELISA. Cells were fixed with 4% PFA and processed for IF.

2.2.1.7 HDV /WHDV infection of HepaRG and primary hepatocytes

HDV infections were done with sera from chronically HDV-infected patients obtained from xxx, Italy. These sera were not quantified for content of viral RNA; therefore, the exact inoculum was unknown. Cells were either infected with 10µl/well GTA-7 serum, 25µl/well BTFZ-serum or 15µl/well GTA-4 serum.

WHDV infections were done with serum from woodchucks; sera were obtained from M. Roggendorf, Hannover. These animals, carrying a chronic WHV-infection, were superinfected with HDV, resulting in formation of WHV-enveloped HDV particles. 20µl/well were used.

differentiated HepaRG Cells or freshly isolated primary hepatocytes (day one after isolation) were infected with HDV or WHDV sera for 16h at 37°C, 5% CO_2. The virus was then washed off thouroughly with 1×PBS, fresh medium was added. On day 5 p.i., cells were fixed with 4% PFA and processed for IF.

2.2.1.8 Binding assay with radiolabeled preS-peptide on PMH

PMH were isolated as described, plated onto collagen-coated 24-well plates and kept in serum-free medium. On day 1 after isolation, cells were incubated with 165 nM/well of HBV preS/2-48^{myristoyl}-Y^{125} for 1h at 37°C, 5% CO_2 (incubation volume: 300µl/well). Incubation was performed in the absence or presence of either 25µM HSA, 1,8µM HDL or both. Following incubation, SN were taken off, cells washed three times with 300µl/well 1×PBS and lysed with 300µl/well 1N NaOH. Counts per minute (cpm) in all fractions were quantified in a γ-counter.

2.2.2 Analysis of infections

2.2.2.1 Immunofluorescence of HBV/ HDV infected cells

On day five p.i. (HDV) or day 12 p.i. (HBV), cells were fixed for 30 min at 4°C with 4% Paraformaldehyde (PFA) and washed with PBS. After permeabilization with PBS/0,25% Triton X-100 for 30min at RT, cells were again washed and incubated overnight with a primary antibody diluted in PBS/ 5% skimmed milk powder. After another washing step, incubation with the secondary antibody, diluted in PBS/ 5% skimmed milk powder was performed for 1h at RT. The cells were again washed; cells that were not grown on coverslips were then stained with 4',6-Diamidin-2-phenylindol (DAPI, dissolved to 1µg/ml in methanol) and washed again; if cells had been plated on cover slips, those were mounted on glass slides with Vectashield® mounting medium. Microscopy was performed on a xxx microscope in a 100× to 400× magnification.

2.2.3 Biochemical methods

2.2.3.1 Peptide synthesis

All peptides were synthesized by Alexa Schieck or Thomas Müller (AG Mier, Department for nuclear Medicine, University clinics Heidelberg) using solid phase synthesis by the Fmoc/tBu method on an Appied Biosystems 433A synthesizer. Fluorescein Isothiocyanat (FITC) was coupled onto the ε-amine group of an additional Lysine on position 49. All peptides were subsequently purified by preparative High Performance Liquid Chromatography (HPLC) on a C18-column, applying a linear gradient from 100% water to 100% Acetonitril in 0,1% Trifluoric Acid (TFA). Analysis of the products was done by chromatography on a Merck

Chromolith® Performance RP18e-column (100 - 4,6mm; 4ml/min), final purification on a Chromolith® SemiPrep RP-18e column (100 - 10 mm; 10 ml/ min). Identity of all peptides was confirmed by mass spectrometry.

2.2.3.2 Serum preparation

Human Blood was taken from healthy donors by medical personnel and collected into serum centrifugation tubes. The blood was let to clot for 10min at RT. For rat serum preparation, rats were sacrificed by CO_2-overdose, fixed in supine and the abdomen was opened. A syringe with a 20G-canula was inserted into the *vena cava inferior* and blood was drawn. This was then let to clot o/n. Dog serum and cynomolgus serum was obtained from animals used for biodistribution studies of HBV preS-peptides. Blood was taken from animals by veterinary personel and let to clot. After clotting, samples were centrifuged for 10 min at 1000rpm. Supernatant serum was taken off, aliquoted and stored at-20°C.

2.2.3.3 Purification of high density Lipoproteins from human serum

SEC on Superdex 75

Serum was isolated as described before. 4ml of sterile filtered serum were applied onto a HiLoad 26/60 Superdex 75 column (prep-grade). 1×PBS was used as running buffer, runs were performed at 2,5ml/min. Fractions of 5ml were collected and analyzed for HDL-content by ApoA1-specific WB.

Ultracentrifugation

4ml of each peak fraction from the SEC were pooled (usually fraction A4-A7) and adjusted to 1,121g/cm^3 by addition of 960mg solid sodium bromide. The solution was then subjected to ultracentrifugation in a SW60-rotor for 24 h at 345.000×g, 10°C. After centrifugation, the solution was ractionated into 8 fractions, 0,5ml each and analyze for HDL-content using an ApoA1-specific antibody.

SEC on Superose 6

The HDL-containing peak fractions from ultracentrifugation were pooled and concentrated too 300µl by centrifugation in a centrifugal filter unit (cut off: 30kDa) for 15 min at 3000×g. The concentrate was applied onto a HR 10/300 Superose 6 column. 1×PBS was used as running buffer, runs were performed at 0,4ml/min. Fractions of 0,5ml were collected and analyzed for HDL-content by ApoA1-specific WB. Peak fractions were again pooled and

concentrated; all fractions were analyze for total protein content by coomassie-stained SDS-PAGE.

2.2.3.4 Size exclusion chromatography (SEC) of peptide-albumin /-serum complexes

Fluorescein Isothiocyanate (FITC)-labeled peptides were dissolved to a final concentration of 100µM (Chromatography on a HR 10/300 Superose 6 column) or 200µM (Chromatography on Smart-S6 column) in 1×TN buffer (20mM Tris, 140mM NaCl, pH7,4). Serum albumin was dissolved to a final concentration of 40mg/ml (HR 10/300 Superose 6 column) or 13,2mg/ml (Smart-S6 column) in 1×TN-Puffer. The peptides were preincubated in given amounts with 150µM (10/300 Superose 6 column) or 30µM (Smart S6 column) or 75µl human serum for 1h at 37°C and applied to the respective column. On the smart S6 column, 50µl were applied, runs were performed at 0,04ml/min with 1×TN as running buffer; on the 10/300 superose 6 column, 300µl were applied, runs were performed at 0,4ml/min. UV-absorption of all elution fractions was measured at 280nm (all proteins) and 490 nm (FITC-specific absorption).

2.2.3.5 Fishing of binding partners for HBVpreS/2-48^{myristoyl} in Serum

HBVpreS/2-48^{myristoyl} -CL was incubated at a final concentration of xxxµM with 1ml of human serum from a healthy, vaccinated donor in a final volume of 10ml for 1h at 4°C in the dark. The solution was then exposed to UV-light for 10min on ice, filled up to 30ml with HisTrap binding buffer and applied onto a 1ml Nickel agarose column at 0,5ml/min. Unspecifically bound proteins were washed off with 5column volumes (CV) of wash buffer (0,5ml/min), elution of bound molecules was performed with a linear gradient from 20mM to 500mM imidazole over 10CV (0,5ml/min). UV absorption of all elution fractions was measured at 280nm.

2.2.3.6 Fishing of binding partners for HBVpreS/2-48^{myristoyl} on primary hepatocytes

Primary Rat Hepatocytes (PRH) were isolated by the method described in xxx and resuspended in 1×PBS. 2×10^{8} cells were then incubated in a volume of 30ml with a final concentration of 1µM HBVpreS/2-48^{myristoyl} CL-peptide at 4°C for 1h in the dark. Following exposure of the suspension to UV-light for 10min on ice, cells were pelleted (28×g, 5min, 4°C), washed twice with 0,5%BSA/PBS, twice with PBS and lysed with HisTrap binding buffer,

6M Urea (rotation for 1h, 4°C; addition of 1protease-inhibitor cocktail (Roche) pellet, EDTA-free). For complete lysis, the solution was treated with ultrasound (3min, 50%). Aggregates were removed by a short ultracentrifugation (53.000×g, 20min, 4°C), the supernatant sterile filtered and applied onto a 1ml nickel sepharose column at 0,5ml/min. Unspecifically bound proteins were washed off with 5column volumes (CV) of wash buffer (0,5ml/min), elution of bound molecules was performed with a linear gradient from 20mM to 500mM imidazole over 10CV (0,5ml/min). UV absorption of all elution fractions was measured at 280nm.

HisTrap binding buffer	**20mM Sodium Phosphate, NaCl, 6M Urea, 20mM Imidazole, pH8,3**
HisTrap wash buffer	20mM Sodium Phosphate, NaCl, 6M Urea, 20mM Imidazole, pH6,3
HisTrap elution buffer	20mM Sodium Phosphate, NaCl, 6M Urea, 500mM Imidazole, pH6,3

2.2.3.7 Mass spectrometry

Mass spectrometry (matrix-assisted laser desorption/ ionisation / time of flight, MALDI-TOF) was performed by the group of Dr. Thomas Ruppert on a Ultraflex TOF/TOF (Bruker).

2.2.4 Assay for membrane activity analysis

2.2.4.1 Liposome production

For leakage assays, liposomes were prepared with a 15mM lipid mastermix solution containing either 85mol% POPC and 15mol%DOPC (inert lipid mixture) or 35 mol% POPC, 25 mol% DOPS, 25 mol% POPE, 5 mol% PI and 10 mol% Cholesterol (physiological mixture).
The lipids were dissolved in Chloroform ad transferred to glass tubes; 100µl of mastermix were used for each final gradient. The chloroform was left to evaporate for 15 min under a nitrogen gas flow; the lipids were then dried thoroughly by applying vacuum for 1h at RT (high vaccum applied by membrane pump, 3bar). Per final gradient, 500µl Buffer A (100mM KCl, 25mM HEPES, 10% glycerol, pH7,4) containing 1% octyl glucoside (OG)were then added to solve the dried lipids and shaken for 1h at RT. For reconstitution of the liposomes, a double volume of buffer A (containing 12,5mM HPTS, 45mM DPX if desired) without OG was then added drop by drop while vortexing the solution. Thereby, the OG concentration fell below the critical micellar concentration(CMC), leading to the formation of liposomes. Removal of the detergent and surplus dye was reached by dialysis of the solution against 5l of buffer A overnight at 4°C. The liposomes were then concentrated by a Nycodenz gradient.

Therefore, the dialyzed solution was mixed with an equal volume of 80% Nycodenz in buffer A, layered with 1/4 volume of 30% Nycodenz in buffer A and 200µl of buffer A. Centrifugation at 55krpm for 3h40, 4°C led to the flotation of liposomes and their efficient separation from remaining free dye.

The floated liposomes were taken off, aliquoted and stored until further usage at -80°C.

2.2.4.2 membrane activity assay of HBV preS derived lipopeptides on liposomes

in a 96well plate, 1µl of HPTS/DPX containing liposomes (corresponds to 80µM in final volume) and 3,5 or 7µl (corresponding to 75-150µM in final volume) preS-peptides were incubated at 37°C in a final volume of 70µl. The preS peptides were dissolved in 50% DMSO /buffer A; if 3,5µl peptide were used, 3,5µl 50%DMSO/buffer A were added to the reaction. During this time, absorption and emission of the HPTS-dye was measured at 460nm and 520nm, respectively, in a Fluoroscan Ascent FL fluorescence plate reader. At the end of the incubation time, 10µl of a 2,5% (w/v) octyl maltoside solution were added; this led to complete lysis of all liposomes and total dequenching of the HPTS dye. The fluorescence signal obtained by the lysis was set as 100%; values obtained during the incubation were expressed as percentage of total lysis employing the following formula:

Fluorescence (%) = ((Ft - Fmin)/(Fmax - Fmin)) * 100

Ft: measured fluorescence at time point t

Fmin: minimal measured fluorescence (corresponding to no membrane activity)

Fmax maximal measured fluorescence (corresponding to total lysis by octyl maltoside).

2.2.4.3 flotation assay with HBV preS-derived lipopeptides on liposomes

50µM preS-peptides dissolved in 50% DMSO/buffer A were preincubated with 640µM lipid in a final volume of 150µl for 30min at 37°C. an equal volume of 80% Nycodenz was added, layered with 700µl of 30% Nycodenz and ~100µl of buffer A in quick seal tubes. Flotation was performed by centrifugation in a TLA120 Rotor for 45min at 4°C, 386 000×g. The gradient was then fractionated from the bottom into 8 fractions, ~100µl per fraction; 15µl of each fraction and 1,5µl input were analyzed by western blot with a preS1-specific antibody.

2.2.4.4 Electron microscopy of liposomes and peptides

peptides were dissolved to 1mM in buffer A (100mM KCl, 25mM HEPES, 10% glycerol, pH7,4). Liposomes containing no dye were used. Increasing amounts of peptide solution were added to 1µl liposome solution, buffer A was added to a final concentration of 15µl; this solution was incubated for 1h at 37°C.

10µl of this preincubated mixture were then pipetted onto a parafilm layer, a pioloform-coated electron microscopy grid (300 mesh, no carbon coating, no glow discharge) was laid on the drop for 10 min so that liposomes could adsorb. surplus solution was removed by short contact with filter paper. Negative staining was performed in two steps; first, a short (5sec) incubation with a first drop of 1% uranyl acetate (UA), second, a longer incubation with a second drop UA (30sec). The grids were then carefully dried on filter paper and stored at RT until microscopy was performed.

2.2.5 Analysis methods

2.2.5.1 SDS-PAGE

Samples to be analyzed were dissolved in 2×SDS sample buffer (200mM Tris/HCl pH6,8, 6%SDS, 20% Glycerol, 10%DTT, 0,1mg/ml bromphenol blue, 0,1mg/ml Orange G) and heated for at least 10min at 95°C. Separation was performed on acrylamid-gels after the method of Lämmli (XXX) or Schägger (XXX).

Composition of gels for electrophoresis by the method of Lämmli

	Stacking gel	**Separating gel**
H_2O_{dd} (ml)	11	17,5
4×Stacking gel buffer (ml)	5	-
4× Separating gel buffer (ml)	-	12,5
BAA (ml)	4	20
Temed (µl)	10	25
APS	Spatula tip	Spatula tip
Final volume (ml)	20	50

Composition of buffers for electrophoresis by the method of Lämmli

4×Stacking gel buffer	**4×Separation gel buffer**	**1× SDS running buffer**
0,5 M Tris/Cl pH 8,8 0,4 % SDS 0,01 % NaN_3	1,5 M Tris/Cl pH 8,8 0,4 % SDS 0,01 % NaN_3	0,025 M Tris 0,086M glycine 0,0035M SDS

Composition of gels for electrophoresis by the method of Schägger

	Stacking gel	**12% sep. gel**	**16% sep. gel**	**20% sep. gel**
H_2O_{dd} (ml)	10,6	10,9	5,6	0,3
3×Schägger gel buffer(ml)	6,7	13,3	13,3	13,3
BAA (ml)	2,7	15,8	21,1	26,4
Temed (µl)	20	40	40	40
APS	Spatula tip	Spatula tip	Spatula tip	Spatula tip
Final volume (ml)	20	40	40	40

Composition of buffers for electrophoresis by the method of Schägger

3× Schägger gel buffer	**Cathode buffer**	**Anode buffer**
3 M Tris pH 8,45 0,3 % SDS	0,1 M Tris 0,1 M Tricin 0,1 % SDS	0,2 M Tris pH 8,9

2.2.5.2 Transfer of proteins separated by SDS-PAGE onto a nitrocellulose membrane (Western blot) and immunodetection

The electric transfer of proteins onto a nitrocellulose membrane was done using the semi-dry method. On top of two filter papers soaked in Schäffer-Nielsen transfer buffer was laid the presoaked membrane. The protein gel was also soaked in buffer and laid onto the membrane, followed by another two layers of soaked filter paper. Applying a voltage of 15V for 30min transferred proteins from the gel onto the membrane.

free binding sites on the membrane were blocked by incubation with TBST-M (1×TBS, 0,05% Tween-20, 5% skimmed milk powder) for at least 1h at RT. The membrane was washed three times for 5min with TBS-T (1×TBS, 0,05% Tween-20) and incubated with the first antibody diluted in TBST-M) (2h at RT or overnight at 4°C). The membrane was again washed (three times, 5min, TBS-T) and incubated for 1h with the secondary antibody (diluted in TBS-T for detection with ECl, diluted in TBS for detection with Licor). for fluorescence-based detection, the blot was then washed four times with TBS and scanned on a Licor®-reader. In case of a peroxidase-coupled secondary antibody, the membrane was washed four times with TBS-T, swung in ECL-reagent (5ml of ECL-I and 5ml of ECL-II) for 2min and exposed to a photosensitive film, which was then developed in a developing machine.

Solutions for western blot

Schäffer-Nielsen-Transfer buffer	**1×TBS**	**1×TBS-T**	**ECL-I**	**ECL-II**
0,05M Tris 0,02M Glycine 0,04% SDS 10% Methanol pH 9-9,4	0,14M NaCl 0,02M Tris pH8	1×TBS with 0,05% Tween-20	100mM Tris-Cl pH 9,35 4,5mM Amino-phthalhydrazid 8,5 mM coumaric acid	100mM Tris-Cl pH 9,35 0,004% H_2O_2

2.2.5.3 Silver staining of SDS-PAGE gels

For visualization of proteins after electrophoresis, gels were stained with silver nitrate. First, the gel was fixed over night or for 1h in Fix-1, then for 30 min in Fix 2 and two times 15min in Fix 3. Following impregnation with Solution A, the gel was washed 3 times with H_2O_{dd} (1min each) and stained with solution B for12min in the dark. After two more washing steps with H_2O_{dd} , developing solution was added, left on the gel until a sufficient stain was reached and discarded. The reaction was stopped by addition of a 3% acetic acid solution for 1min, the gel was then kept in H_2O_{dd}.

Solutions for silver stain

Fix 1	**Fix 2**	**Fix 3**	**Solution A**	**Solution B**	**Solution C**
50% methanol, 12% acetic acid	10% ethanol, 5% acetic acid	10% ethanol	0,02% Sodium thiosulfate, 0,02% formaldehyde in H_2O_{dd}	0,02% Sodium thiosulfate, 0,02% formaldehyde, 0,2% silver nitrate in H_2O_{dd}	0,0003% Sodium thiosulfate, 0,02% formaldehyde, 3% sodium carbonate in H_2O_{dd}

3. Results

In this work, several sets of peptides derived from the HBV preS1-domain have been used. A schematic representation of the respective peptides is given in fig. 3.1. All peptides are modifications of the preS/2-48^{myristoyl}-peptide **(fig. 3.1.A)** corresponding to the preS1 N-terminus of HBV genotype D.

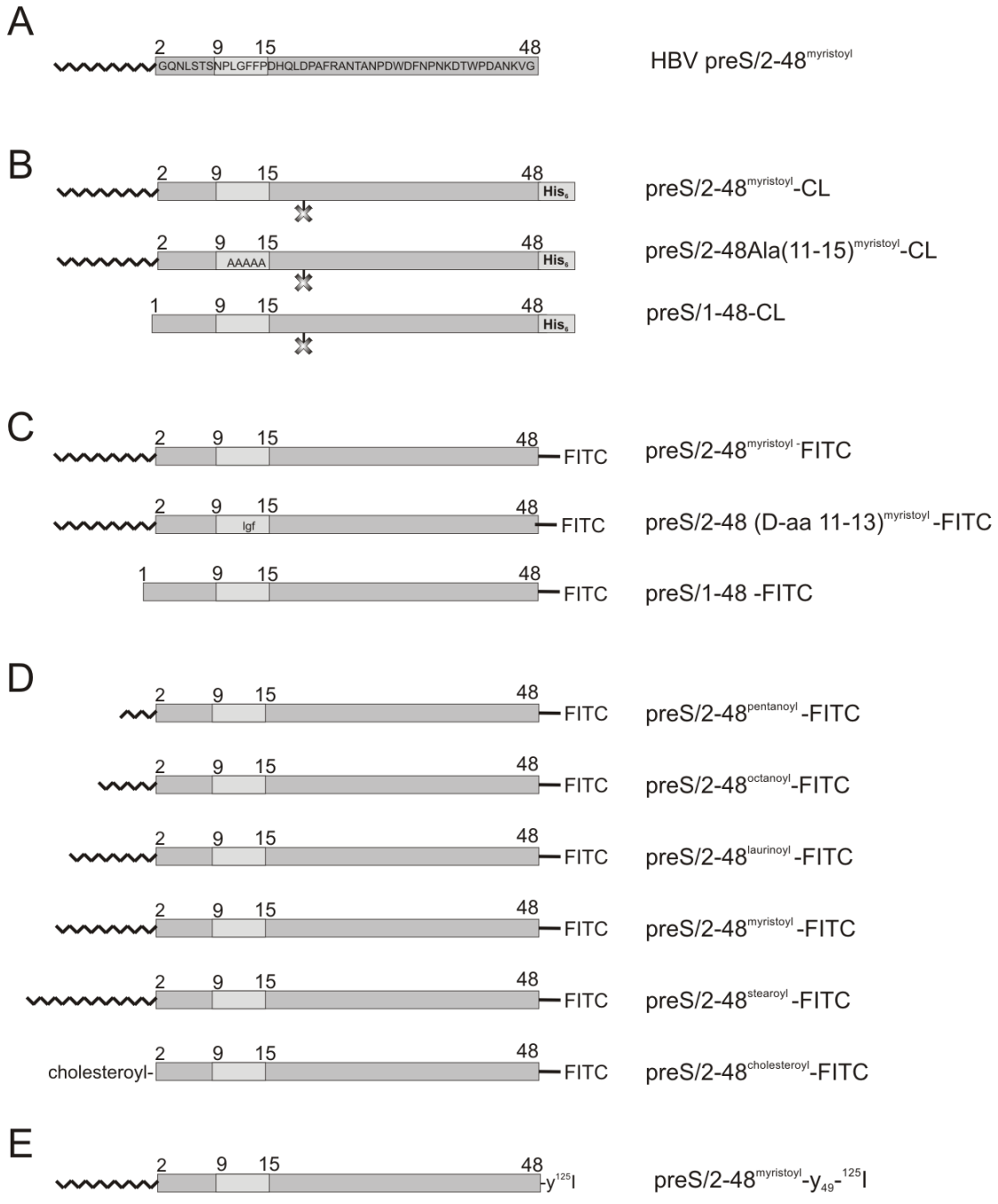

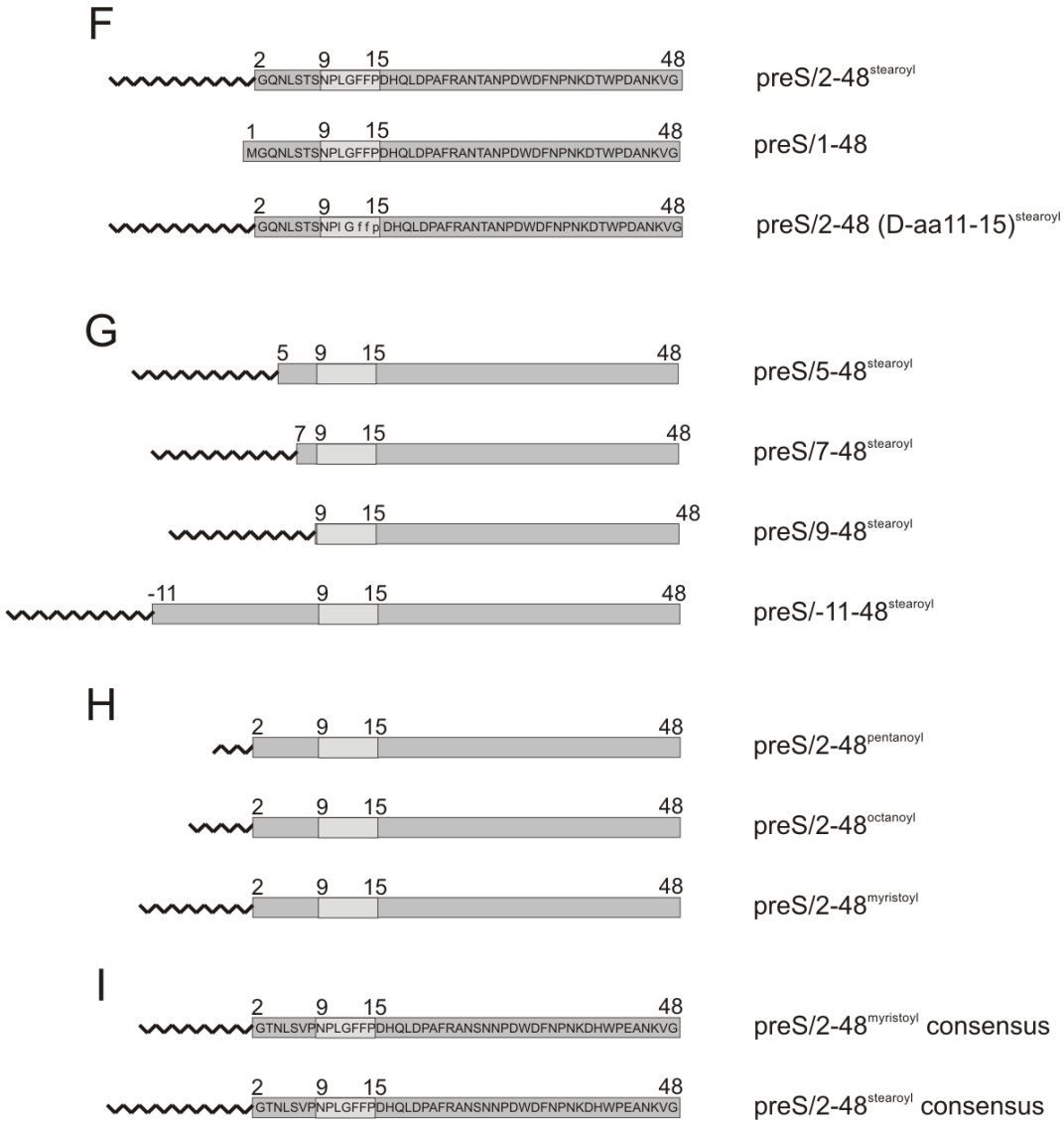

Fig. 3.1: Schematic representation of peptides used in this work. The zigzag line represents the N-terminal acylation, numbers indicate amino acid positions, the essential site is depicted in light gray.
A: The myristoylated wildtype.
B: Crosslinker (CL)-peptides. The star indicates an aryl azide-moiety, the C-terminal His-tag is indicated (His_6).
C, D: Fluorescein- isothiocyanate (FITC)-labeled preS-peptides, either carrying mutations or different N-terminal acylations.
E: Radioisotope labeled preS-peptide. Position of the ^{125}I-labeled D-tyrosine on the C-terminus is indicated.
F-I: Different stearoylated full-length, stearoylated N-terminally shortened or otherwise acylated full length peptides used for membrane activity assays. Unless indicated otherwise, all peptides correspond to the sequence from HBV genotype D.

3.1 Binding of HBV preS1 derived lipopeptides to serum factors

HBV preS-derived lipopeptides comprising the amino acids 2-48 and a N-terminal myristoylation (HBV preS/2-48^{myristoyl}) show a strong liver tropism and marked serum stability

when injected into mice. While mutations in the essential site (amino acids 9-15) abort the liver specificity and leads to equal distribution of the peptide throughout all organs, removal of the fatty acid results in rapid renal excretion [63]. These findings support the hypothesis that one or several serum factors binding and stabilizing the peptide must exist.

In order to assess this putative interaction, a size exclusion chromatography (SEC) assay was employed using fluorescein-isothiocyanate (FITC)-labeled preS-peptides. The FITC-molecule was introduced during solid-phase synthesis, assuring a equimolar ratio of label : peptide. These peptides have been shown to be efficient in inhibiting HBV infection [64]. Peptides were preincubated in absence or presence of serum or serum components and subjected to size exclusion chromatography (SEC) on a superose-6 column. During chromatography, proteins were separated according to their size; large proteins eluted earlier, small proteins later. Every protein eluted at a specific ratio of elution volume (V_e) to void volume (V_0) (V_e/V_0-ratio), the largest proteins eluting with the void volume at a V_e/V_0-ratio of 1,00. Measurement of the UV-absorption of all elution fractions at 280nm and 490nm allowed detection of all proteins or only the FITC-peptide, respectively. A shift in the FITC-specific elution signal would then indicate binding to another protein.

3.1.1. Identification of preS-binding partners

3.1.1.1 HBV preS/2-48^{myristoyl} showed a size shift in SEC when preincubated with serum

For a first assessment of binding, an acylated wildtype (wt) and a non-acylated wt peptide were used (fig. 3.1 C). Serum subjected to SEC eluted in a characteristic pattern, showing several peaks, the largest eluting at an V_e/V_0-ratio of 1,96 **(fig. 3.2 A).** When preincubated with buffer, the preS-peptide eluted at a V_e/V_0-ratio of 2,38 **(fig. 3.2 B).**

Preincubation of the HBV preS/2-48^{myristoyl} -FITC peptide with serum led to a marked shift in the FITC-specific elution signal, now overlapping with the serum-peak at V_e/V_0 =1,96 **(fig. 3.2 C).** This shift, however, was not observed when the non-acylated preS/1-48 FITC peptide was preincubated with serum **(fig. 3.2 C).**

These results clearly indicated an acylation-dependent binding of the preS-peptide to a serum component. Since the non-acylated variant showed no shift in elution, a possible artefact caused by the FITC-molecule could be ruled out.

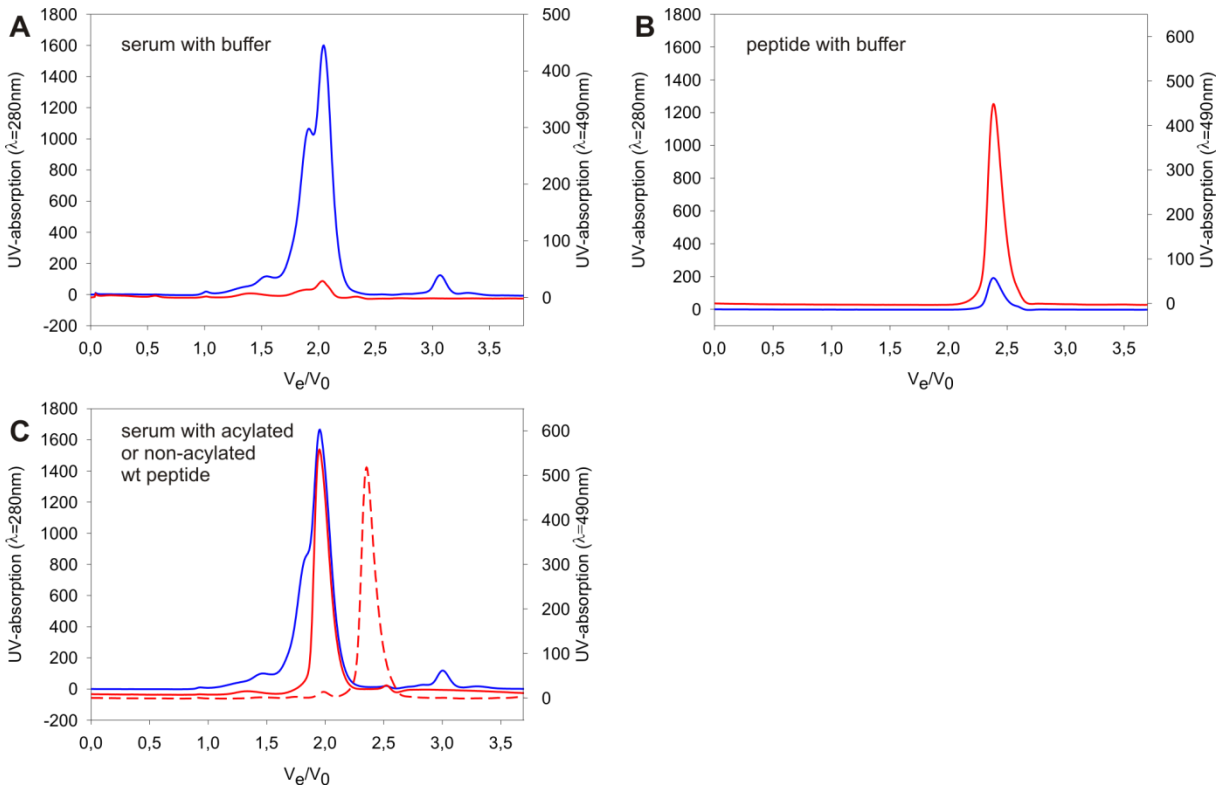

Fig. 3.2: Acylation dependent binding of HBV preS-peptides to serum components. A: 75µl human serum preincubated with TN-buffer (1h, 37°C). Blue curve: UV_{280}. Red curve: UV_{490}. **B:** 50µM HBV preS/1-48 preincubated with TN-buffer. Blue curve: UV_{280}. Red curve: UV_{490} . **C:** 50µM preS/1-48 (dashed red curve) or preS/2-48^{myristoyl} (continuous red curve) preincubated with 75µl serum (corresponds to 160µM albumin). Blue Curve: UV_{280}. Elution profiles from SEC on a HR30/100 Superose 6 column are shown; UV-absorption at 280nm (left y-axis) or 490nm (right y-axis) is given, the elution volumes are normalized for the void volume of the column (V_0, =8ml). Running conditions for all runs: 4°C, 0,4ml/min, running buffer: TN-buffer (20mM Tris, 140mM NaCl, pH7, 4). Representative data of 3 independent experiments are shown.

3.1.1.2 Functional peptides carrying a crosslinker moiety for identification of binding partners

In order to identify the interaction partners of preS-peptides, a biochemical crosslinking assay was used. For this purpose, a photoreactive aryl azide-moiety was coupled to a lysine introduced on position 19 of a set of preS-peptides (fig. 3.1 B). Upon exposure to UV-light, this molecule forms reactive nitrenes that rapidly establish covalent bonds to molecules in close proximity. A hexa-histidine tag (his-tag) was introduced on the C-terminus of those peptides for purification of formed complexes via affinity chromatography on nickel-sepharose columns.

The modified peptides are not altered in their ability to inhibit HBV-infection

To assure that the alterations introduced into these peptides do not influence their ability to inhibit HBV infection, they were added in increasing concentrations to a HBV-infection assay on HepaRG cells. As control, unaltered myristoylated wildtype peptide was used.

While the uncompeted infection led to a HBsAg-secretion of ~30 signal over cutoff (S/CO) **(fig. 3.3, black bar)**, addition of 500nM myristoylated wildtype (wt) peptide reduced secretion about six fold **(fig. 3.3, dark grey bar)**. A similar reduction was observed already at 100nM of the peptide carrying the aryl azide moiety and His-tag (preS/2-48^{myristoyl}-CL). Addition of higher amounts of this peptide did not reduce infection further **(fig. 3.3, light grey bars)**.

In contrast, a crosslinker-peptide where 5 aa in the essential site were replaced by alanine (preS/2-48 Ala11-15^{myristoyl}-CL) did not influence HBV infection, independently of the amount added **(fig. 3.3, white bars).** Thus, the alterations made on the preS-peptide for identification of binding partners do not influence its functionality.

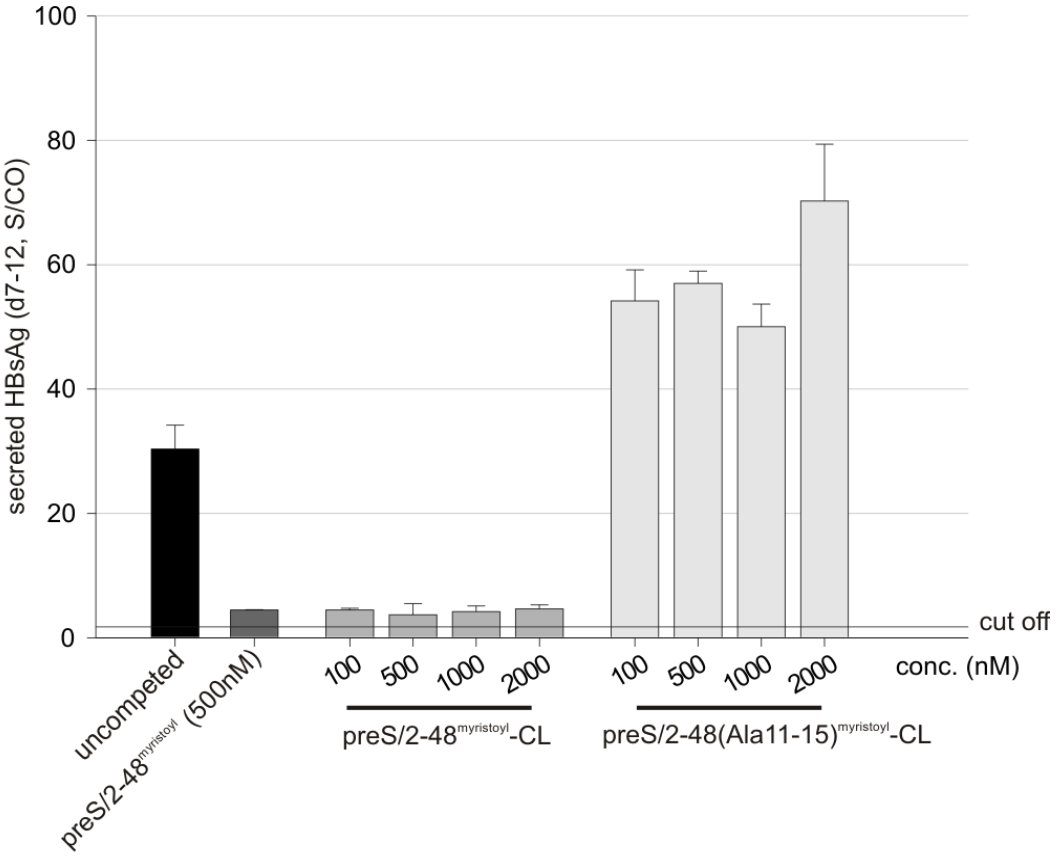

Fig. 3.3: preS/2-48^{myristoyl} -CL inhibits HBV-infection in a sequence-dependent manner. HepaRG cells were infected with a multiplicity of infection [24] of 1×10^4 in the absence of inhibitor or presence of 500nM unaltered WT preS-peptide, 100-2000nM preS/2-48^{myristoyl}-CL or 100-2000nM preS/2-48 Ala11-15^{myristoyl}-CL. Supernatant [60] from day 7-12 was harvested, secreted HBsAg measured by ELISA. Representative data of 3 independent experiments are shown.

3.1.1.3 Human Serum Albumin and Apolipoprotein A1 bind to preS-peptides

In order to identify binding partners, human serum was incubated with preS/2-48^{myristoyl}-CL, preS/2-48 Ala11-15^{myristoyl}-CL or preS/1-48-CL (fig. 3.1 B); formed complexes were purified by affinity chromatography on nickel-sepharose.

Analysis of the elution fractions by preS1-specific western blot (wb) and silver stain SDS-PAGE showed two bands in the elution fractions of the crosslinker assay with acylated wt and mutant peptide **(fig. 3.4, left and middle panel).** The upper band ran at an apparent molecular weight of 70-75 kDa, the lower band at an apparent molecular weight of 30-35 kDa. Assuming that these bands correspond to peptide-serum factor-complexes, subtraction of the peptides´ molecular weight (6,5 kDa) results in binding partners with a molecular weight of 63-68 kDa and 23-28 kDa, respectively.

Neither band showed up in the elution fractions when the non-acylated peptide was used, indicating acylation-dependent, sequence-independent binding **(fig. 3.4, right panel).**

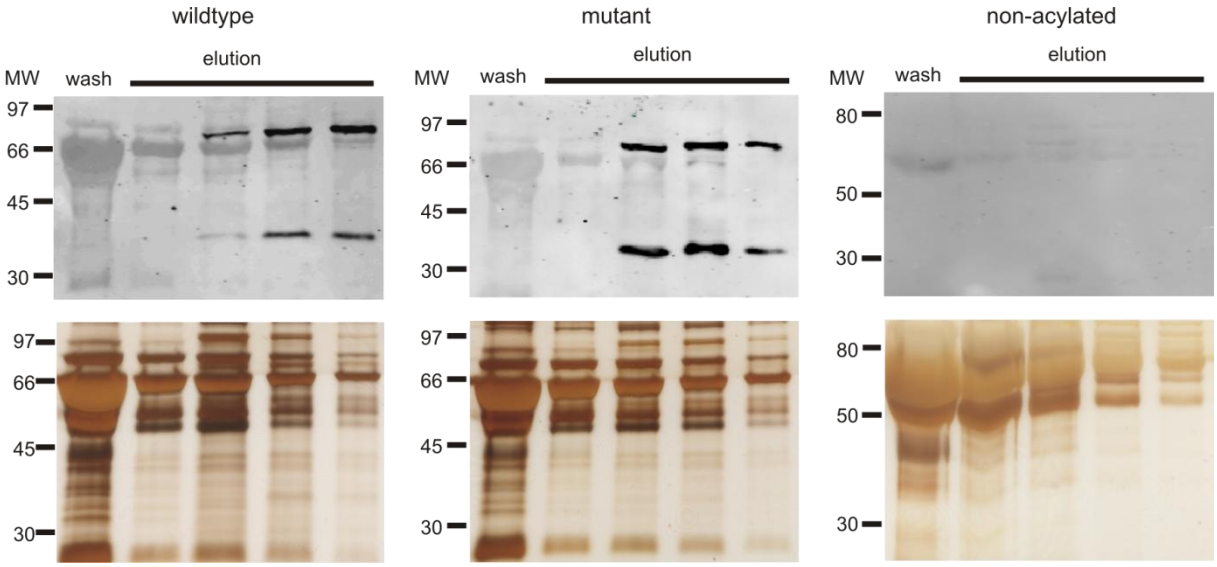

Fig. 3.4: Myristoyl-dependent, sequence-independent binding of preS-peptides to two serum components. 150µM of preS/2-48^{myristoyl}-CL **(left panel),** preS/2-48 Ala11-15^{myristoyl}-CL **(middle panel)** or preS/1-48-CL **right panel)** were incubated with 1ml of human serum for 1h at 37°C, filled ad 10ml with lysis buffer and applied to a nickel-sepharose column in presence of 20mM Imidazole. After washing with 50mM Imidazole, bound molecules were eluted with a 500mM Imidazole step gradient over 10 column volumes. Wash and elution fractions were separated by SDS-PAGE and analyzed by wb using a HBV preS1-specific antibody (Ma18-7) (**upper panels)** or by silver stained SDS PAGE **(lower panels).** Representative data of 2 independent experiments are shown.

Peak fractions of the affinity chromatographies with myristoylated wildtype peptide were analyzed by mass spectrometry (data not shown); proteins corresponding to the preS1-specific bands in WB were identified to be human serum albumin (HSA, upper band) and apolipoprotein A1 (ApoA1, lower band).

With 66 kDa (serum albumin) and 24 kDa (apolipoprotein A1), these proteins correspond to the expected sizes. Both proteins are involved in the systemic transport of hydrophobic substances, which makes them likely interaction partners for an acylated peptide.

Next, the characterization of both interactions, their possible role in the liver tropism and hepatocyte binding of preS-peptides as well as their influence on HBV infection came into focus. In the following, analysis of the albumin-peptide interaction will be presented, followed by data concerning the ApoA1-peptide binding. The influence on hepatocyte binding and HBV-infection has always been assessed in parallel assays; therefore, these data will be presented together in later chapters.

3.1.2 The peptide - HSA interaction

3.1.2.1 HBV preS peptides bound HSA in the SEC-assay

In order to validate HSA as binding partner for preS-peptides, the SEC-assay was performed with purified HSA. Therefore, HSA was incubated either with buffer or with acylated wt, acylated mutant or non-acylated wt peptide (fig. 3.1 C) and subjected to SEC.

HSA eluted as sharp peak at a V_e/V_0-ratio of 2,03 **(fig. 3.5, black curve)**. Preincubation with acylated wt peptide led to the described shift in the 490nm UV-absorption (see chapter 3.1.1.1), indicating binding of the peptide to HSA **(fig. 3.5, green curve).** When a peptide carrying a mutation in the essential site (D-amino acids 11-13) was preincubated with HSA, the size shift was also observed **(fig. 3.5, red curve).** The independence of the interaction from the peptide´s sequence was confirmed by these findings. The non-acylated wt peptide showed no size shift in this assay **(fig. 3.5, blue curve)**, giving additional affirmation of the acylation dependence.

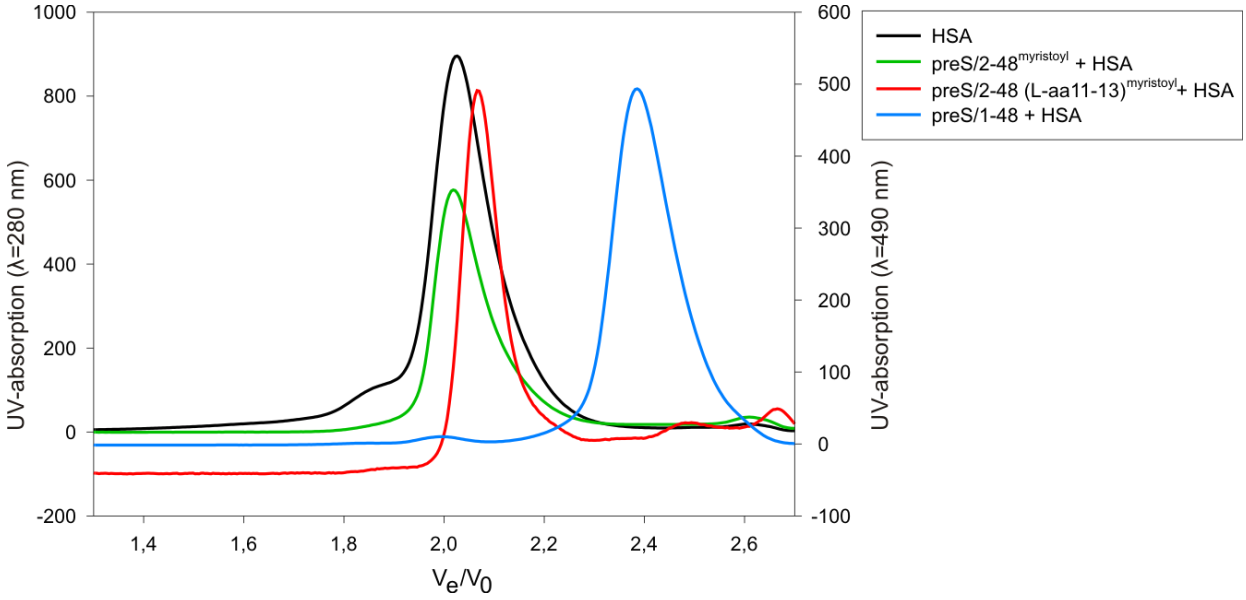

Fig. 3.5: HBV preS-peptides bind HSA in an acylation dependent, sequence-independent manner. 150µM HSA were incubated with TN-buffer (black line) or 50µM HBV preS/2-48 ^{myristoyl} (green curve) , 50µM HBV preS/2-48 (D-AS11-13)^{myristoyl} (red curve) or 50µM of HBV preS/1-48 (blue curve) for 1h at 37°C and subjected to SEC on a superose 6 column. Elution profiles from SEC on a HR30/100 Superose 6 column are shown; UV-absorption at 280nm (left y-axis) or 490nm (right y-axis) is given, the elution volumes are normalized for the void volume of the column (V_0, =8ml).running conditions for all runs: 4°C, 0,4ml/min, running buffer: TN-buffer. Representative data of 2 independent experiments are shown.

3.1.2.2 The peptide-HSA binding depends on the length of the N-terminal acylation

Since the observed interaction was found to depend only on the N-terminal acylation, the influence of the length of the N-terminal fatty acid was assessed. Peptides with wt sequence, carrying C5-, C8-, C12-, C14- or C18 fatty acids or a cholesterol moiety N-terminally (fig. 3.1 D) were preincubated with HSA and subjected to SEC.

Non-acylated peptides did not bind albumin **(fig. 3.6, dark blue curve).** Peptides carrying acylations shorter than C12 showed no binding to HSA; a short fatty acid was not enough to confer a sufficient hydrophobicity for binding, the hydrophilic peptide part dominated **(fig. 3.6, green and red curve).** With a C12-acylation, the on-rate approximately equaled the off-rate, leading to a ~50% binding **(fig. 3.6, pink curve)**, while C14- and C18-acylations led to complete binding of the peptides, being hydrophobic enough for a strong interaction with the fatty acid transporter HSA **(fig. 3.6, grey and orange curve)**. A peptide carrying a cholesteryl moiety on its N-terminus also bound HSA **(fig. 3.6, purple curve).**

The peptide´s affinity to albumin thus increased with the length of the N-terminal fatty acid, therefore, with its hydrophobicity.

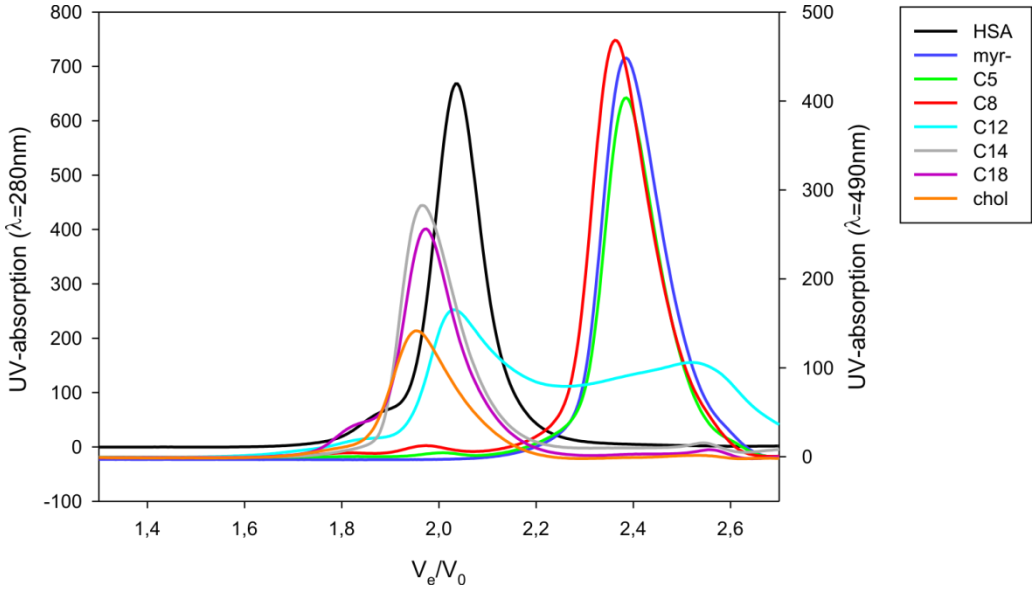

Fig. 3.6: Binding of HBV preS-peptides to HSA depends on the length of the N-terminal acylation.
150µM HSA were incubated with buffer (black curve) or 50µM of a non-acylated (blue curve), C5-acylated (green curve), C8-acylated (red curve), C12-acylated (light blue curve), C14-acylated (grey curve), C18-acylated (orange curve) or cholesteroylated (purple curve) preS-peptide for 1h at 37°C and subjected to SEC on a superose 6 column. Elution profiles from SEC on a HR30/100 superose 6 column are shown; UV-absorption at 280nm (left y-axis) or 490nm (right y-axis) is given, the elution volumes are normalized for the void volume of the column (V_0 =8ml). Running conditions for all runs: 4°C, 0,4ml/min, running buffer: TN-buffer. Representative data of 2 independent experiments are shown.

In order to confirm that the observed shift in the FITC-signal corresponds to the preS-peptide and is not caused by free FITC, three peak fractions from an SEC-run with C14-, C18- and a cholesteroylated peptide preincubated with HSA were analyzed by silver stained SDS-PAGE and HBV preS1-specific wb. For all three peptides, a preS1-specific signal could be detected in the HSA-peak fractions, running below 15 kDa **(fig. 3.7 A)** At this molecular weight, a diffuse band could also be observed in the silver stain gel **(fig. 3.7 B)**. The HSA-band was visible at ~60-70 kDa in the silver stained SDS-PAGE **(fig. 3.7 B)** and also, not distinguishable as clear band, but as background on the wb slightly above 60 kDa **(fig. 3.7 A).** Above the HSA-background, a preS1-specific band was again visible; this band possibly corresponds to albumin-bound peptide. A small fraction of the complex would then have withstood the denaturing and reducing conditions of SDS-PAGE. Taken together, these data confirm that preS-peptides bind to HSA.

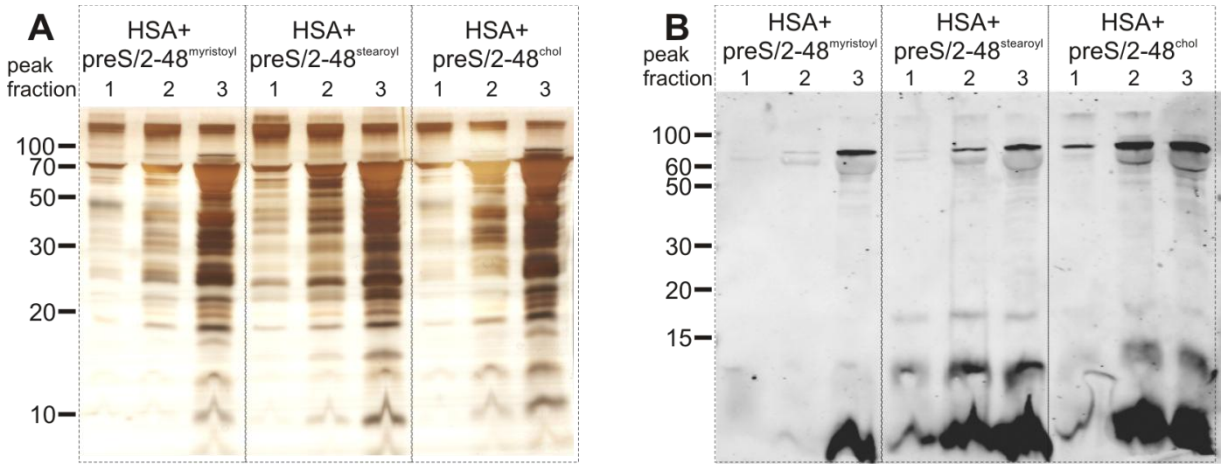

Fig. 3.7: Confirmation of the peptide binding to HSA by western blot and silver stained SDS-PAGE.
Peak fractions from SEC-runs of preincubated HSA with either preS/2-48^{myristoyl}, preS/2-48^{stearoyl} or preS/2-48^{cholesteroyl} were separated by SDS-PAGE on a 14% Schägger-gel.
A: Western blot using a HBV preS1-specific antibody (Ma18-7).
B: Silver stained SDS-PAGE. Sizes of molecular weight markers are indicated.

3.1.2.3 The peptide-HSA binding *in vivo*

Having identified and characterized the peptide-HSA interaction *in vitro*, confirmation of the observed effect *in vivo* was sought. In the course of a preclinical study for Myrcludex B, an HBV preS-derived lipopeptide developed for therapeutic treatment of HBV infection, beagle dogs received intravenous injections of ^{123}I-labeled HBV preS/2-48 ^{myristoyl} (fig. 3.1 E). 10min and 1h after injection, blood samples were taken and serum was prepared. Aliquots of these sera were then subjected to SEC, UV-absorption and radioactivity of elution fractions were measured. Peak fractions were analyzed by coomassie-stained SDS-PAGE. As the values from both times points did not differ, data from the 1h-time point only are shown **(fig. 3.8)**.

In the SEC, the radioactivity peak **(fig. 3.8, dashed line)** overlapped with the UV-peak corresponding to serum albumin **(3.8, black line).** The radioactivity measured was in the same order of magnitude after 10 min and 1h (~1×10^5 counts per minute), showing that the labeled peptide bound rapidly after injection to albumin and remained bound. The coomassie-stained SDS-PAGE of the peak fractions showed a strong band at ~66 kDa **(inlaid panel)**, confirming that this peak indeed corresponds to serum albumin.

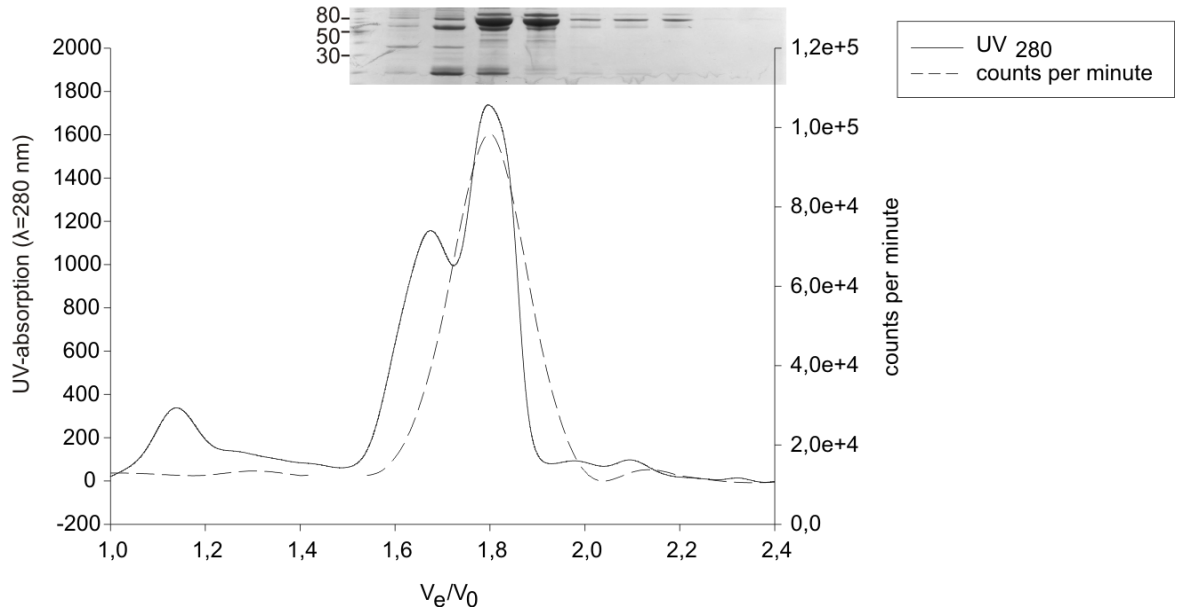

Fig. 3.8: HBV preS-peptides bound to serum albumin *in vivo*. 86MBq/14µg of HBV preS/2-48myr Tyr49-^{123}I peptide were injected subcutaneously into the left hind leg of female beagle dogs that had been anaesthetized with ketamin (10mg/kg) and xylazine (2mg/kg). 1h after Injection, blood was taken, serum was prepared and 300µl were subjected to SEC. Elution profile from SEC on a HR30/100 Superose 6 column is shown; Left y-axis: UV-absorption at 280nm. Right y-axis: measured radioactivity. Elution volumes are normalized for the void volume of the column (V_0, =8ml). Running condition: 4°C, 0,4ml/min, running buffer: TN-buffer.

3.1.2.4 The dissociation constant (K_D) for the peptide-HSA binding was found to be in the micromolar range

In order to determine the strength of the peptide-HSA interaction, increasing amounts of FITC-labeled preS-peptides were incubated with a fixed amount of HSA (30µM final concentration) and subjected to SEC. The amount of peptide was varied over a broad range (1µM-90µM final concentration). In this range, saturation of the albumin and therefore the appearance of a second peptide UV_{490}-peak, corresponding to unbound peptide, was expected. Integration of the elution profile peaks at UV=490nm corresponding to bound peptide and unbound peptide was then performed using the Unicorn-software (GE Healthcare). Exemplary runs for three selected peptide concentrations are shown in **fig. 3.9 A**. When preincubation was performed with the C12-acylated peptide **(fig. 3.9 A, upper row)**, a peak corresponding to unbound peptide was detectable already at 5µM peptide. While the bound peptide-peak increased when more peptide was added, the unbound-peptide peak rose at a higher rate. The C14-acylated peptide **(fig. 3.9 A, middle row)** was entirely bound to albumin up to an equimolar ratio; higher peptide concentrations led to appearance of an unbound peptide-peak. The C18-acylation conferred binding to albumin even at a molar excess of peptide **(fig. 3.9 A, lower row)**.

For calculations, the peak corresponding to bound peptide was integrated between V_e/V_0 = 1,4 - 2,4; The concentration of unbound peptide was calculated by integrating between V_e/V_0 = 2,4 and 3,4.

The dissociation constant K_D of an interaction is defined by the concentration at which 50% of the ligands binding sites are occupied (θ = 0,5 with θ= fraction of occupied ligand binding sites). This value θ can be calculated by the formula $\theta = \frac{[RL]}{[RL\,] + [R]}$ with [RL] corresponding to the concentration of the receptor-ligand complex and [R] to the concentration of the unbound receptor. In this case, the receptor was HSA and the ligand the peptide. The concentration of the HSA-peptide complex [*HSA*-peptide] was calculated for each peptide concentration by the formula $[HSA - pep] = \frac{shifted\ peak\ 490nm\ integrated}{all\ peaks\ 490nm} \times [input\ peptide]$. This allowed the calculation of θ by $\theta = \frac{[HSA-pep]}{[HSA\ total\,]}$. The obtained values were then plotted against the input peptide concentration. A linear fit curve was drawn using the Graphpad software which also allowed calculation of the K_D and the maximal bound peptide per HSA, B_{max} **(fig. 3.9 B)**.

This assay was performed with the C12-, the C14- and the C18-acylated preS-peptide (fig. 3.1 D).

In this way, the dissociation constant for preS/2-48 ^{lau} (C12)-HSA-interaction was determined to be of 63,25 µM **(fig. 3.9 B, green curve)**; for the preS/2-48 $^{myr\ 120}$-HSA of 17,78 µM **(fig. 3.9 B, red curve).** PreS/2-48^{stea} (C18) was found to bind to HSA with a maximal amount of 10 peptide molecules per HSA **(fig. 3.9 B, blue curve)**, leading to a K_D-value of 289,7 µM.

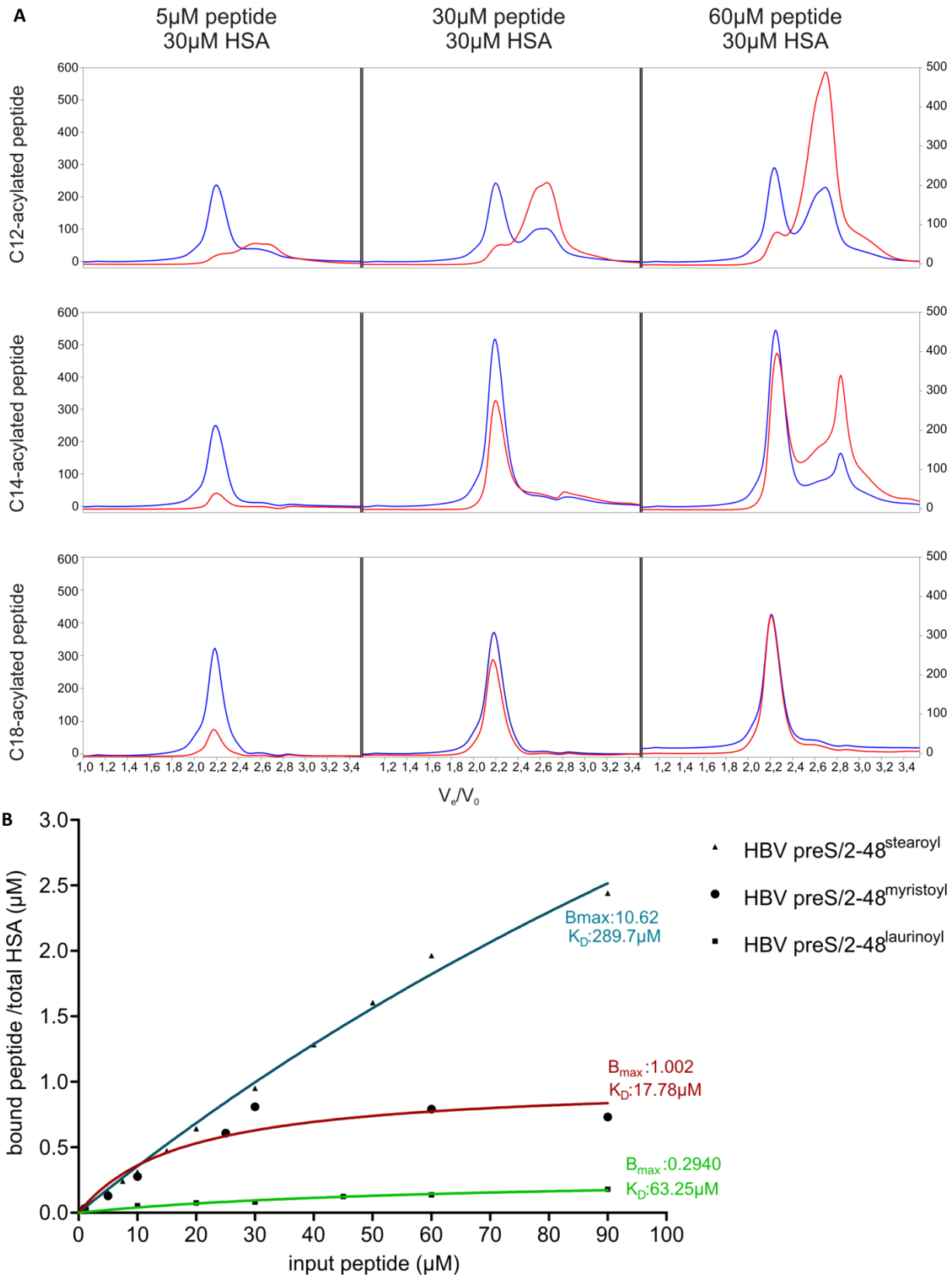

Fig. 3.9: Binding curves for the peptide-HSA interaction. A: Increasing amounts of either C12-, C14- or C18- acylated HBV preS-peptide were incubated with 30µM HSA and subjected to SEC on a Smart-Superose 6 column; exemplary runs with 5µM, 30µM and 60µM of each peptide are shown. Left y-axis: UV-absorption at 280nm. Right y-axis: UV-absorption at 490nm.

B: Ratios of bound peptide /total albumin were calculated and plotted against the amount of input peptide. Linear regression curves were calculated according to the "one site - specific binding" model (GraphPad software). calculated values of the respective maximal binding (B_{max}) and the dissociation constant (K_D) are indicated. Binding studies have been performed twice with the myristoylated peptide and once with the stearoylated and the laurinoylated peptide.

3.1.3 PreS-peptides bound to Serum components from other species

In the course of preclinical studies for Myrcludex B as therapeutic agent against HBV infection, biodistribution studies have been performed in different species such as rats, cynomolgus monkeys and beagle dogs. Albumin binding of preS peptides to albumin or serum from these species was assessed.

Binding could be detected when using serum albumin from rats **(fig. 3.10 A)**, rat serum **(fig. 3.10 B)**, beagle dog serum **(fig. 3.10 C)** or cynomolgus monkey serum **(fig. 3.10 D).** While the preS-peptide bound to primary hepatocytes from rat and beagle dog, it did not bind to hepatocytes from cynomolgus monkeys [64], nor could liver tropism be detected in these animals (A. Schieck, personal communication). The N-terminal acylation therefore confers binding to albumin in a wide range of species; the differences in liver tropism indicate that the albumin-interaction plays no role in the transport of the peptide to the liver.

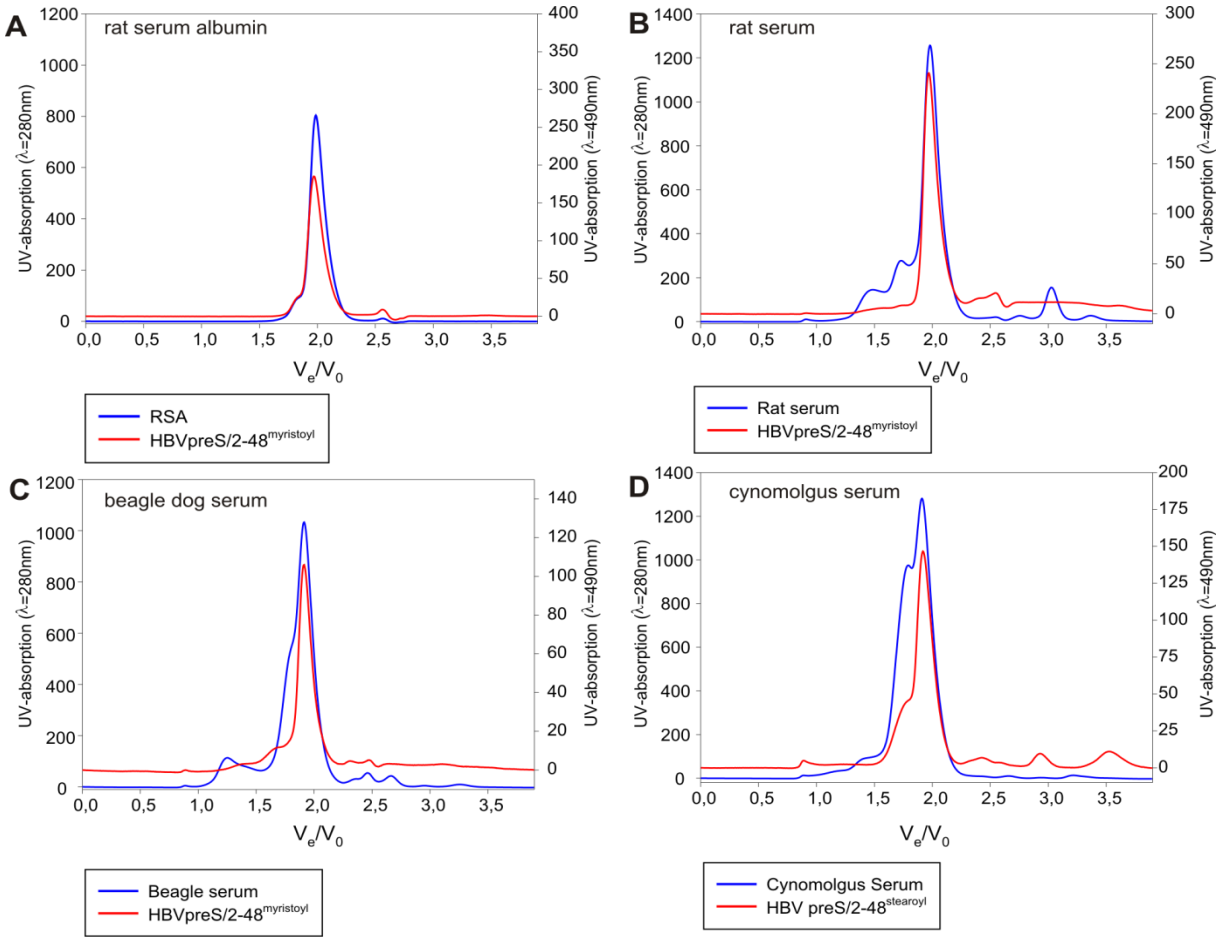

Fig. 3.10: HBV preS-peptides bind to albumin from other species. 150µM RSA **(A)** or 75µl serum from rat **(B),** beagle dog **(C)** or cynomolgus monkey **(D)** were incubated with 50µM of HBVpreS/2-48^{myristoyl} (HBVpreS/2-48^{stearoyl} for the cynomolgus serum) for 1h at 37°C and subjected to SEC. Elution profiles from SEC on a HR30/100 Superose 6 column are shown; UV-absorption at 280nm (left y-axis) or 490nm (right y-axis) is given, the elution volumes are normalized for the void volume of the column (V_0, =8ml). Running conditions for all runs: 4°C, 0,4ml/min, running buffer: TN-buffer. Representative data of 2 independent experiments are shown.

3.1.4 Binding of HBV preS-peptides to high density lipoproteins

Apolipoprotein A1, the main protein constituent of high density lipoproteins (HDLs), was identified as binding partner for preS derived lipopeptides. This interaction was therefore analyzed *in vitro* by the SEC-assay.

3.1.4.1 HDLs were purified from human serum

For assessment of HDL-peptide binding, HDLs were purified from human serum by a three-step purification method. This consisted of a preparative gel filtration on a superdex 75 column, flotation by ultracentrifugation followed by SEC on a Superose 6 column.

Separation of human serum on a superdex 75 column

When serum was subjected to SEC on a superdex 75 column, serum components eluted in two main peaks **(fig. 3.11).** The first peak eluted between V_e/V_0 of 1,0 and 1,2, the second between V_e/V_0 of 1,3 and 1,5. Analysis of the elution fractions by ApoA1-specific wb showed a positive signal in very early elution fractions (V_e/V_0-ratio of 1,2) **(fig. 3.11).** This elution volume was close to the void volume of the column and corresponded to a molecular weight of 380 kDa (calculated using the UNICORN-software, based on standard run on the same column). Monomeric uncomplexed ApoA1 has a molecular weight of 24 kDa, and would thus be expected to elute at later fractions. This indicates that this positive signal indeed corresponds to high molecular weight complexes such as HDLs.

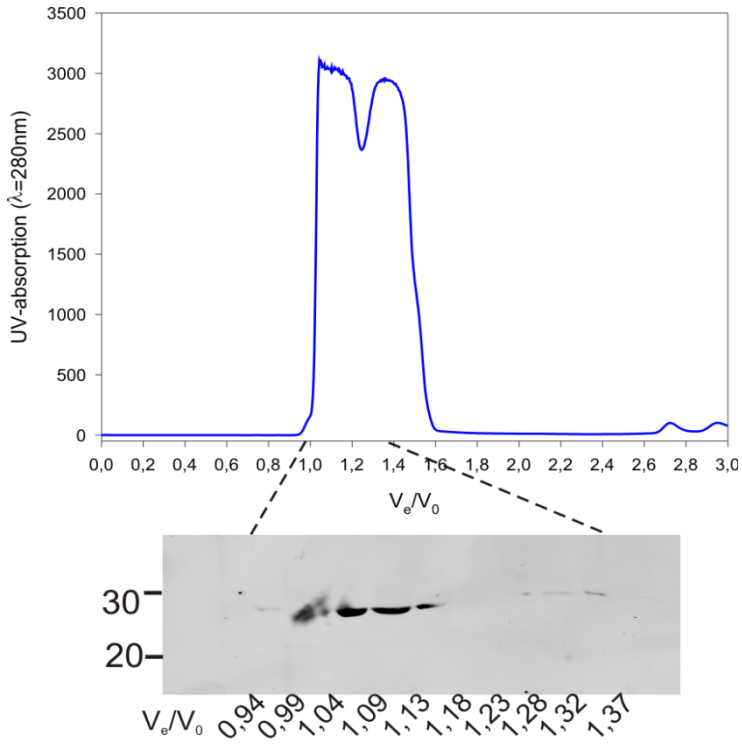

Fig. 3.11: High density lipoproteins elute close to the void volume when serum is subjected to SEC on Superdex 75.
Upper panel: Elution profile from SEC on a HiLoad 26/60 Superdex 75 column; UV-absorption at 280nm (y-axis) is given, the elution volumes are normalized for the void volume of the column (V_0, = 105ml).running conditions for all runs: 4°C, 2,5ml/min, running buffer: 1×PBS.
Lower panel: western blot of SDS-PAGE from the elution fractions. 10µl of each fraction were separated by SDS-PAGE and blotted onto nitrocellulose; first antibody: mouse anti human ApoA1. Sizes of the molecular weight marker are indicated.

Flotation by ultracentrifugation

The different lipoproteins present in the serum differ by their relative density [117]. This feature can be used for their separation. If the density of a solution is adjusted to the density of the lipoproteins of interest, ultracentrifugation will lead to the flotation of these particles. Peak fractions from the S75 column were pooled, adjusted to the density of HDLs (1,121g/cm^3) using sodium bromide and subjected to ultracentrifugation. Analysis of the gradient fractions by coomassie-stained SDS-PAGE and WB showed that the ApoA1-signal was enriched in the top fractions after ultracentrifugation **(fig. 3.12).** This step therefore led to a further purification of the HDLs from other serum proteins. The presence of other protein contaminants in the top fractions after ultracentrifugation, made an additional step necessary.

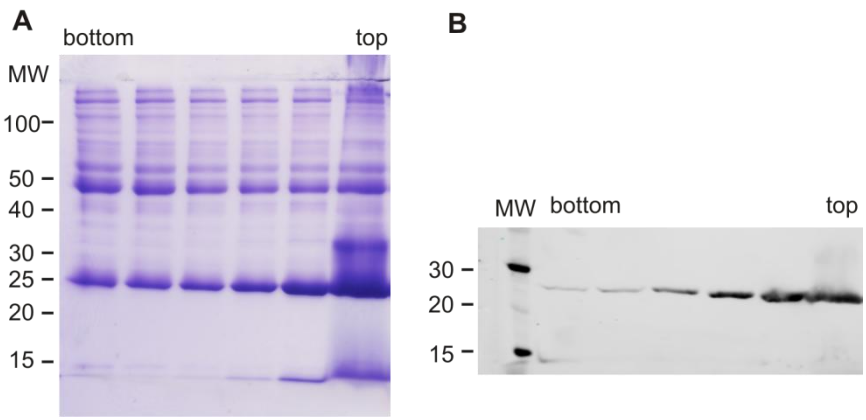

Fig. 3.12: HDLs float up in ultracentrifugation at a density of 1,121g/cm^3. 10µl of each fraction after centrifugation were applied onto a SDS-PAGE which was either coomassie-stained **(A)** or blotted onto nitrocellulose **(B).** First antibody: mouse α human ApoA1. Sizes of the molecular weight markers are indicated.

Separation on a Superose 6 column

In order to further purify the obtained HDL and to separate them from the sodium bromide, the pooled top fractions from ultracentrifugation were concentrated and applied onto a HR30/100 Superose 6 column. The elution profile of this run showed a clear peak at a V_e/V_0-ratio of 1,30 **(fig. 3.13 A);** in these fractions, a marked band of ~25 kDa was visible in the coomassie-stained SDS-PAGE **(fig. 3.13 B)**. Eluting much earlier than free ApoA1 would have (expected V_e/V_0-ratio: ~2,0), this peak was likely to correspond to HDLs.

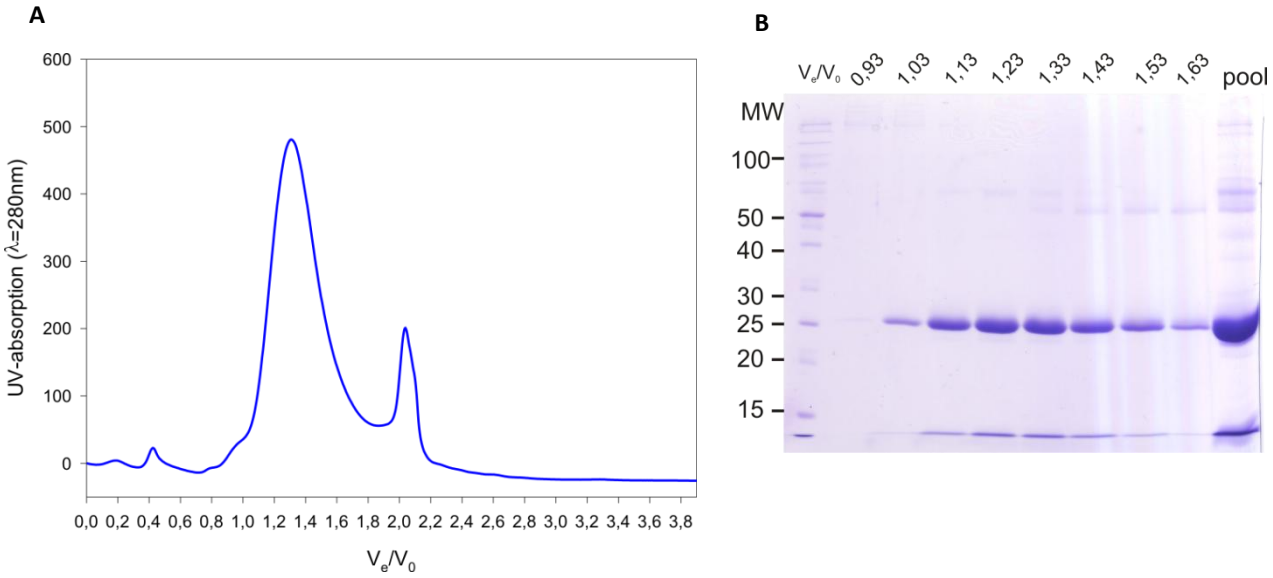

Fig. 3.13: SEC on Superose 6 as third purification step leads to a concentrated and pure HDL-preparation.
A: Elution profile from SEC on a HR 30/100 Superose 6 column; UV-absorption at 280nm (y-axis) is given, the elution volumes are normalized for the void volume of the column (V_0, =8ml).running conditions for all runs: 4°C, 0,4ml/min, running buffer: 1×PBS.
B: Coomassie-stained SDS-PAGE of the elution fractions from A and of pooled peak fractions. Sizes of the molecular weight markers are indicated in kDa.

Next, peak fractions from the Superose 6-elution were pooled and concentrated. When a sample of this concentrate was analyzed by coomassie-stained SDS-PAGE **(fig. 3.13B, right lane)**, several other bands were also visible besides the prominent ApoA1-band. Since HDLs contain ApoA-II (17 kDa), ApoA-IV (44 kDa), ApoC-I-III (6,6 kDa, 8,9 kDa and 8,8 kDa, respectively) ApoD (22 kDa) and ApoE (10 kDa), some of these bands may be attributed, although not with certainty, to HDLs.

Quantification of the protein content in the pooled fraction revealed a concentration of 1,97mg/ml. In human plasma, ApoA-I has a concentration of 1,3mg/ml. The purification method therefore led to a 1,5-fold enrichment of the HDLs. Having reached a satisfying purity, these HDLs were used for subsequent analyses.

3.1.4.2 HDL bound HBV preS derived lipopeptides depending on their N-terminal moiety

In the following experiment, a C14- a C18-acylated or a cholesteroylated peptide with wt sequence were preincubated with HDLs and subjected to SEC. The purified HDLs eluted as a clear peak when subjected to SEC on a Superose 6 column **(fig. 3.14, black curve)** at a V_e/V_0-ratio of 1,60. This ratio differed slightly from the one observed during purification of the HDL; this is probably due to usage of a different Superose 6 column, as these show slight variations in their separation behavior. Small peaks eluting in later fractions might either be

co-purified contaminants or HDL protein constituents that had dissolved from the lipoproteins.

When a myristoylated preS-peptide was preincubated with HDLs and subjected to SEC, only a small amount of peptide shifted to an earlier elution volume **(fig. 3.14, red curve).** A stearoylation on the peptide´s N-terminus conferred stronger binding, the largest part of the peptide-signal having shifted to earlier elution volumes **(fig. 3.14, blue curve).** When the assay was performed with a preS-peptide carrying a cholesterol-moiety, however, the entire peptide was bound to HDLs **(fig. 3.14 green curve)**.

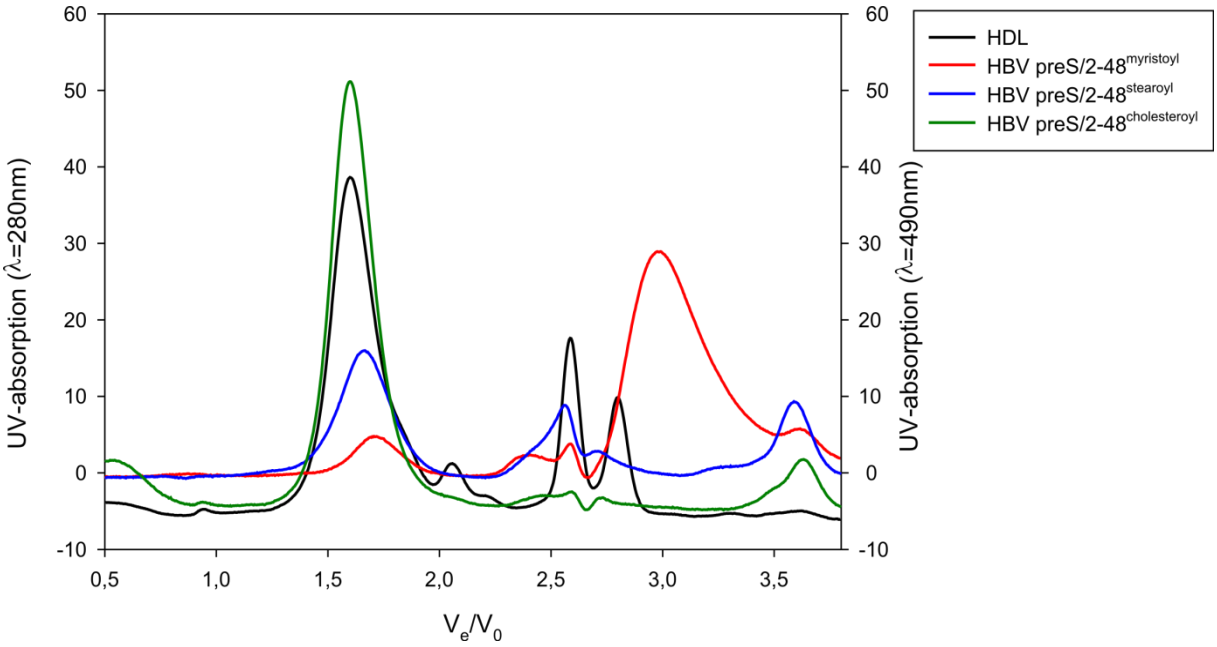

Fig. 3.14: The N-terminal moiety determines the binding to HDLs. 100µl of purified HDLs were preincubated either with buffer (black curve) or with 50µM of HBVpreS/2-48^{myristoyl} (red curve), HBVpreS/2-48^{stearoyl} (blue curve) or HBVpreS/2-48^{cholesteroyl} (green curve) for 1h at 37°C and subjected to SEC. Elution profiles from SEC on a HR 30/100 Superose 6 column; UV-absorption at 280nm (left y-axis) and 490nm (right y-axis) are given, the elution volumes are normalized for the void volume of the column (V_0, =8ml). Running conditions for all runs: 4°C, 0,4ml/min, running buffer: 1×TN. Representative data of 2 independent experiments are shown.

Although ApoA1 has been identified as binding partner using a myristoylated preS-peptide, the weak interaction between HDL and preS/2-48^{myristoyl} observed here may be due to the different assay conditions. In the crosslinker-assay, formed complexes are stabilized by formation of covalent bonds. In the SEC-assay, weak complexes formed by hydrophobic interactions only dissociate more easily.

However, as seen for the peptide-HSA-interaction, the hydrophobicity of the N-terminal moiety influences the binding to HDL, the strongest binding being observed for a cholesteroylated peptide.

3.1.5 Neither HDL nor HSA influenced peptide binding to primary hepatocytes

HBV preS peptides have been shown to bind to a wide range of primary hepatocytes [64], a cell type involved in metabolism of fats and fatty acids. While the existence of a specific receptor for albumin is a subject of discussion, the role of albumin in binding and uptake of fatty acids into hepatocytes has often been postulated (introduction chapter 1.6.2). HDLs are known to bind via ApoA1 to the scavenger receptor B1 (SRB1) [133] and thereby get taken up by the cell. The finding that HBV preS peptides bind to serum albumin and HDLs raised the question whether these interactions influence peptide binding to hepatocytes.

In this assay, radiolabeled wt preS-peptide was incubated with freshly isolated primary mouse hepatocytes (PMH). Thereafter, the supernatant [60] was taken off, the cells washed three times with PBS and lysed with NaOH. Radioactivity of all fractions was measured. Before incubation, cells were thoroughly washed to remove secreted proteins. The incubation itself was performed in serum-free medium in the absence or presence of HSA, HDLs or a combination of both. All assays were done in triplicates, using one peptide-mastermix.

After incubation, the SN of the cells contained ~5×10^5 cpm (**fig. 3.15**, peptide only, black bars) or ~7×10^5 cpm when HSA or HDL were added (**fig. 3.15,** grey bars). This difference was not statistically significant ($p>0,05$). With each washing step, radioactivity decreased, showing slight, but not significant differences; the final cell pellet then contained ~3×10^4 cpm (peptide only) or ~$2\text{-}3\times10^4$ cpm (peptide + HSA/HDL). Therefore, addition of either substance or combination of both did not influence peptide binding to PMH.

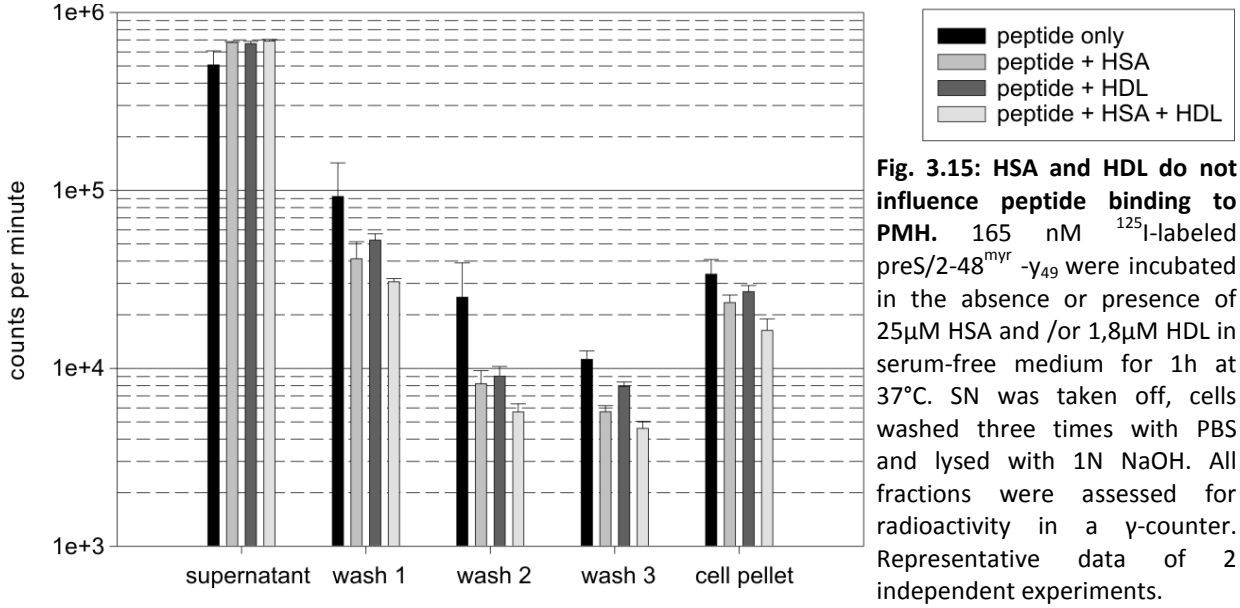

Fig. 3.15: HSA and HDL do not influence peptide binding to PMH. 165 nM ^{125}I-labeled preS/2-48^{myr} -γ_{49} were incubated in the absence or presence of 25µM HSA and /or 1,8µM HDL in serum-free medium for 1h at 37°C. SN was taken off, cells washed three times with PBS and lysed with 1N NaOH. All fractions were assessed for radioactivity in a γ-counter. Representative data of 2 independent experiments.

3.1.6 Liver tropism was not impaired in a ApoA1-deficient mouse

In order to assess whether the peptide binding to HDLs has an effect on the peptides´ liver tropism, radiolabeled myristoylated wt HBV preS-peptide was injected into a mouse deficient for Apolipoprotein A1. As control, a wildtype mouse was used. The lack of ApoA1 expression was controlled by analyzing liver samples from both mice for ApoA1 content in western blot **(fig. 3.16A)**.

When comparing the radioactivity signal in the ApoA1 deficient mouse to the one in the wt mouse, no difference in liver tropism could be detected **(fig. 3.16 B)**. While the signal at the site of injection was comparable in both mice, the signal in the liver was slightly increased in the ApoA1 deficient mouse. It can therefore be concluded that the peptide-HDL interaction has no positive effect on liver tropism.

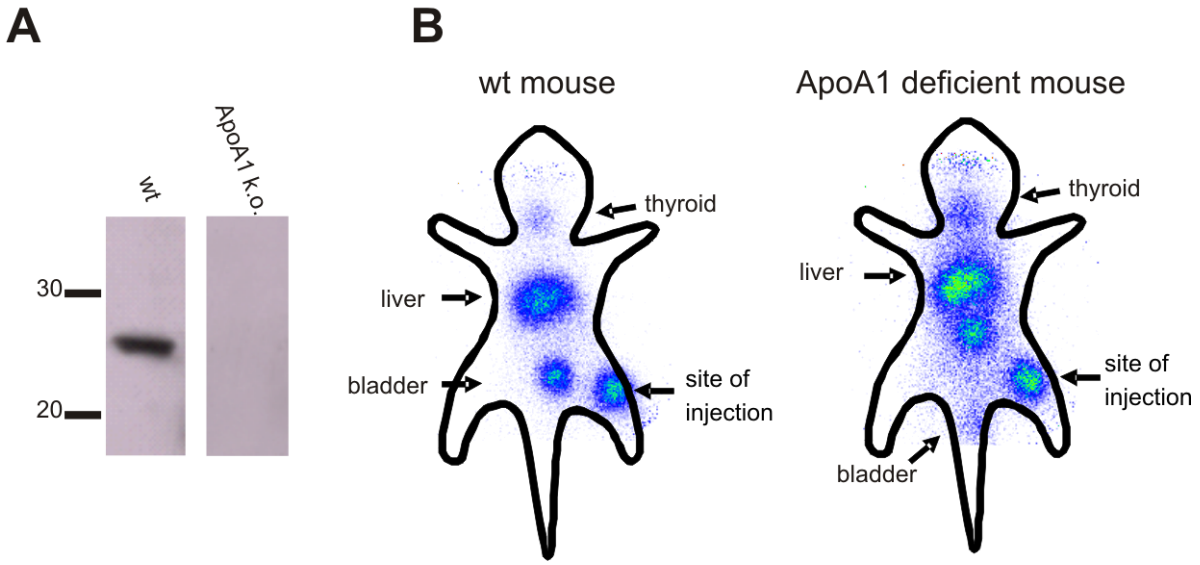

Fig. 3.16: The peptides´ liver tropism is not impaired in ApoA1 deficient mice. I^{125}-labeled HBVpreS/2-48^{myristoyl} was injected subcutaneously into WT C57BL6 mice (left) or C57BL6/ApoA1(-/-) mice (right). Scintigraphic imaging was performed 8h after injection **(B)**. Mice were then sacrificed; liver samples were taken and analyzed by mouse ApoA1-specific western blot **(A)**.Mice were kindly provided by K. Matuschewski.

3.1.7 Addition of HSA or HDL did not influence HBV infection

In the previous experiments, the interaction of preS-peptides with HSA or HDL has been studied. In order to obtain a first hint whether a possible HBV-HSA or HBV-HDL interaction has an influence on HBV-infection, both substances were added to an HBV-infection assay on primary human hepatocytes (PHH) in the presence of fetal calf serum (FCS).

When HSA was added to the infection assay, the amount of secreted HBsAg in the supernatant of day 7 to 12 increased by ~40% **(fig. 3.17 A)** in comparison to the control

infection. Inhibition of infection by wt preS-peptide reduced the HBsAg secretion to about the same level as when no albumin was added.

Addition of purified HDLs lead to a decrease of infection by ~30% in comparison to the control infection **(fig. 3.17 B)**. Again, the addition of preS-peptides reduced infection to control level. The observed effects are only moderate, neither HSA or HDL appeared to have a strong effect on HBV infection. The observation that infection inhibition was not altered confirms indirectly that neither factor has a role in binding of preS-peptides to hepatocytes.

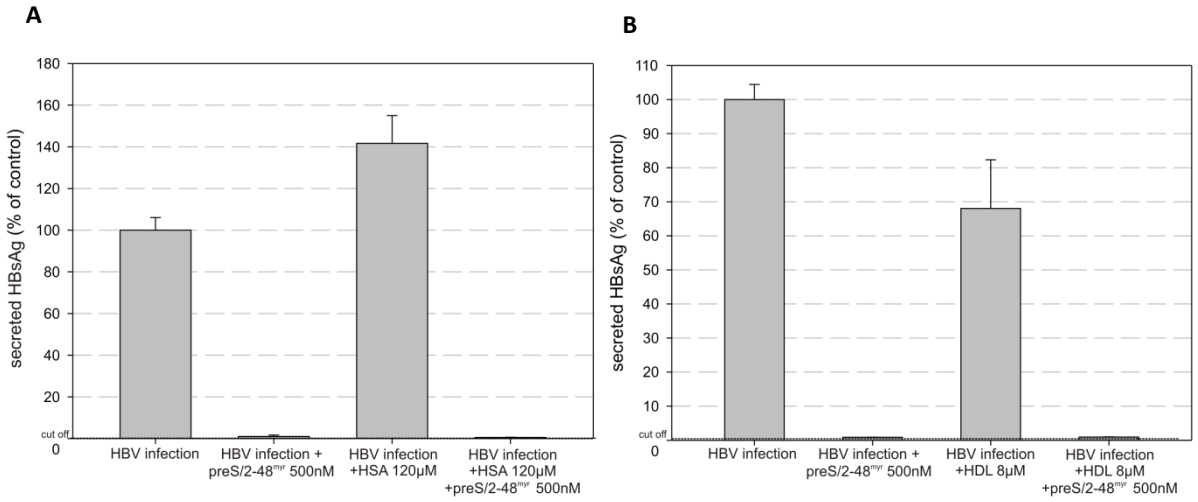

Fig. 3.17: Neither HSA nor HDL have an influence on HBV infection or infection inhibition. PHH were infected with a MOI of 1×10^4 in the absence of inhibitor or presence of 500nM preS-peptide and absence or presence of 120µM HSA **(A)** or 8µM HDL **(B)**. Supernatants from day 7-12 were harvested, secreted HBsAg was measured by quantitative ELISA. Representative data of 3 independent experiments are shown.

3.2 Attempts to identify a cellular interaction partner for HBV preS-peptides

It could be shown that His-tagged HBV preS-peptides containing an aryl azide-moiety (crosslinker-peptides) could efficiently be used for identification of binding partners in human serum (chapter 3.1.1.3). It was therefore assessed whether these peptides would also allow identification of a receptor molecule on hepatocytes.

Therefore, primary hepatocytes from rats were isolated and incubated with either acylated wt CL-peptide, acylated mutant CL-peptide, non-acylated wt CL-peptide or no peptide for 1h at 4°C. Following UV-light exposure, cells were lysed, suspensions were separated from cell debris and subjected to affinity chromatography on a nickel-sepharose column.

Fig. 3.18 shows a typical elution profile from this assay when performed with WT peptide. During application of the sample, the UV-absorption **(fig. 3.18, blue curve)** rose sharply and remained above detection limit. The column was then washed with 5% of the high-imidazole

elution buffer **(fig. 3.18, red curve)**. This led to a relatively high UV-absorption, being caused by unspecifically bound material being washed off. Subsequent elution was performed in three steps: a flat linear gradient over 10 column volumes [2] from 5% to 50% elution buffer, leading to elution of weakly bound molecules; a sharper linear gradient over 5CV from 50% to 100% elution buffer, causing elution of strongly bound substances; and a high-imidazole wash over 10CV at 100% elution buffer. Monitoring of conductivity **(fig. 3.18, green curve)** gave information about the actual increase of the high-salt elution buffer during the elution.

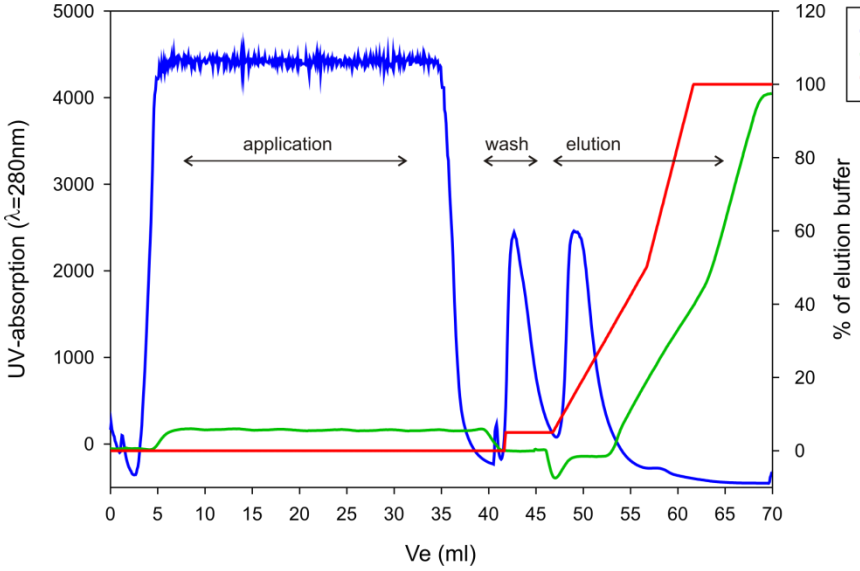

Fig. 3.18: Affinity chromatography of an incubation of wt crosslinker peptide with primary rat hepatocytes. 30ml lysate from cells preincubated with 1µM HBV preS/2-48^{myristoyl}-CL were applied onto a 1ml Ni^{2+} -column; after a low imidazole wash, bound proteins were eluted with a 2-step linear imidazole gradient. During the run, UV-absorption at 280nm and conductivity were monitored.

When elution profiles from these assays performed with the different peptides were compared, no remarkable differences could be observed. The first two large peaks from the column wash and the first linear gradient step appeared in all elution profiles. At the second linear gradient step, however, a shoulder could be detected in the wt-elution profile but not in any of the other elution profiles **(fig. 3.19).**

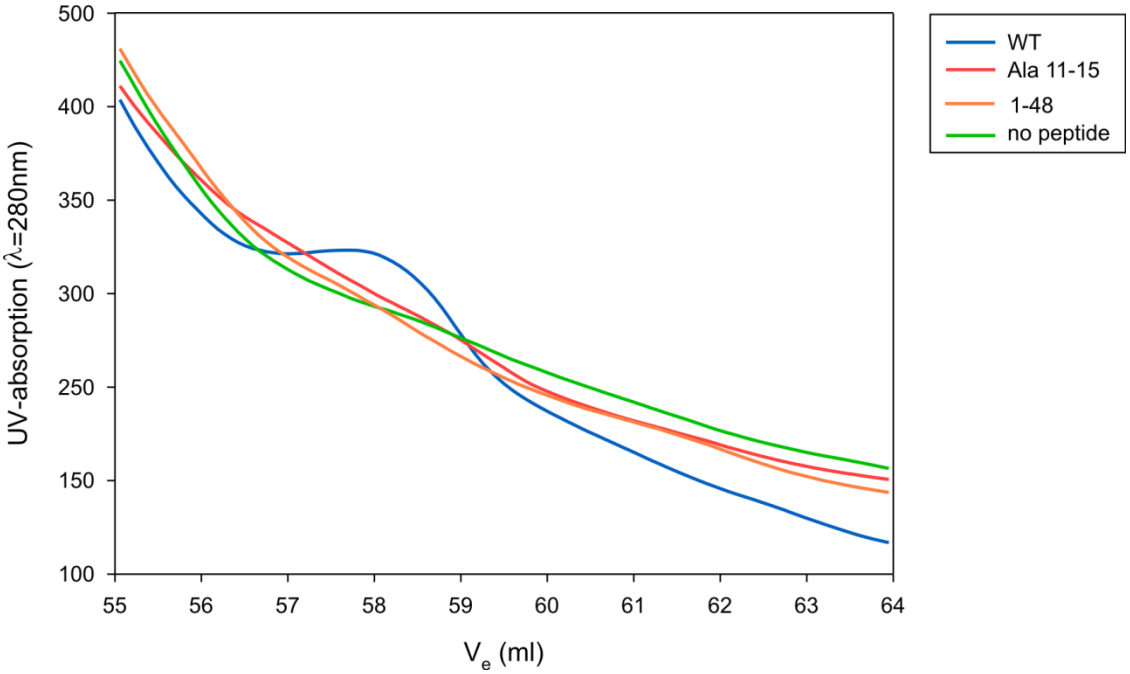

Fig. 3.19: Comparison of the elution profiles from crosslinker assays on primary rat hepatocytes. 30ml lysate from cells preincubated with 1µM HBV preS/2-48^{myristoyl}-CL, 1µM preS/2-48 (Ala 11-15)^{myristoyl}-CL , 1µM preS/1-48-CL or no peptide were applied onto a 1ml Ni^{2+} -column; after a low imidazole wash, bound proteins were eluted with a 2-step linear imidazole gradient. A detail of overlay from the second step is shown.

Elution fractions from these chromatography runs were then analyzed by HBV preS1-specific wb for preS peptide-protein complexes.

Western blots for crosslinker-assay with wt-, mutant and non-acylated peptides are shown in fig. 3.20. For more clarity, elution profiles are overlaid in the wb.

A large amount of protein eluted during the first linear gradient step, visible as background stain in all three wb. In the fractions corresponding to the shoulder in the second linear elution step, a low-molecular weight band (~15 kDa) was visible in the wb for wt **(fig. 3.20 A)**, but not in the wb for acylated mutant **(fig. 3.20 B)** or non-acylated peptide **(fig. 3.20 C)**. Attempts to identify the proteins of this band, however, did not yield results.

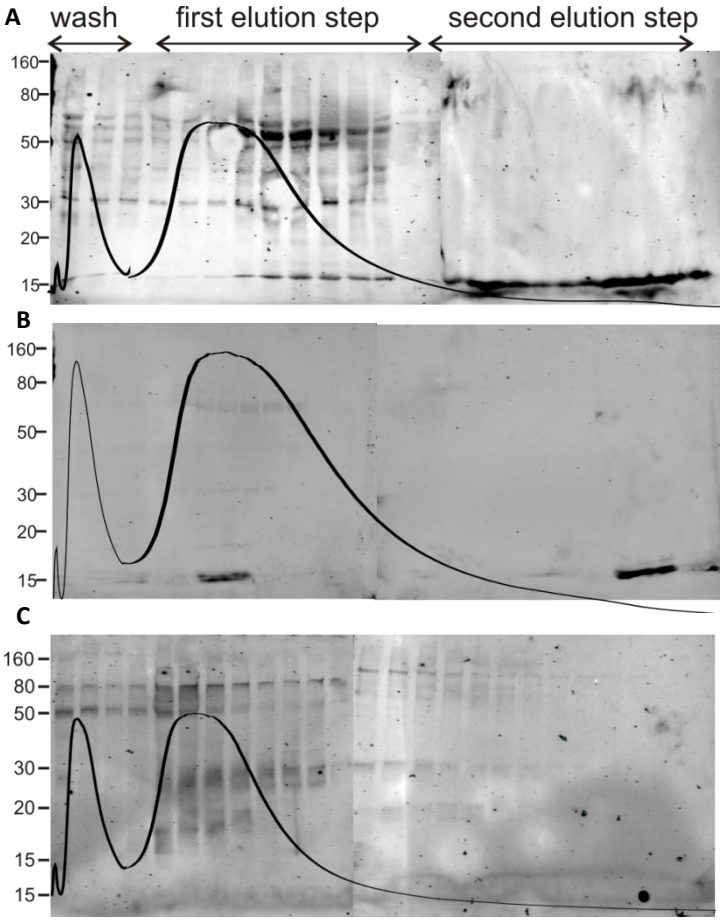

Fig. 3.20: Western blots of elution fractions from crosslinker-assays with wildtype (A), acylated mutant (B) or non-acylated peptide (C). Samples of each elution fraction were applied onto a 12% Lämmli-gel and blotted onto nitrocellulose. Complexes of preS-peptides to cellular proteins were detected by using a HBV preS1-specific antibody (Ma18/7).

In summary, no cellular interaction partner for HBV preS1-derived peptides could be identified.

3.3 Membrane activity of HBV preS-derived peptides

HBV infection has been shown to depend on the presence and intactness of the HBV L-protein preS1-domain [20] and on its N-terminal acylation [28, 42]. Until now, it is unclear how HBV enters hepatocytes, a specific receptor has not been identified (introduction chapter 1.2.6). A crucial step in the entry of enveloped viruses is uncoating. This usually occurs by fusion of the viral membrane with a host cell membrane, either the plasma membrane or an endosomal membrane. A role of the HBV preS-sequence in membrane fusion has been discussed recently [85]. Using a set of preS-derived peptides well characterized for their ability to inhibit HBV-infection [62] and their binding to hepatocytes [64], we assessed these peptides´ membrane activity in a liposome-based leakage assay. Association to membranes was studied by a coflotation assay; electron microscopy studies of preincubated peptides with liposomes were performed to visualize a possible structural alteration.

3.3.1 The liposome-based membrane activity assay

Liposomes containing 8-hydroxypyrene-1,3,6-trisulfonic acid (HPTS), a fluorescent dye, and *p*-xylene-bis-puridinium bromide (DPX), a substance that quenches HPTS when present in high concentration, were used. Incubation with membrane active substances, such as detergents or membrane dissolving or channelizing proteins, leads to leakage of HPTS and DPX from the liposome, thereby dequenching of the HPTS and an increase of fluorescence (fig. 3.21). Here, membrane activity of the preS-peptides was analyzed.

After addition of peptides to liposomes, plates were incubated at 37°C and emission on a HPTS-specific wavelength was measured. After incubation, detergent was added, leading to lysis of all liposomes, dequenching of all HPTS and maximal fluorescence signal. This absorption was set as 100%, values obtained during incubation were calculated as percentage of the lysis value. A schematic representation of this assay is given in fig. 3.21.

This assay can be used in order to determine whether a peptide or protein exhibits membrane activity, i.e. whether it is able to perturb membranes in such a way that the membrane becomes permeable for small molecules. As such, it does not allow the conclusion that a peptide mediates fusion, since no conclusions on fusion of liposomes, but only on leakage of dye can be drawn.

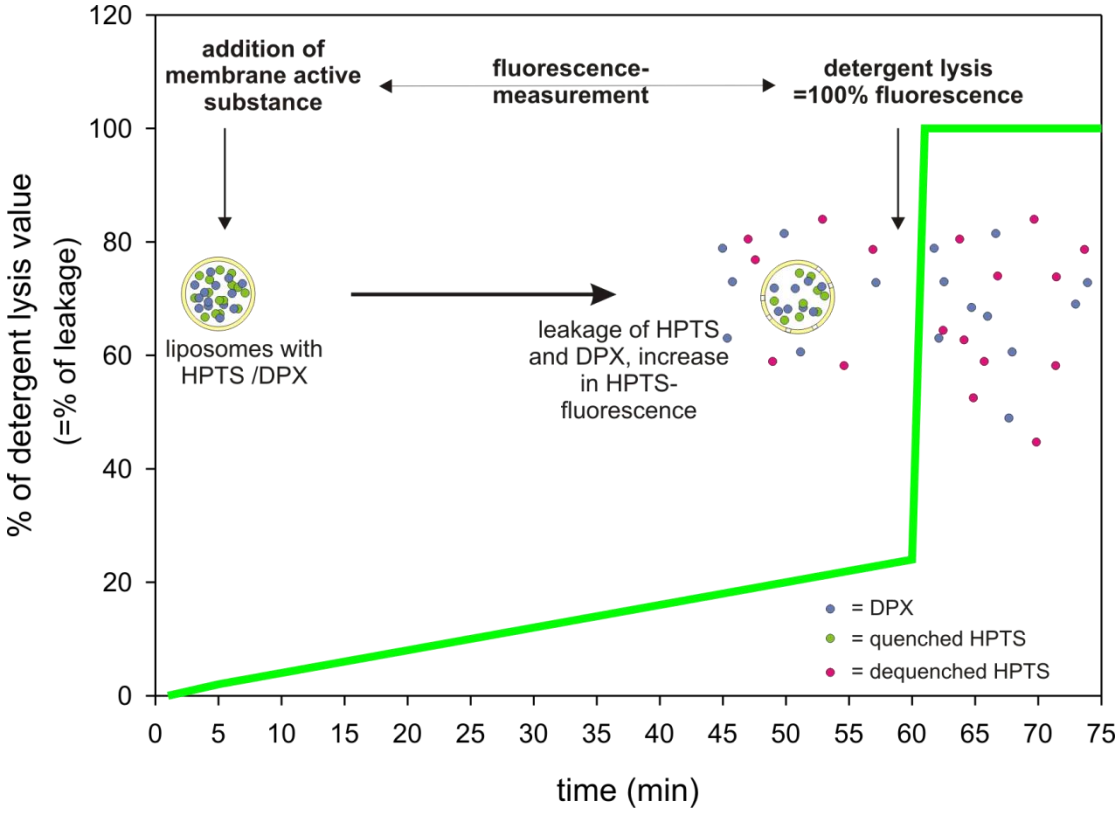

Fig. 3.21: Principle of the membrane activity assay. Liposomes containing HPTS and DPX (in a concentration that quenches HPTS-fluorescence) are incubated with a membrane active substance. This substance leads to leakage of HPTS and DPX from the liposomes and therefore dequenching of HPTS. After incubation time, detergent is added in order to lyse all liposomes. During incubation, fluorescence is measured; the value obtained by detergent lysis is set as 100%.

In all the following experiments, liposomes consisting of phosphatidylserine (PS) and phosphatidylcholine (PC) were used.

3.3.1.1 The wildtype PreS-peptide showed a concentration-dependent membrane activity

First, it was addressed whether a wt preS-peptide is membrane active. Therefore, increasing concentrations of a wt peptide were added to liposomes. Addition of 50 µM stearoylated wildtype peptide led to a ~9% increase in fluorescence over 120min **(fig. 3.22, orange curve)**; this activity was found to increase at 100µM peptide **(fig. 3.22, red curve)**. No leakage was observed when no peptide was added **(fig. 3.22, green curve)**, indicating that the liposomes used here were stable under the chosen conditions. The HBV preS-peptide therefore exerts membrane activity in a concentration-dependent manner.

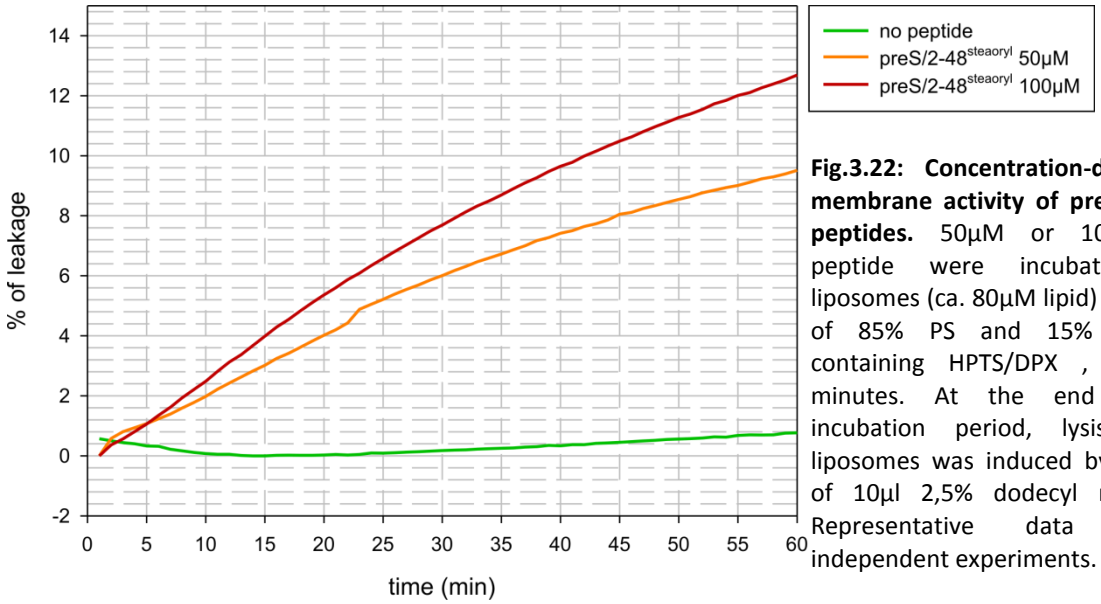

Fig.3.22: Concentration-dependent membrane activity of preS-derived peptides. 50µM or 100µM wt peptide were incubated with liposomes (ca. 80µM lipid) consisting of 85% PS and 15% PC and containing HPTS/DPX , over 60 minutes. At the end of the incubation period, lysis of all liposomes was induced by addition of 10µl 2,5% dodecyl maltoside. Representative data of 3 independent experiments.

3.3.1.2 Membrane activity of preS depended on the integrity of the essential site

Next, it was analyzed whether the correct sequence and the N-terminal acylation are required for the peptide´s membrane activity. Therefore, a peptide where 5 amino acids in the essential site had been replaced by their respective d-amino acids or a non-acylated peptide were used. Addition of the acylated mutant peptide did not lead to a significant increase in fluorescence **(fig. 3.23, orange curve)** nor was leakage observed when a non-acylated peptide was added **(fig. 3.23, blue curve)**. The essential site and the acylation are required for the peptide´s membrane binding and inhibitory activity, showing thus a strong correlation between infection inhibtion, membrane binding and membrane activity.

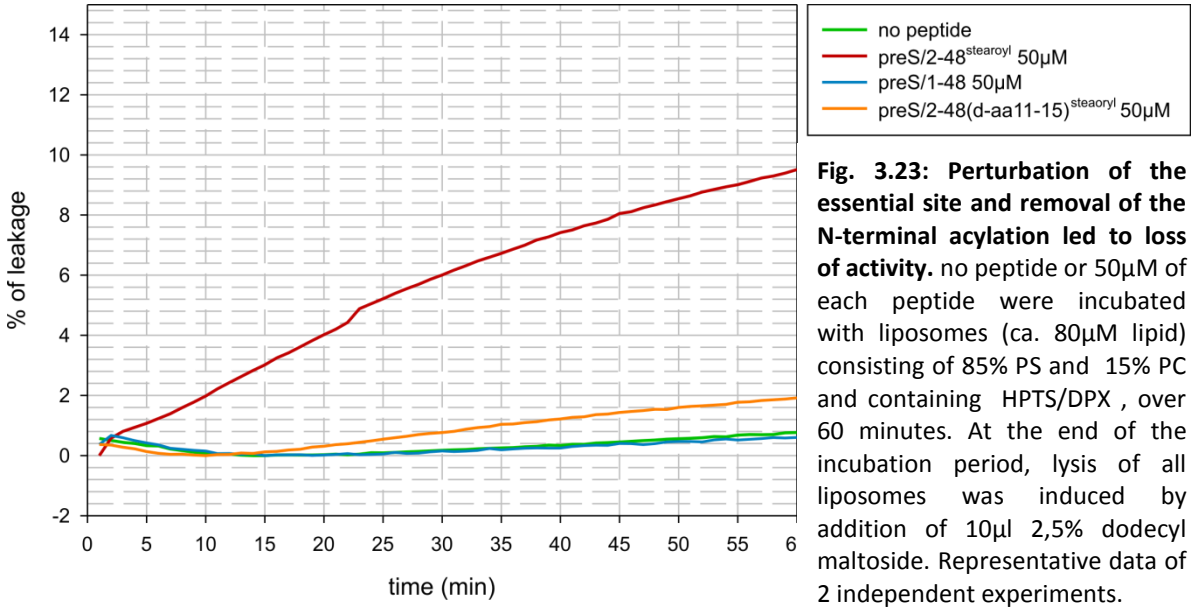

Fig. 3.23: Perturbation of the essential site and removal of the N-terminal acylation led to loss of activity. no peptide or 50µM of each peptide were incubated with liposomes (ca. 80µM lipid) consisting of 85% PS and 15% PC and containing HPTS/DPX , over 60 minutes. At the end of the incubation period, lysis of all liposomes was induced by addition of 10µl 2,5% dodecyl maltoside. Representative data of 2 independent experiments.

3.3.1.3 Deletions of the N-terminal amino acids were tolerated up to amino acid 7

The N-terminus of the preS-peptide is required for its inhibitory activity; deletion are tolerated only up to aa 6 [62]. Therefore, the role of the preS-N-terminus in membrane activity was assessed. Peptides with N-terminal deletions up to aa 9 or a peptide with the 11 additional amino acids from genotype B were used. Comparison of these peptides with regard to their membrane activity showed that peptides lacking 3 aa **(fig. 3.24, yellow curve)** or 5aa **(fig. 3.24, dark blue curve)** perturb membranes similar to wt peptides **(red curve)**. Deletion of 7aa **(fig. 3.24, pink curve)** reduced fluorescence signal stronlgy. Interestingly, a peptide comprising the additional N-terminal 11 amino acids of genotype B **(fig. 3.24, light blue curve)** led to a marked increase in membrane activity, showing a five times increase compared to the 2-48 peptide. This is in contrast to infection inhibition by preS-peptides, where the additional 11 aa of genotype B did not increase infection inhibition [62] . Taken together, this indicates that the extreme N-terminal part of preS1 is involved in perturbation of lipid membranes.

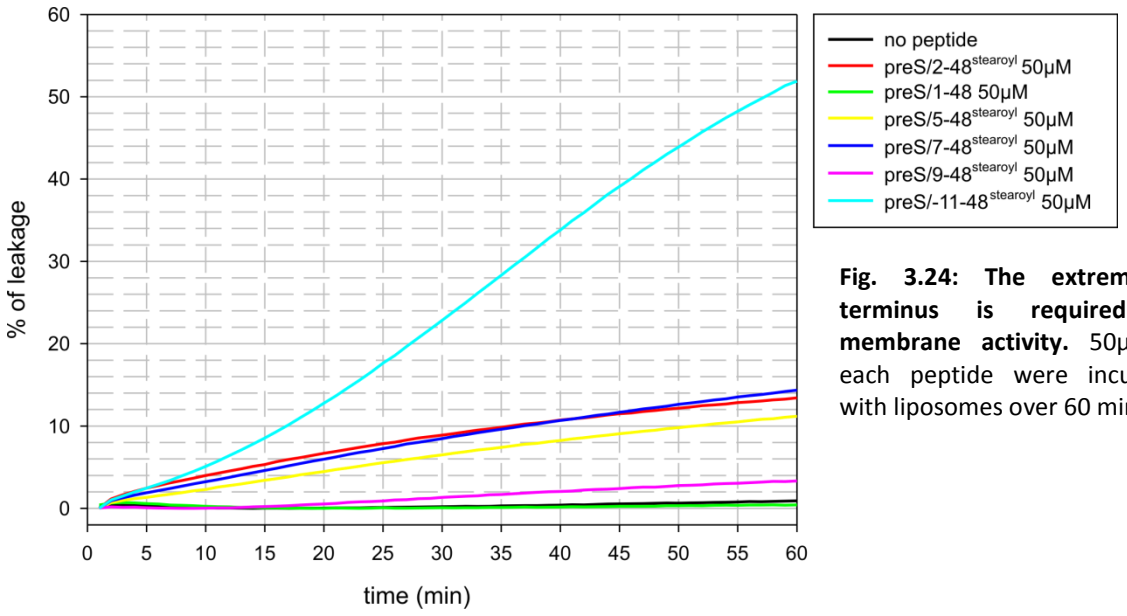

Fig. 3.24: The extreme N-terminus is required for membrane activity. 50µM of each peptide were incubated with liposomes over 60 minutes.

3.3.1.4 The N-terminal acylation required a minimal length for membrane activity

Due to their hydrophobicity, acylations of proteins or peptides are often determinants for membrane interaction, being responsible for initial contact with membranes or targeting a protein to certain membrane compartments [134,135]. The preS-acylation is therefore likely to play a role in the peptide´s membrane activity. The membrane activity assay was therefore performed with peptides carrying shorter acylations.

Incubation of liposomes with a C5- **(fig. 3.25, orange curve)** or C8-acylated preS-peptide **(blue curve)** did not raise the fusion signal over the background signal obtained when no peptide was added **(fig. 3.25, green curve).** A C14-acylated peptide **(fig. 3.25, red curve)** did induce leakage similar to values observed before for C18-acylated peptides.

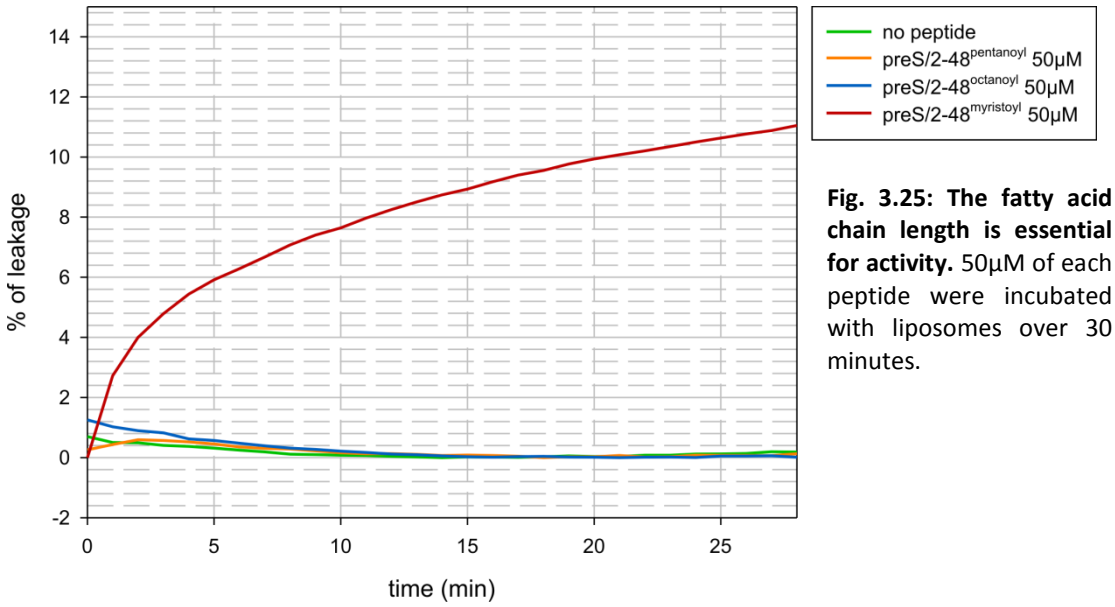

Fig. 3.25: The fatty acid chain length is essential for activity. 50µM of each peptide were incubated with liposomes over 30 minutes.

Also, the activity of a C14 and a C18-acylated peptide whose sequence corresponded to the consensus sequence from different HBV-genotypes was compared to the activity of the genotype D stearoylated wildtype, since the consensus-peptide shows an increased inhibitory activity in HBV-infection. Comparison of a C14- **(fig. 3.26, blue curve)** to a C18-acylated peptide **(fig. 3.26, green curve)** showed an increase in fluorescence by ~7% with increasing acylation chain length. Interestingly, a stearoylated peptide with a consensus sequence from the different HBV genotypes **(fig. 3.26, green curve)** was more active than a stearoylated peptide with genotype D wildtype sequence **(3.26, red curve).**

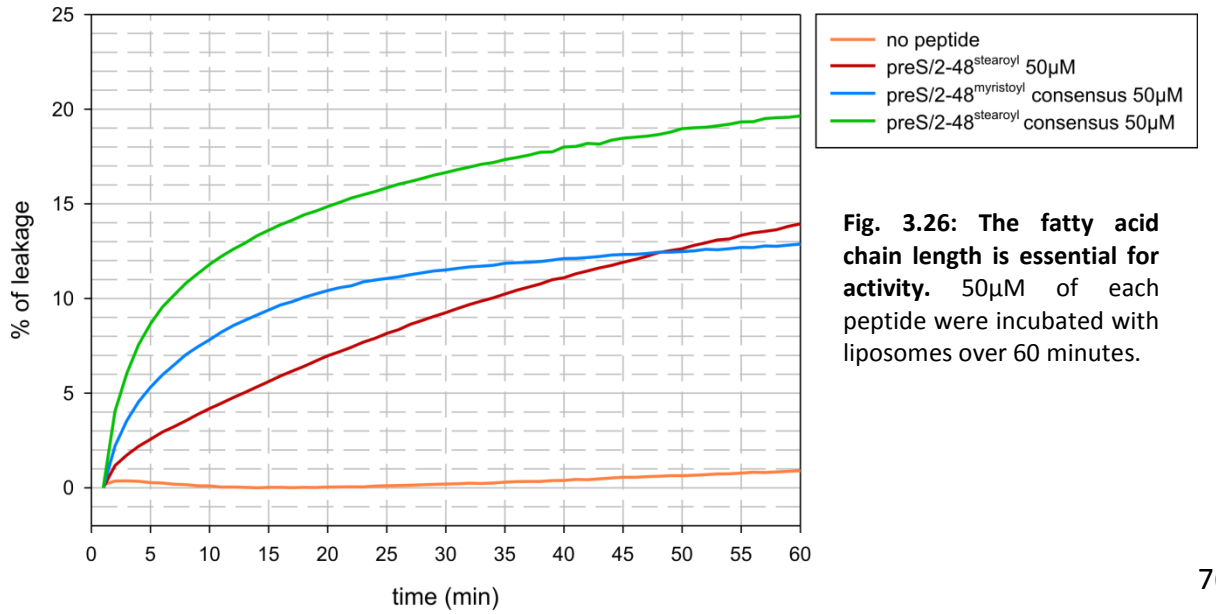

Fig. 3.26: The fatty acid chain length is essential for activity. 50µM of each peptide were incubated with liposomes over 60 minutes.

Taken together, it was shown that HBV preS-peptides were able to disturb phospholipid membranes depending on their sequence integrity and on the N-terminal acylation, which had to be of a minimal length. These features correlated with their ability to inhibit HBV infection and with their specificity in hepatocyte membrane binding, indicating a possible role in fusion of the viral membrane with a host cell membrane.

3.3.2 After coincubation, preS-peptides showed coflotation with liposomes

In order to assess whether the observed membrane activity of preS-peptides results from weak, transient interaction or is the result of a binding or insertion, coflotation assays were performed. Therefore, acylated wt, non-acylated wt or acylated mutant peptides were incubated with or without liposomes for 1h at 37°C. In a subsequent ultracentrifugation on a nycodenz-gradient, liposomes were floated; the usage of fluorescently labeled liposomes allowed a visual control of their flotation (data not shown). These gradients were then fractionated, the fractions were assessed for their peptide content in wb using a preS1-specific antibody. As input control, input peptide was loaded.

When wt peptide was incubated without liposomes, ultracentrifugation led to accumulation of all peptide signal on the bottom of the gradient **(fig. 3.27 A, left panel).** After addition of liposomes to the incubation, a part of the peptide signal was detectable on the top of the gradient, indicating coflotation of peptides with liposomes **(fig. 3.27 A, right panel)**. Performing this assay with a non-acylated peptide did not lead to peptide flotation **(fig. 3.27 B);** interestingly, an acylated mutant peptide did float up when incubated with liposomes **(fig. 3.27 C).**

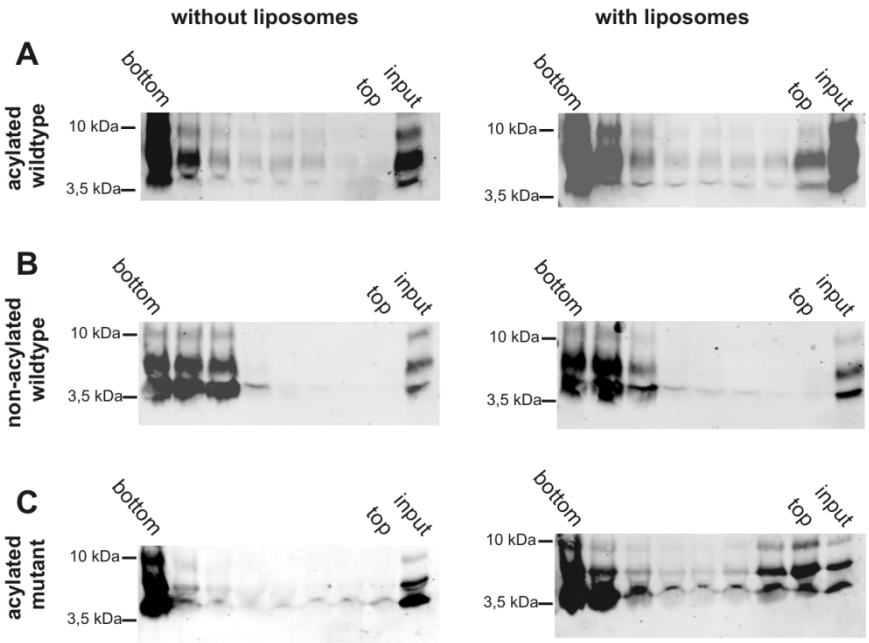

Fig. 3.27: Acylation-dependent, sequence independent binding of HBV preS-peptides to phospholipid liposomes.
50µM of peptide and 640µM lipid or buffer were coincubated at 37°C for 1h. Subsequent ultracentrifugation on a nycodenz-gradient (40%-30%-buffer) for 1h at 380.000×g was followed by fractionation. All fractions were subjected to SDS-PAGE and transferred onto nitrocellulose-membranes. HBVpreS-peptides were detected using a preS1-antibody (Ma18-7). Representative data of 2 independent experiments.

PreS-peptides therefore showed an acylation-dependent binding to liposomes which was strong enough to withstand the relatively harsh conditions of ultracentrifugation. This hints towards an insertion of the fatty acid and possibly a part of the peptide into the phospholipid membrane.

3.3.3 HBV preS-peptides caused structural alterations in liposomes

In order to analyze whether the membrane activity described above leads to disruption and alteration of liposomal membranes, increasing amounts of peptides were coincubated with liposomes and subsequently analyzed by negative stain electron microscopy. For reduction of staining background, liposomes were prepared in a low salt phosphate buffer; peptides were dissolved in the same buffer.

Without the addition of peptide, liposomes of different sizes (100nm - 500nm) could be observed **(fig. 3.28 A)**, appearing to some extent folded, but generally intact. When the incubation was done in the presence of 8µM wt peptide, very little membranous structures were left; instead, filamentous shapes associated with electron dense material could be observed **(fig. 3.28 B)**. An increase of the peptide concentration to 16µM led to almost complete disappearance of intact liposomes, aggregations of electron dense material could be observed **(fig. 3.28 C).** These morphological changes could not be observed when liposomes were incubated with an acylated mutant **(fig. 3.28 D)** or a non-acylated peptide **(fig. 3.28 E).** At higher peptide concentrations, electron dense material was found to be associated to liposomes, but this did not seem to affect their structure.

In conclusion, HBV wt preS-peptides appear to have a dose-dependent effect on liposomal integrity which is absent in mutant peptides.

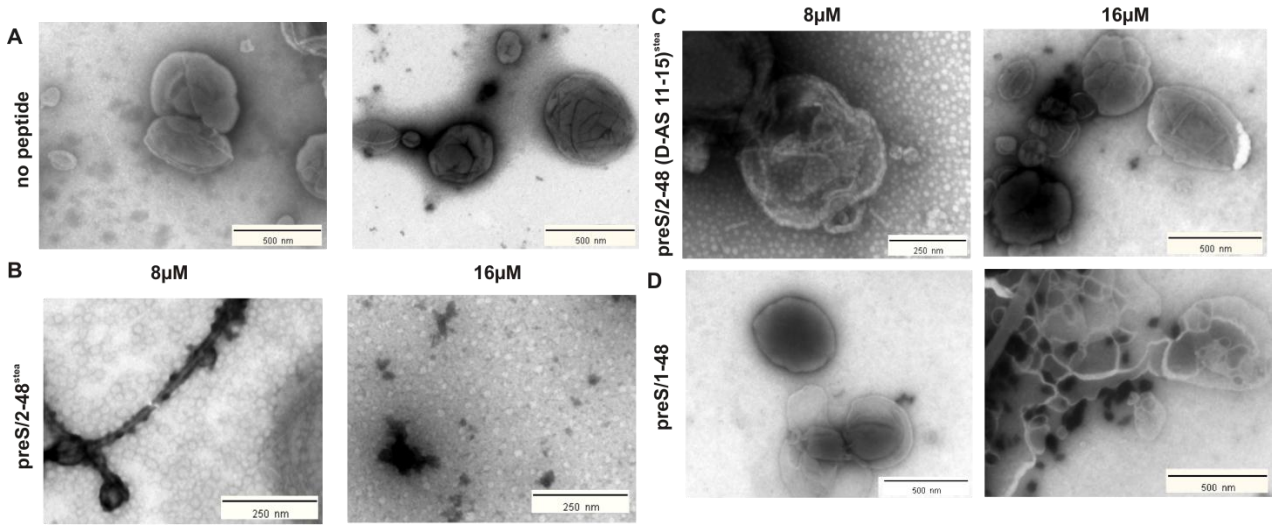

Fig. 3.28: Sequence- and acylation dependent structural membrane alterations induced by preS-peptides. Liposomes (3mM lipid) were incubated without or with (8-16 µM) of acylated wildtype, non-acylated wildtype or acylated mutant peptides for 1h at 37°C. After adsorption onto pioloform-coated EM-grids, negative staining with 1% uranyl acetate was performed. Micrographs were taken on a Leica EM 900. Representative data of 3 independent experiments.

3.4 Analysis of HBV and HDV infection on Hepatocytes from different rodent species

HBV is known to have a very restricted host range (see introduction chapter 1.2). This is generally assumed to be due to the specificity of the unknown HBV-receptor, thought to be present only in a small range of species. However, HBV infects primary hepatocytes from *Tupaia belangeri* [36], a tree shrew belonging to the order of Scadentia within the clade of Supraprimates which also comprises the Primates, the Rodentia (rodents) and the Lagomorpha (hares and rabbits). The fact that HBV preS-derived peptides bind to primary hepatocytes from different species within this clade raised the question whether other species can be infected with HBV.

HDV is thought to share a common entry pathway with HBV; yet, since HDV is an RNA-virus replicating without DNA-intermediate, it is less likely to face restriction of replication once it successfully entered a cell. Therefore, analysis of HDV infection in the different species was included.

Rats, rabbits, hamsters and guinea pigs were chosen as animals for preparation of primary hepatocytes that were then infected with either HBV or HDV. All infections were controlled by parallel infection in the presence of the inhibitory preS-peptide in order to assess specificity.

Furthermore, cells were infected with woodchuck-hepatitis delta virus (WHDV), a virus originating from an HDV-infection of woodchucks that were infected with woodchuck hepatitis virus (WHV) [128]. WHDV therefore carries the envelope proteins from WHV. Belonging to the order of rodentia, woodchucks are phylogenetically close to rats, guinea pigs and hamsters.

As read out, quantitative ELISA of secreted HBsAg and Immunofluorescence analysis (IF) was performed for HBV infections. The HDV-infections were assessed by IF only.

All infection experiments were done twice; a parallel HepaRG infection, using one inoculum mastermix, was performed every time.

3.4.1 HBV infection

3.4.1.1 HBV preferentially infected differentiated HepaRG cells

As it has been described before, differentiated HepaRG cells are susceptible to HBV-infection [38]. IF analysis of infected HepaRG cells revealed a generally cytoplasmatic and less often nuclear distribution of the core antigen. Infection was clearly restricted to the so-called "islands" of differentiated cells. Addition of 500nM HBV preS1-peptide led to a strong reduction in HBV-infection **(fig. 3.29)**, as described by literature.

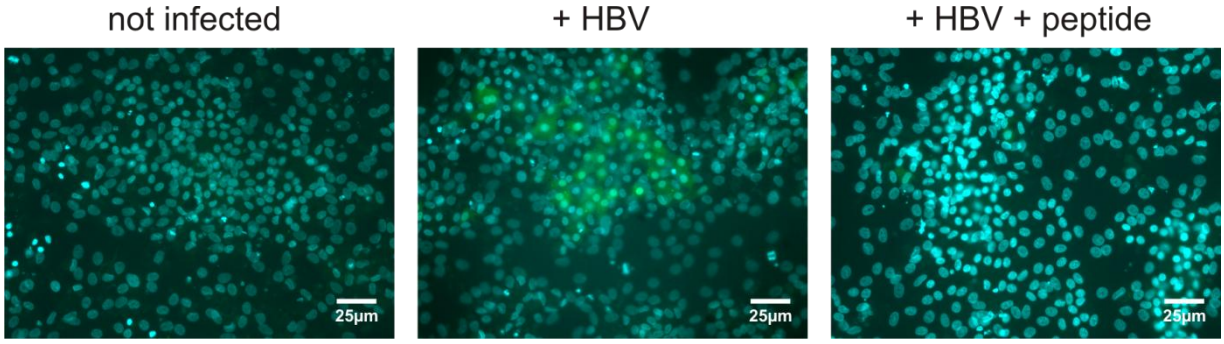

Fig. 3.29: Infection of HepaRG cells with HBV. Differentiated HepaRG cells were inoculated with an multiplictiy of infection [24] of 10^4 for 16h in the absence or presence of 500nM HBVpreS/2-48^{myr}. On day 12 p.i., cells were fixed, permeabilized and stained for HBcAg. Representative data of 8 independent experiments.

3.4.1.2 Primary hepatocytes from rat and rabbit were not susceptible to HBV infection

Hepatocytes from rat (PRH) or rabbit (PRaH) were prepared as described in material and methods and infected on day 1 after isolation with HBV. Analysis of HBsAg in SN from day 7-12 p.i. showed no secreted antigen in the case of either species **(fig. 3.30).**

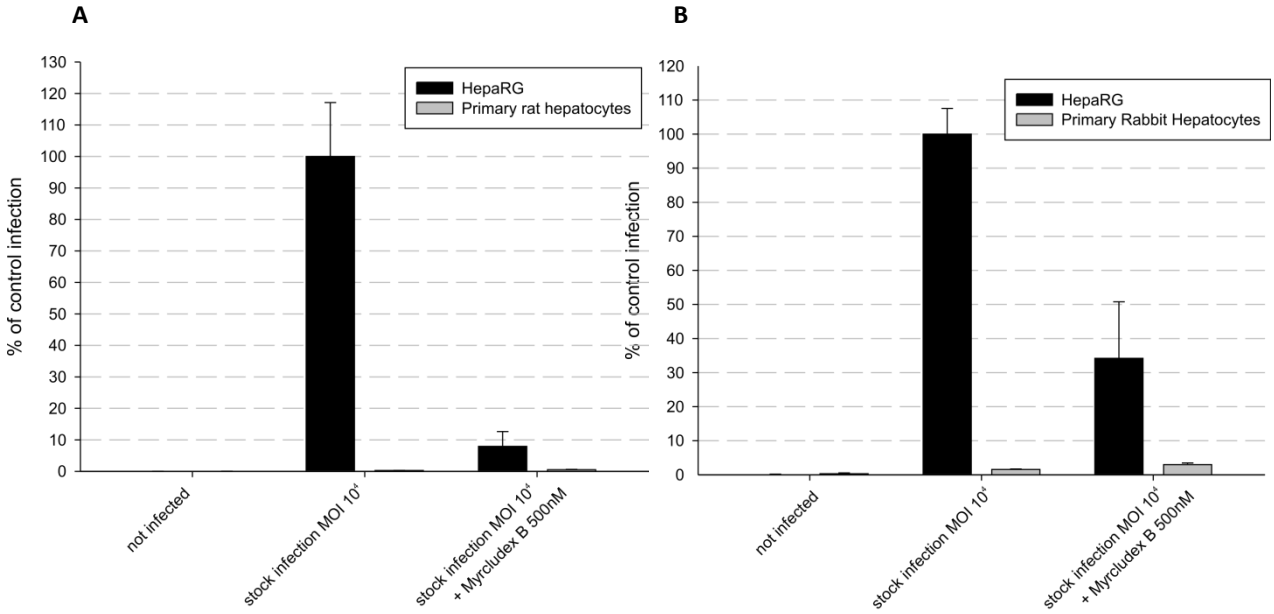

Fig. 3.30: HBV infection of primary rat (A) or rabbit (B) hepatocytes. On day 1 after isolation, cells were infected for 16h with a MOI of 10^4 in the absence or presence of 500nM HBVpreS/2-48^{myr}. A control infection of HepaRG cells was done in parallel with an inoculum mastermix. SN of day 7-12 were harvested, secreted HBsAg was measured by ELISA and is expressed as percentage of control infection of HepaRG. Representative data of 2 independent experiments.

Immunofluorescence of these cells showed no HBcAg specific stain in cells from either species **(fig. 3.31 and fig. 3.32)**, confirming the above results. It has to be mentioned that PRH were found to be very sensible to seeding density and were difficult to cultivate, detaching from plates or forming clumps within two days after plating. Due to this, focusing on a single cell layer in fluorescence microscopy proved to be challenging.

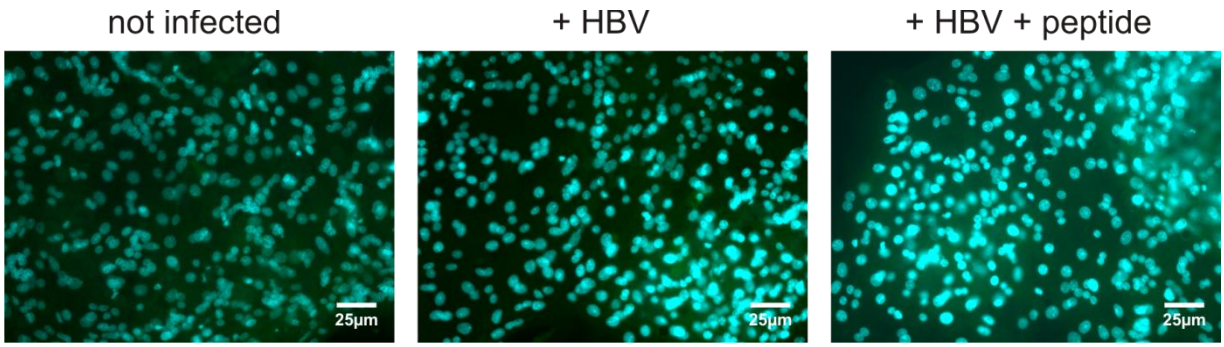

Fig. 3.31: Infection of PRH with HBV. Freshly isolated PRH were inoculated with an MOI of 10^4 for 16h in the absence or presence of 500nM HBVpreS/2-48^{myr}. On day 12 p.i., cells were fixed, permeabilized and stained for HBcAg. Representative data of 2 independent experiments.

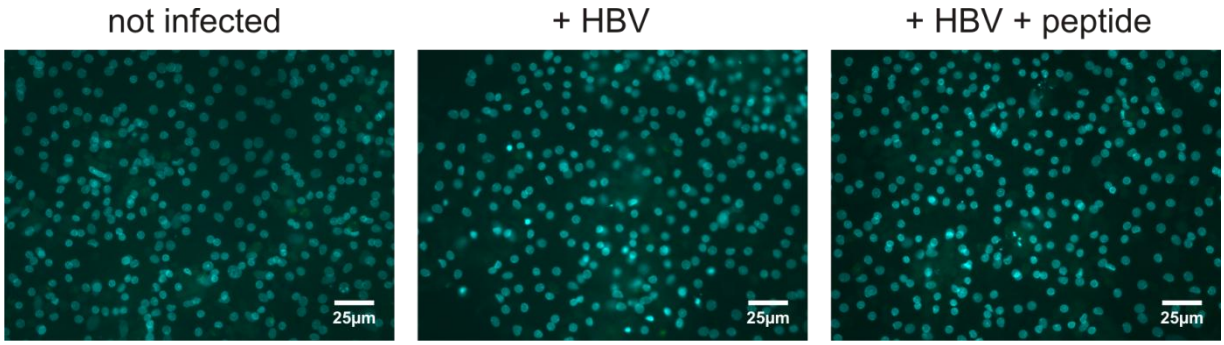

Fig. 3.32: Infection of PRaH with HBV. Freshly isolated primary rabbit hepatocytes were infected with an MOI of 10^4 for 16h in the absence or presence of 500nM HBVpreS/2-48^{myr}. On day 12 p.i., cells were fixed, permeabilized and stained for HBcAg. Representative data of 2 independent experiments.

3.4.1.3 Primary hepatocytes from hamster and guinea pig showed susceptibility to HBV

Interestingly, infection of primary hepatocytes from hamster (PHaH) and guinea pig (PGH) led to secretion of HBsAg into the supernatant of day 7-12 after infection **(fig. 3.33).** Infection of PHaH led to secretion levels reaching ~80% of the HepaRG control infection and could be reduced by addition of preS/2-48^{myristoyl} to ~15%. Infection of PGHs led to HBsAg levels of ~60% of the control infection; on these cells, infection could not be inhibited with the peptide.

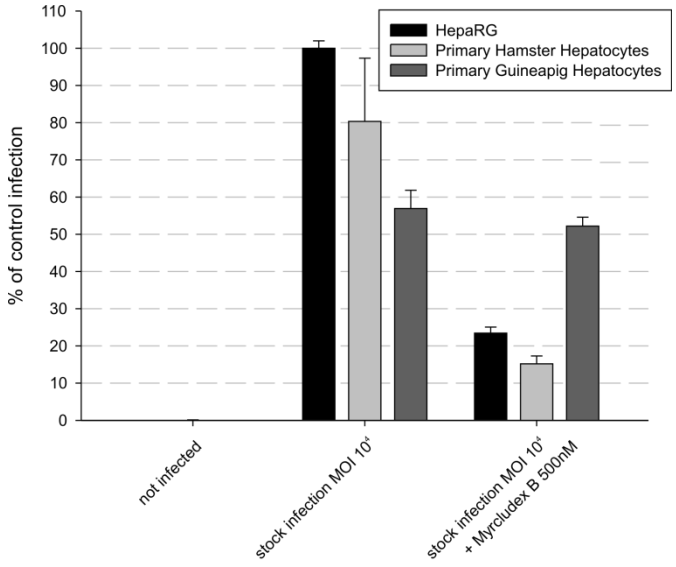

Fig. 3.33: HBV infection of primary hepatocytes from hamster (light grey bars) or guinea pig (dark grey bars). On day 1 after isolation, cells were infected for 16h with a MOI of 10^4 in the absence or presence of 500nM HBVpreS/2-48^{myr}. A control infection of HepaRG cells was done in parallel with an inoculum mastermix. SN of day 7-12 were harvested, secreted HBsAg was measured by ELISA and is expressed as percentage of control infection of HepaRG. Representative data of 2 independent experiments.

This observation could be confirmed by immunofluorescence against HBcAg **(fig. 3.34).** The typical cytoplasmatic staining, forming either speckles or being equally distributed, was detectable in cells from both species. Only few infected cells could be detected in the PHaH-infection when the preS-peptide was added.

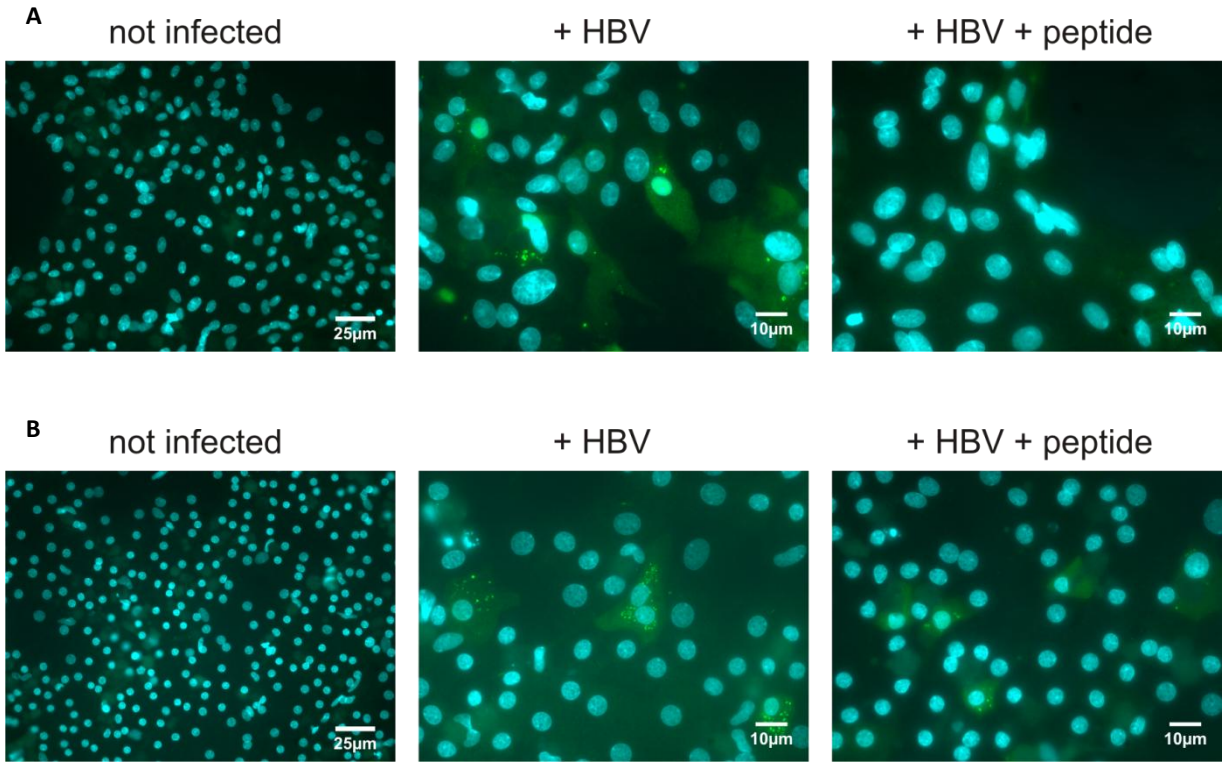

Fig.3.34: Infection of PHaH or PGH with HBV. Freshly isolated primary hepatocytes from hamster **(A)** or guinea pig **(B)** were infected with an MOI of 10^4 for 16h in the absence or presence of 500nM HBVpreS/2-48^{myr}. On day 12 p.i., cells were fixed, permeabilized and stained for HBcAg. Representative data of 2 independent experiments.

3.4.2 HDV infection

3.4.2.1 Infection of HepaRG with HDV led to typical nuclear staining

When inoculated with serum from HDV-infected patients, HepaRG cells got infected with HDV. Immunofluorescence staining against the HDAg led to a typical nuclear staining which is due to the HDsAg present in the nucleus where it promotes replication (introduction chapter 1.5.4). This HDV infection could be inhibited with the preS-peptide **(fig. 3.35).** HepaRG cells also proved to be susceptible to infection with the Woodchuck HDV. This infection could not be inhibited by addition of the HBV preS1-derived peptide. In the WHDV-infection, the HDAg accumulated preferentially in the nucleus; an occasional cytoplasmatic stain could be observed.

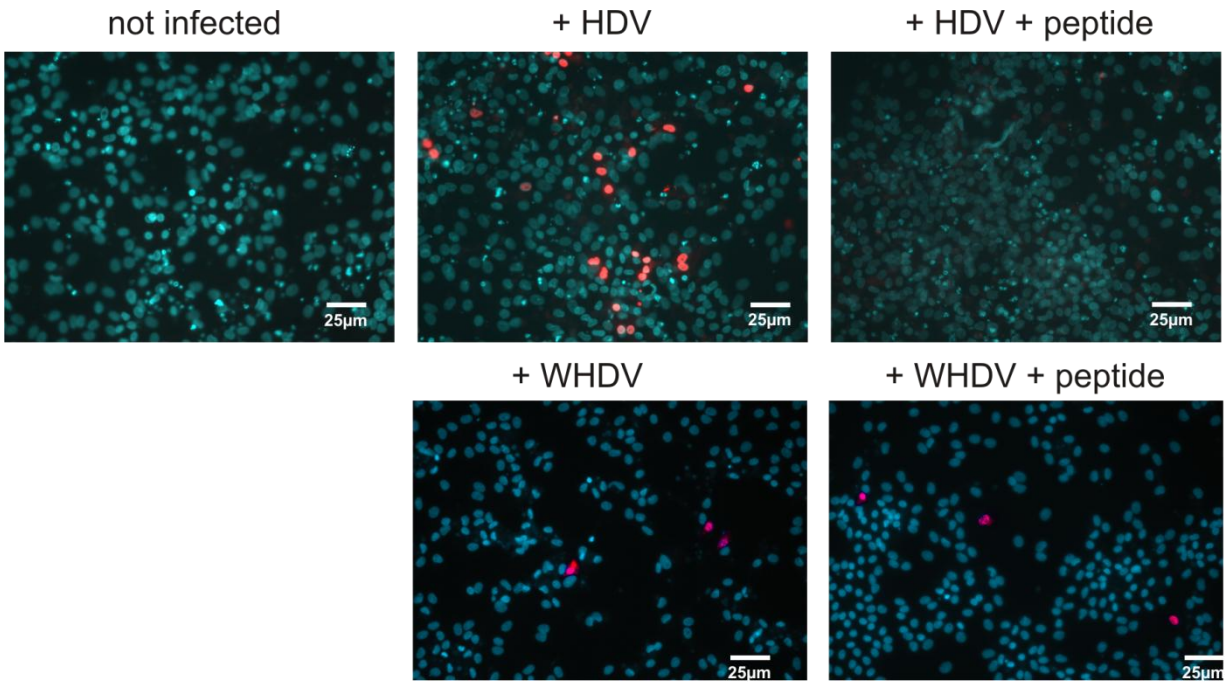

Fig. 3.35: Infection of HepaRG cells with HDV and WHDV. Differentiated HepaRG cells were inoculated with serum from a HDV-positive patient or serum from WHV-HDV-infected woodchucks for 16h in the absence or presence of 500nM HBVpreS/2-48^{myr}. On day 5 p.i., cells were fixed, permeabilized and stained for HDAg. Representative data of 2 independent experiments.

3.4.2.2 Primary rat hepatocytes are not susceptible to HDV but to WHDV

When PRH were incubated wit HDV-positive serum, no infection could be detected by IF **(fig. 3.36)**. A high background staining was often visible, forming blot-like dots between cells. Since no specific nuclear staining was observed, this was not regarded as HDV-infection. However, these cells were susceptible to WHDV infection.

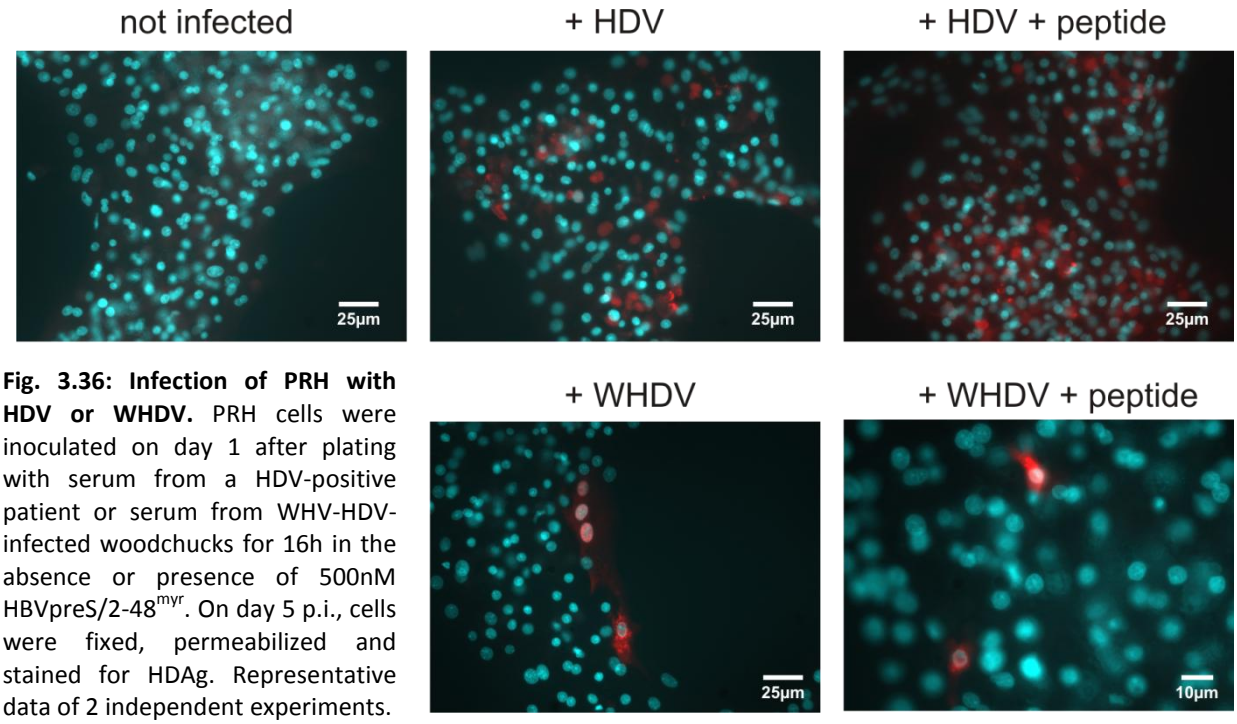

Fig. 3.36: Infection of PRH with HDV or WHDV. PRH cells were inoculated on day 1 after plating with serum from a HDV-positive patient or serum from WHV-HDV-infected woodchucks for 16h in the absence or presence of 500nM HBVpreS/2-48^{myr}. On day 5 p.i., cells were fixed, permeabilized and stained for HDAg. Representative data of 2 independent experiments.

3.4.2.3 Primary rabbit hepatocytes could be infected with HDV at a low rate

Inoculation of PRaH with HDV led to a positive staining in IF **(fig. 3.37)**, yet only very few cells were found to be infected. This infection was found to be sensitive to inhibition by the preS-peptide, since no infected cell could be detected in cells treated with HDV and preS-peptide. PRaH cells could also be infected with WHDV; addition of the preS-peptide did not lead to abrogation of WHDV infection.

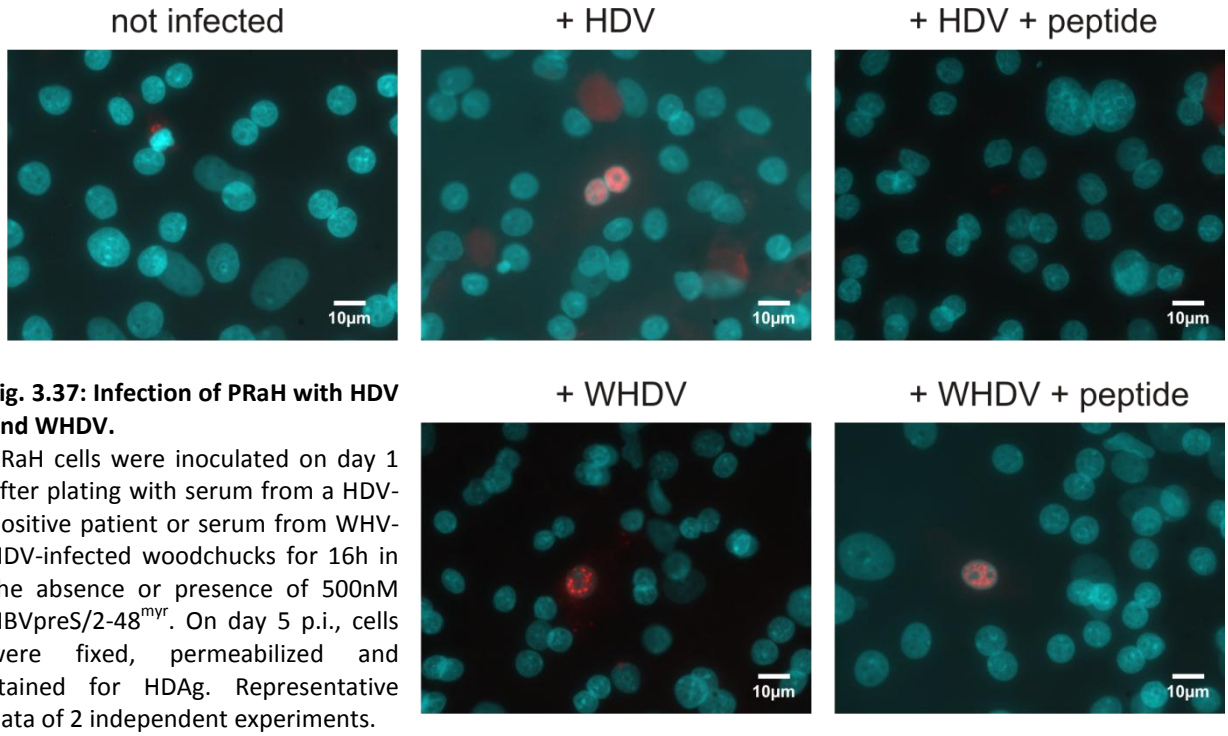

Fig. 3.37: Infection of PRaH with HDV and WHDV.
PRaH cells were inoculated on day 1 after plating with serum from a HDV-positive patient or serum from WHV-HDV-infected woodchucks for 16h in the absence or presence of 500nM HBVpreS/2-48^{myr}. On day 5 p.i., cells were fixed, permeabilized and stained for HDAg. Representative data of 2 independent experiments.

3.4.2.4 Primary hamster hepatocytes and primary guinea pig hepatocytes were not susceptible to HDV but could be infected with WHDV

Infection of PHaH with HDV did not lead to any detectable positive staining **(fig. 3.38)**. A background staining as described for PRH was found; its blot-like appearance, however, did not convincingly look like infected cells. PHaH were found to be susceptible to WHDV infection, although this resulted in a relatively weak, dot-like cytoplasmatic staining. Since this stain was always associated to nuclei and in the focal plane, it was seen as real infection. As for PRaH, WHDV infection could not be inhibited by addition of the preS-peptide.

The same was shown for HDV and WHDV infection of PGH **(fig. 3.39)**. Again, background staining was observed in the case of HDV-infection. WHDV led, as for PHaH, to cytoplasmatic staining in infected cells.

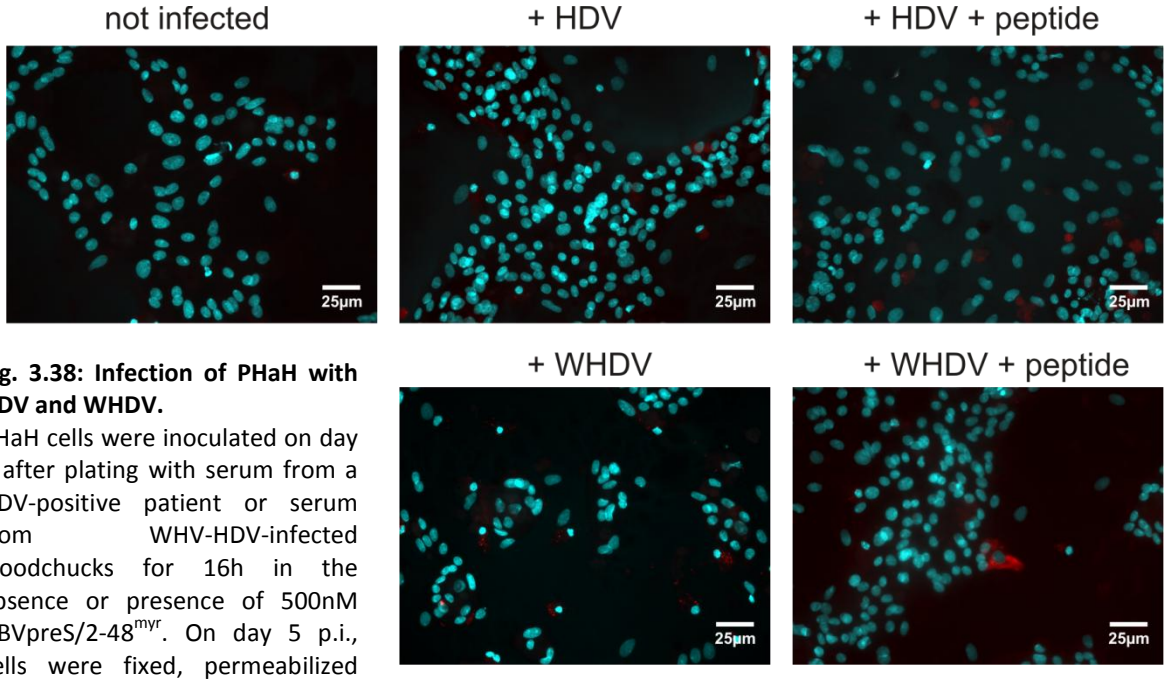

Fig. 3.38: Infection of PHaH with HDV and WHDV.
PHaH cells were inoculated on day 1 after plating with serum from a HDV-positive patient or serum from WHV-HDV-infected woodchucks for 16h in the absence or presence of 500nM HBVpreS/2-48^{myr}. On day 5 p.i., cells were fixed, permeabilized and stained for HDAg. Representative data of 2 independent experiments.

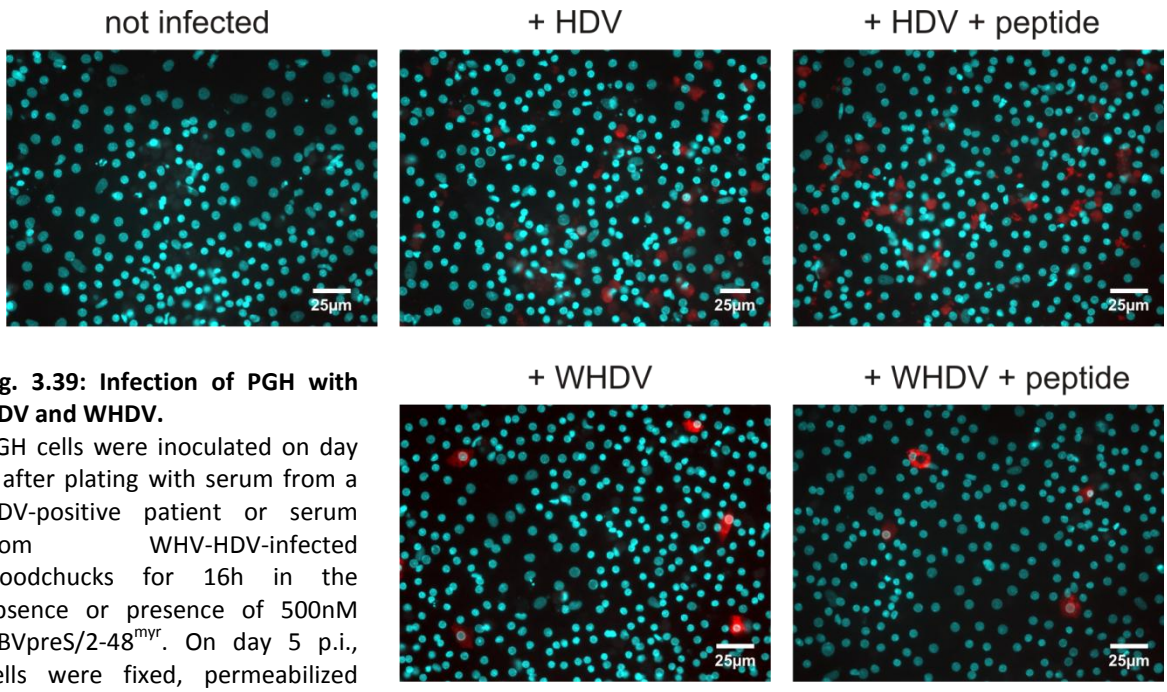

Fig. 3.39: Infection of PGH with HDV and WHDV.
PGH cells were inoculated on day 1 after plating with serum from a HDV-positive patient or serum from WHV-HDV-infected woodchucks for 16h in the absence or presence of 500nM HBVpreS/2-48^{myr}. On day 5 p.i., cells were fixed, permeabilized and stained for HDAg. Representative data of 2 independent experiments.

The data from all infection experiments are summarized in table 3.1.

Tab. 3.1: Summary of infection experiments on primary hepatocytes from different species.
HBV: hepatitis B virus. HDV: hepatitis delta virus. WHDV: woodchuck hepatitis delta virus. + : infection or inhibition of infection; - : no infection or no inhibition of infection, respectively.

	rat	rabbit	hamster	guineapig
HBV	-	-	+	+
inhibition by preS-peptide	-	-	+	-
HDV	-	+	-	-
inhibition by preS-peptide	-	+	-	-
WHDV	+	+	+	+
inhibition by preS-peptide	-	-	-	-

4. Discussion

4.1. Binding partners for HBV preS-peptides in serum

4.1.1 PreS-peptides bind serum factors in an acylation-dependent manner

Biodistribution studies on HBV preS-derived peptides revealed their marked stability in serum and rapid targeting to the liver [63]. The retention in the body was shown to depend on the N-terminal acylation, whereas the liver specificity required the intact peptide sequence, especially the essential domain aa 9-15. This led to the assumption that serum factors binding preS-peptides exist, preventing their excretion and possibly mediating binding to liver cells.

In this work, the association of preS-peptides with serum factors was demonstrated and analyzed by a size exclusion chromatography (SEC) based assay. SEC has been shown to be an appropriate tool to study protein-protein interactions or interaction of small molecules with serum components[136]. It is therefore a valid assay for the question addressed here.

In this work, it was observed that FITC-labeled preS-peptides showed a size shift when preincubated with serum, indicating their binding to a serum factor. The detection of only one shifted FITC-specific peak suggested binding mainly to one serum protein. The observed size shift can be attributed to the peptide and does not result from a FITC-dependent serum factor binding, since a non-acylated FITC-labeled peptide did not show an altered elution behavior (fig. 3.2 C). Furthermore, western blot analysis of elution fractions from a preincubation of peptide with albumin showed that peptide can be detected in albumin-peak fractions (fig. 3.7), arguing for a binding of the authentic preS-peptide.

4.1.2 Identification of albumin and apolipoprotein A1 as binding partners for preS-peptides

Subsequently, crosslinker-peptides (CL-peptides) were used to identify binding partners for preS-peptides in human serum. The alterations introduced into these peptides did not modify their ability to inhibit HBV infection. They could be shown to be active in HBV infection inhibition in a sequence-dependent manner (fig. 3.3).

When an unaltered preS-peptide (IC_{50} of 400 pmol) is added in increasing amounts to an HBV-infection, the secreted S-antigen decreases to below background level [62]; the wt CL-

peptide showed an inhibition ability similar to the unaltered wt peptide. Addition of higher concentrations of the wt CL-peptide did not reduce infection further; this is possibly due to an abreaction of the aryl azide moiety with primary amines in the cell supernatant during incubation. While an unaltered peptide diffuses to the cell surface during incubation, a fraction of the CL-peptide might react off unspecifically after a certain time and would then not be at disposition anymore.

Addition of the mutant CL-peptide led to an apparent increase in HBV-infection. The reason for this is unknown.

These CL-peptides were then used for identification of interaction partners from human serum.

Photoactiveable crosslinker molecules have been shown before to be an efficient tool for the identification of interaction partners.

Introduction of a phenylalanine with a trifluoromethyl-diazirin-moiety (TMD-Phe) into preprolactin was shown to allow its crosslinking to different proteins of the endoplasmatic reticulum [137]. Others have described the usage of this modified phenylalanine for crosslinking of a transmembrane peptide to lipids [138]. Photo-crosslinking is therefore a useful method for identification of different interaction partners.

In this work, the CL-peptides allowed identification of two interaction partners in human serum. For both acylated wt CL-peptide and mutant CL-peptide, HSA and Apolipoprotein A1 were found crosslinked to preS-peptides (fig. 3.4). No binding to serum components was found when the non-acylated wt peptide was used. In the elution fractions for the acylated peptides, HSA could be seen as background stain in the wash fraction (fig. 3.4); whereas the preS-peptide-HSA complex eluted later. Although the western blot and silver stain allowed no absolute quantification of bound and unbound HSA, it can be concluded that the larger part of HSA remained unbound. The input molar ratio HSA : peptide in this assay was ~ 4:1, therefore, a proportion of HSA was expected to be unbound.

The ratio of peptide-HSA-complex to peptide-ApoA1-complex appeared to be ~1:1; ApoA1 is present in serum with ~54µM; therefore, the HSA : ApoA1 : peptide ratio was 12:1:3. This hints towards a higher affinity of preS-peptides for ApoA1 than for HSA.

In contrast to this are the observations from SEC of peptides preincubated with serum. While a large part of the peptide signal shifted to overlap with the HSA-peak, no FITC-signal could be detected in fractions corresponding to uncomplexed ApoA1 or to HDL.

Both interactions were confirmed by the SEC-assay (fig. 3.5, 3.14); albumin-binding was confirmed with albumin or serum from other species (fig. 3.10).

4.1.3 The affinity for HSA increases with the fatty acid chain length

The HSA-binding was shown to increase with the length of the N-terminal fatty acid (fig. 3.6). While neither a C5- nor a C8-acylated peptide bound in the SEC-assay, C12-acylation conferred partial binding. The relative broadness of the bound peptide-peak and its tailing out indicates that dissociation of C12-acylated peptide from HSA during the SEC occured, indicating a rather low affinity. C14-, C18-acylated peptides and a cholesteroylated peptide were all completely bound. A C12-acylated peptide bound with a maximal amount of 0,3 peptides per HSA-molecule (K_d = 63µM), C14-acylated peptides bound with a K_d of 18µM and with maximally 1 peptide /HSA-molecule. Analyzing the binding of C18-acylated preS revealed a maximal amount of 10 peptides per HSA-molecule (fig. 3.9).

Short fatty acids such as octanoic acid (C8) are known to bind HSA with rather low affinity (K_d ~1 µM) at two distinct binding sites on the molecule [139]. For C12- and C14- fatty acids, 7 common binding sites have been described [121]. For myristic acid [120] and stearic acid (C18) [126], dissociation constants of 460nM and 14nM, respectively, have been reported. Peng and colleagues studied the binding of cholesterol to HSA and reported a rather high dissociation constant of 400µM and one binding site per HSA-molecule [140]. No reports on the binding of acylated peptides to albumin are known.

As the K_d-values reported for fatty acids are lower than those found in this work for acylated peptides, it is obvious that the hydrophilic peptide part decreases the peptides´ affinities for HSA. This explains why peptides with short acylations (C5, C8) do not bind HSA, while the short fatty acids themselves are known to bind albumin.

For larger HSA-ligands, different dissociation constants have been reported. Short cationic antimicrobial peptides have been shown to bind HSA with K_d in the range of 4.3 - 22,2µM [130]. The K_d-values reported here lie in the range of 18-63µM and are therefore in accordance with values for large ligands. This suggests that preS-peptides do not bind on one of the smaller fatty acid binding sites, but rather to one of the two larger ligand sites. The overall hydrophobicity of the molecule is the critical feature in this step, arguing for Sudlow site I as the binding site for preS-peptides. In order to assess this in more detail, however, structural analysis or probe displacement studies would be necessary.

An important point is the difference in the binding of C14- and C18-acylated preS-peptides observed here. The C14-acylated peptide binds with a K_d of 17µM and a maximum of 1 molecule per molecule HSA (fig. 3.9). In contrast, the C18-acylated peptide was calculated to have a maximal number of 10 binding sites and a K_d of 280µM. These K_d-values are in discrepancy with the values reported for fatty acids alone, where C18-FA bind with a ~10 times higher affinity than C14-FA. One possible explanation is the existence of a low-affinity, unspecific secondary binding of the C18-aclyated peptide to HSA in addition to specific binding. A possible way to analyze this would be the incubation of HSA with increasing amounts of unlabeled C18-peptide in the presence of a constant amount of FITC-labeled C18-peptide; subsequent SEC would show whether the specific binding of 1 molecule peptide exists after saturation of unspecific binding.

Another possible reason for the large number of C18-peptide binding sites might be an allosteric enhancing effect on binding by the peptide itself. Chuang and coworkers have analysed the effect of fatty acids on drug binding by HSA [124]. Using a photoreactive radiolabeled probe, they showed that addition of long chain fatty acids has competitive and allosteric effects on probe binding, regulating HSA-binding in a very complex manner. It is possible that the C18-acylated peptide has an enhancing effect by binding secondary sites that cannot be reached by the C14-acylated peptide, thus leading to low affinity binding of additional peptides.

4.1.4 PreS-peptide binding to albumin takes place *in vivo*

The peptide-albumin interaction could be shown to take place *in vivo* in beagle dogs (fig. 3.8). 10 minutes after intravenous injection of radiolabeled peptide, 75% of the injected dose was found in the liver; this value was stable over 1h (A. Schieck, unpublished data). 10 min and 1h after injection, the preS-peptide was found bound to albumin when serum was subjected to SEC. The detected radioactivity was in the same order of magnitude at both time points and corresponded to ~ 10% of the injected dose. This argues for a relatively stable albumin-binding that keeps the peptide in the serum and prevents it from degradation.

4.1.5 Does the albumin binding influence liver tropism or binding to hepatocytes?

The role of HSA binding in liver tropism of preS-peptides could not be studied directly, since no animal model being deficient in albumin or expressing low albumin levels was accessible. Therefore, indirect arguments for the role of HSA in liver tropism have to be taken into account.

First, mutant peptides also bind HSA but are not targeted to the liver. Non-acylated peptides do not bind HSA and are rapidly excreted from the body (fig. 3.5; [63]). This argues against a role for HSA-binding in liver tropism.

Another argument is the finding that the addition of 300mg/ml β-cyclodextrin to the peptide-HSA preincubation did abolish the peptide-albumin interaction in SEC, but it has no influence on liver tropism of the peptide (data not shown, personal communication A. Schieck). The cyclodextrin bound the peptide more strongly than HSA did, but did not alter its biodistribution. In this case, another molecule has taken over the stabilizing role without affecting liver tropism.

An influence of the HSA-peptide interaction onto hepatocyte binding could not be detected in this work. This was assessed by adding HSA to an incubation of preS-peptides on primary mouse hepatocytes (fig. 3.15). Neither was an altered amount of peptide found in the supernatant after incubation, nor were peptide amounts in wash fractions or cellular fractions influenced by HSA. It has to be mentioned, however, that the albumin concentration used here (25µM) was ~20 times lower than the physiological concentration (500µM). This concentration was chosen to match the HSA : peptide ratio of the SEC-assay while keeping the amount of input radioactivity as low as possible. Higher albumin concentrations might yield different results.

A striking discrepancy exists between these *in vitro* data and the *in vivo* biodistribution study in beagle dogs mentioned above. While only 1% of the peptide was bound to hepatocytes after 1h incubation *in vitro* (fig. 3.8), 75% of the peptide was in the dog liver already 10min after intravenous injection (A. Schieck, unpublished data). This discrepancy is unlikely to be due to an unknown serum factor, since none other could be identified by the two independent assays in this work (SEC-shift assay and crosslinker- fishing experiment). Nor can saturation be the reason; the concentration chosen for the in vitro assay (165nM) lies within the range where no saturation of peptide binding to hepatocytes was detected (up to 3,2µM) [64]. It is more likely that this difference is due to the in vitro situation; the isolation procedure itself stresses the hepatocytes, leading to partial dedifferentiation [141]As

dedifferentiation of primary hepatocytes leads to loss of peptide binding [64], the use of isolated hepatocytes might lead to decreased peptide binding compared to an *in vivo* assay.

Concerning albumin-mediated binding and/or uptake of different substances by the liver, many controversial reports have been made. Until now, it is still under debate how the dissociation of the fatty acid from albumin and the entry into the target cells occurs. First studies on an albumin receptor have been performed by Weisiger and colleagues [142]. Observing a saturable binding of oleate in perfused rat livers only when albumin concentrations rose with the oleate concentrations, they postulated a saturable receptor for the albumin-oleate complex on hepatocytes. This receptor was thought to be present with ~10^7 binding sites per cell. This was questioned by Stollman and coworkers [143] who injected bilirubin in a perfused rat liver in absence or presence of albumin and monitored uptake and biliary excretion of the bilirubin. Observing an unaltered uptake speed in all conditions, they argued against a specific carrier-protein. Many further studies on the uptake of fatty acids or other HSA-ligands by the liver have been performed in the past decades. Some state that the hepatic uptake of HSA ligands is not altered by the presence of albumin [144]; [145]. Others tried to show that albumin does indeed alter the uptake kinetics [146] or that there exists a receptor for polymerized albumin [147]; [148]. Reed and colleagues [149] described a two-phase binding profile of albumin onto hepatocytes, consisting of a saturable- and a non-saturable component; They deduced 3,9×10^6 high-affinity binding sites per cell and a dissociation constant of 1,9 µM. As conclusion, they proposed that membrane-glycoproteins on the hepatocytes bind albumin and induce a conformational change in the molecule, thereby facilitating the delivery of albumin transported ligands. A cell surface-induced conformational change in the albumin was also postulated to reduce the affinity for its ligand [150]. A rather recent theory claims a role for the unstirred water layer on hepatocytes in fatty acid uptake, saying that the presence of serum albumin would alter this layer and thereby facilitate fatty acid uptake into hepatocytes [151]. Taken together, no direct evidence for an albumin receptor has been given yet, and the role for HSA in uptake of its ligands by the liver is unclear.

In 1979, Hansson and colleagues [152] described a receptor for polymerized albumin on HBsAg-particles. After coating microtiter plates with polymerized albumin, they studied binding of HBsAg-particles isolated from a patient and deduced albumin as receptor for HBV on the hepatocyte surface. This interaction has not been confirmed since.

Several groups reported interaction of albumin with the HBV preS2-sequence. A receptor for polymerized albumin on an HBsAg polypeptide was suggested [153]. Krone and coworkers described binding of monomeric HSA to HBsAg-particles via the preS2-domain [154]; polymerized HSA was thought to mediate binding between virus-like particles and hepatocytes by binding to the preS2-domain and to the liver cell surface [155]. Since then, the preS2-domain has been shown convincingly to play no role in HBV infection [40]; it is therefore unlikely that an interaction of preS2 with albumin plays a role in HBV entry.

4.1.6 Apolipoprotein A1 was identified as binding partner for HBV preS-derived peptides

ApoA1 is the major protein constituent of high density lipoproteins, complexes of triglycerides, phospholipids and cholesterol esters. It is present in the blood at a concentration of ~50µM.

Using the CL-peptides described above, ApoA1 was identified as interaction partner for HBV preS-peptides (fig. 3.4). These bound ApoA1 to an approximately equal amount as they bound HSA, although albumin is present in a 12 fold higher concentration in serum.

HDL could efficiently be purified from human serum by SEC (fig. 3.11, 3.13) and density adjusted ultracentrifugation (fig. 3.12), yielding a preparation with ~1,9mg/ml (80µM) containing almost no contaminating proteins. Optimisation of the purification protocol might be possible, especially at the ultracentrifugation step. Analysis of the coomassie-stain of fractions (fig. 3.12) showed that a signal of the correct size (24kDa), although weaker than in the top fraction, was also detected in lower fractions. The flotation of HDLs was therefore not entirely efficient. This might either be due to suboptimal run conditions and thus be corrected by altering these (different run time, better adjustment of the density), or the HDLs in lower fractions correspond to HDLs having slightly higher densities than the ones floated. HDL-populations in serum are inhomogeneous and vary with the amount of cholesterol and fatty acids bound; therefore, the collected top fraction might be devoid of certain HDL-subpopulations.

In the SEC-shift assay, preincubation of C14-acylated peptides and HDL led to a relative weak binding (fig. 3.14). The C18-acylation conferred stronger binding, whereas a cholesteroylated peptide shifted completely in size. Preincubation of HSA, HDL and FITC-labeled preS/2-

$48^{myristoyl}$ led to binding of the peptide to HSA, no binding to HDL could be detected (data not shown). As the fishing assay was performed with a myristoylated CL-peptide, there is a discrepancy between these two results. The reason for this can be found in the technical differences between the two assays. As the crosslinker-assay leads to formation of covalent bonds between the interaction partners, the formed complexes are very stable. SEC on the other hand was performed under native conditions; the runs were performed in the same buffer as the preincubation. Therefore, the binding depended purely on the hydrophobic interactions between HSA and peptide or HDL and peptide, respectively. As hydrophobic interactions are weaker than covalent bonds, these are more likely to dissociate. This again argues for the HSA-peptide interaction being stronger than the HDL-peptide interaction.

4.1.7 Apolipoproteins, HCV and HBV

Another virus replicating in the liver, the hepatitis C virus [2], depends heavily on its interaction with lipoproteins [2]. HCV is a single strand RNA virus, it belongs to the family of Flaviviridae and forms the only representative of the genus Hepacivirus.

HCV particles have been found to be associated with very low density lipoproteins and low density lipoproteins [118] and depend on the secretion of these for their particle formation [156]. HCV particles from serum of chronically infected patients were found in VLDL-fractions; viral peak fractions were rich in apolipoprotein B100. Also, HCV particles from serum subjected to density gradient centrifugation showed a large variation in their density [118, 157, 157, 158]. Furthermore, one of the receptors HCV requires for entry into hepatocytes is the lipoprotein-receptor scavenger receptor B1 (SRB1) [159]. HCV therefore exploits a physiological metabolism pathway not only for particle formation but also for infection.

Such lipoprotein associations have not been reported for HBV. Purification of HBV from human serum does not lead to copurification of apolipoproteins (S. Seitz, unpublished data); In sucrose density gradients, purified HBV particles run as one sharp peak in a high density fraction [160], lipoproteins are likely to run in lower density fractions.

Mehdi and colleagues reported binding of Apolipoprotein H to recombinant HBsAg [161]. They reported a specific, preS-independent interaction and speculated about a possible role for HBV-entry via the LDL-receptor on hepatocytes. This binding was later described to be enhanced after anti-Apo H antibody-binding to the ApoH [162]. In our hands, ApoH had no

effect on HBV infection, nor did an ApoH overexpressing cell line show enhanced susceptibility (A. Schulze, unpublished data). Since no further reports on ApoH playing a role in HBV infection were published, this molecule is unlikely to play a role.
Taken together, it has not been shown so far that HBV associates to lipoproteins or requires an interaction with lipoproteins for successful infection.

4.1.8 Does the peptide-HDL interaction play a role in liver tropism or peptide binding to hepatocytes?

The finding that HBV preS1 peptides bind ApoA1 raised the question whether HDLs play a role in hepatocyte binding by preS-peptides or in HBV entry itself. HDLs are normally taken up into hepatocytes by interaction of the apolipoprotein A1 with the scavenger receptor B1 (SRB1) [163]. A possible role of ApoA1 in mediating peptide or virus uptake into hepatocytes via this receptor could be imagined.
Biodistribution was not altered in a mouse deficient for ApoA1 (fig. 3.16), nor could an influence of HDLs onto peptide binding to hepatocytes be detected (fig. 3.15); addition of purified HDLs to peptide on primary mouse hepatocytes did not lead to a significant increase or decrease in binding. HBV-infection showed a slight decrease in the presence of HDLs, yet no convincing evidence could be obtained. The HDL-concentration used here was under the physiological concentration, addition of higher amounts of HDLs might give further indications.
Cholesteroylated peptides bound HDLs better than acylated peptides (fig. 3.14). Interestingly, biodistribution of a cholesteroylated peptide in mice differs from that of myristoylated or stearoylated peptide; almost no liver tropism is detectable, the peptide is rapidly excreted from the body [63]. Also, liver tropism of the peptide was not impaired in an ApoA1 deficient mouse (fig. 3.16); rather, a slightly increased signal in the liver of the ApoA1 deficient animal was found. It is therefore possible that peptide binding to HDLs inhibits dissociation of the peptide in the liver and retains it in the blood.
A cholesteroylated peptide showed no difference in its infection inhibition behaviour (A. Schulze, unpublished data). This confirms the role of the N-terminal acylation as being merely an anchoring to the plasma membrane and that hepatocyte binding is independent of the liver targeting.

In summary, it could be shown that HSA and HDL bind HBV preS peptides depending on the N-terminal acylation and independent on the intactness of the site necessary for infection inhibition and hepatocyte binding. These interactions are likely to fulfill only a stabilizing function, preventing renal excretion or even protease degradation in the serum.

4.2 Attempts to identify cellular interaction partners for HBV preS-peptides

Since the crosslinker-peptides could be used to identify interaction partners for HBV preS-peptides in serum, it was assessed whether they would allow a similar procedure on hepatocytes. These peptides have been shown to bind in a saturable , competable way to a cytoskeleton-linked protein on the plasma membrane of primary rat hepatocytes, arguing for a proteinacious receptor molecule [64]. Therefore, these cells were used in a crosslinker-assay in order to identify this protein.

Cells were incubated with wt CL-peptide or variations thereof, lysed and subjected to affinity chromatography (fig. 3.18/3.19).Although differences were observed in the elution profiles, no cellular protein could be identified as specific interaction partner. Western blot analysis of the elution profiles showed a wt-specific band at a low molecular weight (15kDa, fig. 3.20). Mass spectrometry of this band did not yield any results.

A possible explanation for the failure of this assay might be the high reactivity of the aryl azide moiety. This molecule is known to react off unspecifically even in the dark, since it forms highly reactive nitrenes. Insertion of the peptides´ fatty acid into the hepatocyte membrane might have led to crosslinking to membrane lipids. Attempts to extract lipids from the elution fractions by methanol-chloroform-extraction, however, did not look promising. Also, if the peptide shows an initial attachment to heparane sulfate proteoglycans as it has been described for HBV [39], this assay would probably lead to peptide-proteoglycan-complexes that would not be detected in western blot.

4.3 Membrane activity of HBV preS-derived peptides

In this work, preS-peptides have been shown to disturb membranes of phospholipid-liposomes in a concentration-dependent manner (fig. 3.22). This membrane activity depends

on the intact sequence of the peptide (fig. 3.23); a replacement of five amino acids in the essential site by their respective D-enantiomers led to complete abrogation of the membrane activity. Non-acylated peptides were also defective in membrane disruption (fig. 3.24). Deletions in the N-terminus proved to be tolerated up to amino acid 7, further deletion reduced membrane activity. Addition of the 11 amino acids from genotype B led to a marked increase in this function (fig. 3.24).

Increasing fatty acid-chain length had a positive effect on the leakage; while neither a C5- nor a C8-acylation led to measurable membrane disruption, a C14-acylated peptide was active, a C18-acylated peptide even more so (fig. 3.25/3.26). C18-acylated peptides with a consensus sequence from the different HBV-genotypes proved to be more efficient than a genotype D peptide (fig. 3.26). Furthermore, the preS-peptides were found to associate tightly to phospholipids membranes in an acylation-dependent manner (fig. 3.27) and to disrupt these in an acylation- and sequence-dependent manner (fig. 3.28).

In all points, these peptides show coherence in their requirements for membrane activity with the features required in Dane-particles for HBV-infectivity [62,42,28,20]. Two discrepancies could be observed. First, peptides carrying the additional 11 aa of genotype B are slightly less active in infection inhibtion [62] but show a marked increase in membrane activity. Second, peptides where the N-terminal 6 amino acids are deleted show a drop in infection inhibition [62] while their membrane activity is not altered. This suggests that the HBV pres1 N-terminus plays a role in viral membrane fusion that independent from the peptide´s inhibitory activity. For such a step, viral proteins often exhibit fusion peptides that adapt a secondary structure only when exposed to a certain trigger (introduction chapter 1.4.2). So far, no secondary structure of the HBV preS1 N-terminus has been reported. Chi and colleagues found pre-structured motifs in the HBV preS1 sequence; they analyzed recombinantly expressed preS -11-108 by nuclear magnetic resonance [164] [164] and found "pre-structured domains" comprising amino acids 1-9, 11-14, 16-33 and 26-29 [165]. Also, secondary structure for the aa 2-20 was determined by NMR, but only when peptides were held in a detergent milieu (personal communication S. Urban). A schematic representation of this structure is given in fig. 4.1 A. This structure consists of an alpha-helix spanning aa2-8, followed by a loop that spans aa 8-18 and contains several hydrophobic residues, and another alpha-helix. A lateral insertion of this helix into a phospholipid membrane as in fig. 4.1. B would be possible; the

more hydrophilic alpha-helices would interact with the more hydrophobic heads of the phospholipids, the loop would insert itself into the membrane.

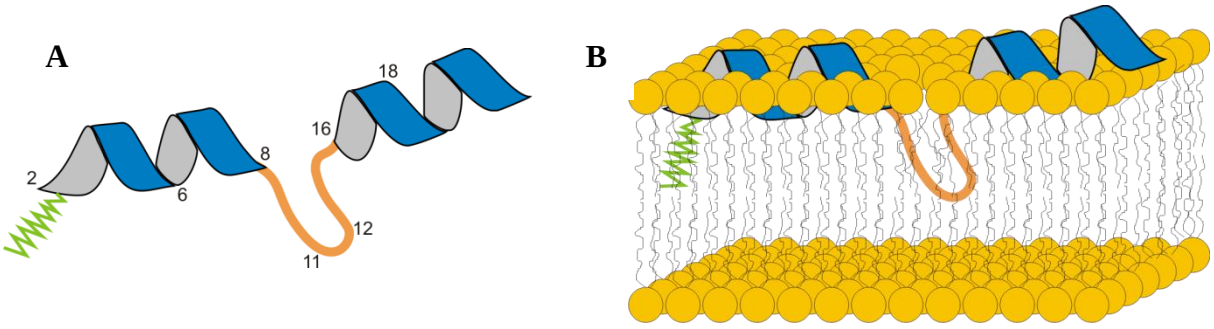

Fig. 4.1: Predicted model of the secondary structure of the HBV preS-peptide 2-22 in detergent milieu.
A: Schematic drawing of the predicted peptide secondary structure.
B: Model of the peptide insertion into a phospholipid membrane. The green line represents the N-terminal acylation; alpha-helices are depicted in blue, the loop structure in orange. Phospholipid heads are depicted in yellow, their lipid tail in black. Numbers of amino acids are indicated. Model of data from S. Urban/ B. Simon.

The above model can be used to explain the differences observed in membrane activity. The Acylation of a minimal length is required for attachment to the target membrane. The domains spanning aa2-8 and 16-22 form helices that lie laterally in the target membrane; the additional 11 aa of genotype B, although their structure in a membrane environment is unknown, might stabilize this lateral insertion. Deletions ahead of the loop formed by aa8-16 do not affect the membrane destabilization. Alterations in the loop are deleterious; replacement of these hydrophobic residues would strongly affect the ability to insert itself into a hydrophobic environment.

Taken together, the findings of this work suggest that the HBV preS1 is an intrinsically unstructured domain that adopts its conformation at the host membrane. After interaction of preS with a specific receptor protein, the N-terminal myristoylation would confer association to the target membrane, followed by formation of a secondary structure in the preS1-N-terminus; this might be induced by contact to phospholipids. This part would then insert itself into the host membrane and destabilize it. The N-terminal acylation would primarily serve as membrane targeting signal [135], the correct sequence being essential. An exposure of the myristoyl-moiety only after a primary attachment to the host cell, a so-called "myristoyl-switch", is possible. The HBV preS1-domain might therefore be a viral fusion peptide that plays a role during viral entry.

4.4 Primary hepatocytes from other species are susceptible to HBV and HDV

The results of infection experiments on primary hepatocytes from different species and of published data concerning HBV or HDV infection of other species are summarized in table 4.1. Rat hepatocytes were suceptible neither to HBV (fig. 3.30/3.31) nor to HDV (fig. 3.36). Rabbit hepatocytes could not be infected with HBV (fig. 3.30/3.32) but were susceptible to HDV infection (fig. 3.37). Both hamster and guinea pig hepatocytes were susceptible to HBV infection (fig. 3.33/3.34); in hamster cells, but not in guinea pig cells, infection could be inhibited with the preS-peptide. Neither hamster hepatocytes nor guinea pig hepatocytes were susceptible to HDV (3.37).
All primary hepatocytes were susceptible to WHDV; in none of these cells could WHDV infection be inhibited by addition of the preS-peptide.

It is not exactly known what step in viral entry is responsible for the restricted host range in HBV; several findings suggest that restriction happens early. For one, transfection of mouse hepatocytes, which are known to be not susceptible to HBV infection, with the HBV-genome leads to production of infectious virus [166]. Transgenic mice containing the HBV genome were also shown to sustain replication of the virus [167]. Also, lipofection of HBV DNA containing capsids into non-susceptible hepatoma cells led to viral replication and virion formation [49]. Therefore, the restriction in infection that leads to the narrow host range is likely to take place at an earlier step such as receptor binding, uptake or viral fusion.
Only few other species have been shown to be susceptible to HBV and /or HDV. The tree shrew *Tupaia belangeri* was shown to be susceptible to HBV-infection [168]; infection could later be shown to be inhibited by HBV preS-peptides [60]. Tupaia hepatocytes have also been reported to be susceptible to HDV [169]; no infection inhibition has been reported. Woodchucks, who are susceptible to infection with woodchuck hepatitis virus (WHV) [170], are not susceptible to HBV infection but to HDV infection [128]. A WHDV-infection has been shown on primary human hepatocytes [171]. The phylogenetic relation of these species (fig. 4.1) shows that they are distributed over the superorder of euarchontoglires. Tupaias, the only small animal model susceptible to HBV known so far, belongs to the same grandorder (Euarchonta) as man; all species tested in this work belong to the other grandorder within the Euarchontoglires, the Glires.

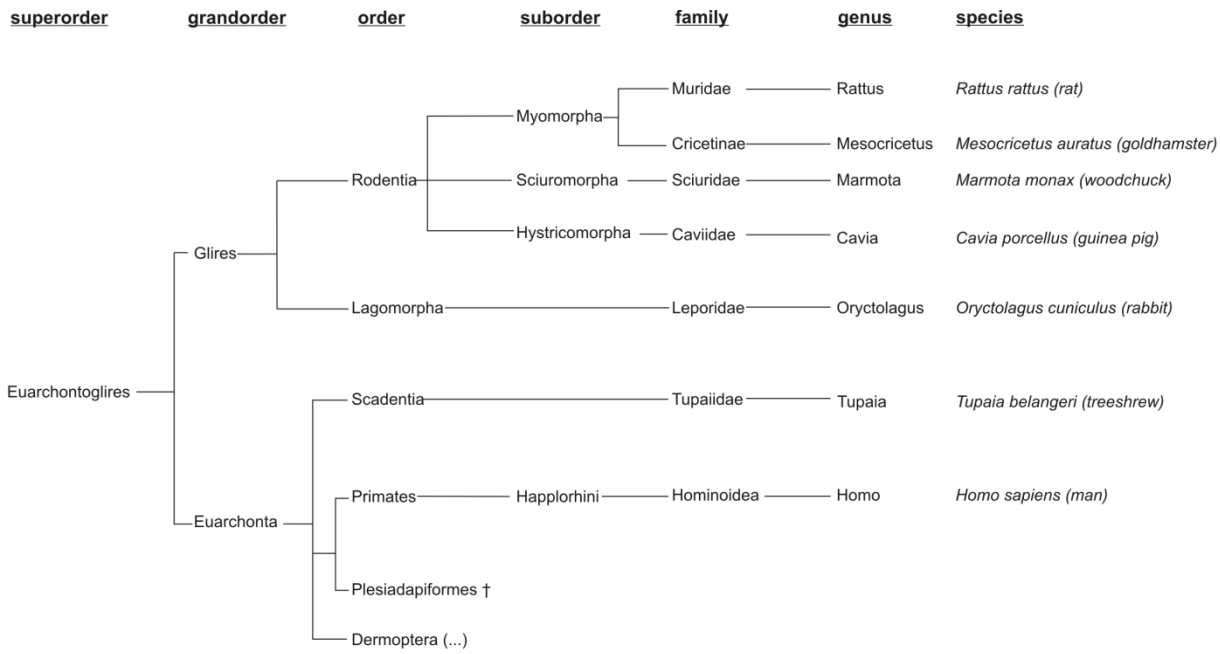

Fig. 4.2: Phylogenetic relation of the superorder Euarchontoglires. Relations are shown as dendrogram; lengths of connective lines do not represent distances of relation. †: extinct order. (...): suborders and further branches not shown. (Data from: Animal Diversity Web)

A summary of data from this work and from literature on the different infections is given in table 4.1.

	HBV infection	HBV infection preS-peptide inhibition	HDV infection	HDV infection preS-peptide inhibition	WHDV infection	WHDV infection preS-peptide inhibition
Rattus rattus (rat)	-		-		+	-
Mesocricetus auratus (goldhamster)	+	+	-		+	-
Marmota monax (woodchuck)	-		+	+	+	-
Cavia porcellus (guinea pig)	+	+	-		+	-
Oryctolagus cuniculus (rabbit)	-	-	+	+	+	-
Tupaia belangeri (treeshrew)	+	+	+	n.d.	n.d.	
Homo sapiens (man)	+	+	+	+	+	-

Tab. 4.1: Summary of species susceptibility to hepatitis B virus (HBV), hepatitis delta virus [2] [2] and woodchuck hepatitis delta virus (WHDV). Species are indicated; **+**: infection or infection inhibition by preS-peptides detected. **-**.: no infection or infection inhibition by preS-peptides detected. **nd**: no data. blank field: if no infection is reported, no statement on inhibition is given.

Since the species analyzed in this work are more closely related to woodchucks than to primates, successful infection of hepatocytes from these animals with WHDV suggests a conserved receptor molecule for the WHV- L-protein within this grandorder (Glires). No detection of HDV antigen in hamsters, rats and guinea pigs is not due to a block of replication itself, since HDAg could be detected in the case of WHDV infection. The successful infection of rabbit hepatocytes, but not of hamster, rat or guinea pig hepatocytes with HDV suggests that the receptor for the HBV L-Protein is present in the Lagomorpha-order but absent in the Rodentia-suborders of Myomorpha and Hystricomorpha. This theory is contradicted by infection of guinea pig- and hamster-hepatocytes by HBV observed in this work. As infection of primary guinea pig hepatocytes could not be inhibited by the preS1-peptide, it could be argued that this is unspecific uptake, possibly caused by the high viral titre and the presence of Polyethylenglycol (PEG) which has been discussed as enhancer of unspecific uptake. Infection of primary hamster hepatocytes, however, was sensible to inhibition by the preS1-peptide, indicating specific receptor-mediated infection.

It is possible that these species express a slightly altered receptor for the HBV L-protein that allows infection under the described conditions. The absence of viral spread during the course if the infection, which is usually observed when primary human hepatocytes are infected, suggests that the observed infection is rather inefficient and spread therefore not possible.

Taken together, these data indicate that HBV entry and replication is possible in primary hepatocytes from species belonging to rather distant animal orders. If hamsters can be infected with HBV, these animals might be a useful small animal for the further study of HBV infection.

5. References

1. **Sweet,R.M. & Eisenberg,D.** Correlation of sequence hydrophobicities measures similarity in three-dimensional protein structure. *J Mol. Biol.* **171**, 479-488 (1983).

2. **Makuwa,M. *et al.*** Hepatitis viruses in non-human primates. *Journal of Medical Primatology* **35**, (2006).

3. Previsiani,N. & Lavanchy,D. Hepatitis B. 2002. WHO-Report

4. MacCallum FO. Collection of specimens for virus investigations. Monthly Bulletin of the Ministry of Health and the Public Health Laboratory Service 6, **229-232**. (1947).

5. **Blumberg,B.S. & Alter,H.J.** A "New" Antigen in Leukemia Sera. *JAMA: The Journal of the American Medical Association* **191**, (1965).

6. **Prince,A.M., Fuji,H.I.R.O., & Gershon,R.K.** IMMUNOHISTOCHEMICAL STUDIES ON THE ETIOLOGY OF ANICTERIC HEPATITIS IN KOREA. *American Journal of Epidemiology* **79**, 365-381 (1964).

7. **Prince A M**. An antigen detected in the blood during the incubation period of serum hepatitis. *Proceedings of the National Academy of Sciences of the United States of America* 60[3], 814-821. 1968.

8. Hepatitis web study. University of washington . 2011.

9. **Maddrey,W.C.** Hepatitis B: An important public health issue. *Journal of Medical Virology* **61**, (2000).

10. **Berquist,K.R. *et al.*** Hepatitis B antigens in serum and liver of chimpanzees acutely infected with hepatitis B virus. *Infect. Immun.* **12**, (1975).

11. **Ganem,D. & Prince,A.M.** Hepatitis B virus infection--natural history and clinical consequences. *N Engl J Med* **350**, (2004).

12. **Mahoney,F.J.** Update on diagnosis, management, and prevention of hepatitis B virus infection. *Clin Microbiol Rev* **12**, (1999).

13. **Lavanchy,D.** Hepatitis B virus epidemiology, disease burden, treatment, and current and emerging prevention and control measures. *J Viral Hepat* **11**, (2004).

14. **Kim,K.-H., Kim,N.D., & Seong,B.-L.** Discovery and Development of Anti-HBV Agents and Their Resistance. *Molecules* 15, 5878-5908. (2010).

15. **Lok,A.S.-F. *et al.*** Evolution of hepatitis B virus polymerase gene mutations in hepatitis B e Antigen–negative patients receiving lamivudine therapy. *Hepatology* **32**, (2000).

16. **Schaefer,S.** Hepatitis B virus taxonomy and hepatitis B virus genotypes. *World J Gastroenterol* **13**[1], 14-21. (2007).

17. **Dane,D.S., Cameron,C.H., & Briggs,M.** Virus-like particles in serum of patients with Australia-antigen-associated hepatitis. *Lancet* **1**, (1970).

18. **Gavilanes,F., Gonzalez-Ros,J.M., & Peterson,D.L.** Structure of hepatitis B surface antigen. Characterization of the lipid components and their association with the viral proteins. *Journal of Biological Chemistry* **257**, (1982).

19. **Bruss,V. & Ganem,D.** The role of envelope proteins in hepatitis B virus assembly. *Proceedings of the National Academy of Sciences of the United States of America* **88**, (1991).

20. **Le Seyec,J., Chouteau,P., Cannie,I., Guguen-Guillouzo,C., & Gripon,P.** Infection Process of the Hepatitis B Virus Depends on the Presence of a Defined Sequence in the Pre-S1 Domain. *J. Virol.* **73**, (1999).

21. **Petitpas,I., Grüne,T., Bhattacharya,A.A., & Curry,S.** Crystal structures of human serum albumin complexed with monounsaturated and polyunsaturated fatty acids. *Journal of Molecular Biology* **314**, (2001).

22. **Nassal,M. & Schaller,H.** Hepatitis B virus replication--an update. *J Viral Hepat.* **3**, 217-226 (1996).

23. **Heermann,K.H. *et al.*** Large surface proteins of hepatitis B virus containing the pre-s sequence. *J. Virol.* **52**, (1984).

24. **Peterson,D.L., Nath,N., & Gavilanes,F.** Structure of hepatitis B surface antigen. Correlation of subtype with amino acid sequence and location of the carbohydrate moiety. *Journal of Biological Chemistry* **257**, (1982).

25. **Ganem,D.** Hepadnaviridae and Their Replication (eds. Fields,B., Knipe,D. & Howley,P.) (Lippincott-Raven, Philadelphia, 1996).

26. **Persing,D.H., Varmus,H.E., & Ganem,D.** The preS1 protein of hepatitis B virus is acylated at its amino terminus with myristic acid. *J. Virol.* **61**, (1987).

27. **Duronio,R.J., Rudnick,D.A., Adams,S.P., Towler,D.A., & Gordon,J.I.** Analyzing the substrate specificity of Saccharomyces cerevisiae myristoyl-CoA:protein N-myristoyltransferase by co-expressing it with mammalian G protein alpha subunits in Escherichia coli. *Journal of Biological Chemistry* **266**, (1991).

28. **Bruss,V., Hagelstein,J., Gerhardt,E., & Galle,P.R.** Myristylation of the Large Surface Protein Is Required for Hepatitis B Virusin VitroInfectivity. *Virology* **218**, (1996).

29. **Bruss,V.** Envelopment of the hepatitis B virus nucleocapsid. *Virus Research* **106**, (2004).

30. **Eble,B.E., MacRae,D.R., Lingappa,V.R., & Ganem,D.** Multiple topogenic sequences determine the transmembrane orientation of the hepatitis B surface antigen. *Mol. Cell. Biol.* **7**, (1987).

31. **Eble,B.E., Lingappa,V.R., & Ganem,D.** The N-terminal (pre-S2) domain of a hepatitis B virus surface glycoprotein is translocated across membranes by downstream signal sequences. *J. Virol.* **64**, (1990).

32. **Bruss,V.** A short linear sequence in the pre-S domain of the large hepatitis B virus envelope protein required for virion formation. *J Virol* **71**, (1997).

33. **Bruss,V., Lu,X., Thomssen,R., & Gerlich,W.H.** Post-translational alterations in transmembrane topology of the hepatitis B virus large envelope protein. *Embo J* **13**, (1994).

34. **Ostapchuk,P., Hearing,P., & Ganem,D.** A dramatic shift in the transmembrane topology of a viral envelope glycoprotein accompanies hepatitis B viral morphogenesis. *Embo J* **13**, (1994).

35. **Will,H. *et al.*** Cloned HBV DNA causes hepatitis in chimpanzees. *Nature* **299**, (1982).

36. **Walter,E., Keist,R., Niederöst,B., Pult,I., & Blum,H.E.** Hepatitis B virus infection of tupaia hepatocytes in vitro and in vivo. *Hepatology* **24**, (1996).

37. **Glebe,D. *et al.*** Pre-S1 Antigen-Dependent Infection of Tupaia Hepatocyte Cultures with Human Hepatitis B Virus. *J. Virol.* **77**, (2003).

38. **Gripon,P. *et al.*** Infection of a human hepatoma cell line by hepatitis B virus. *Proceedings of the National Academy of Sciences of the United States of America* **99**, (2002).

39. **Schulze,A., Gripon,P., & Urban,S.** Hepatitis B virus infection initiates with a large surface protein–dependent binding to heparan sulfate proteoglycans. *Hepatology* **46**, (2007).

40. **Ni,Y., Sonnabend,J., Seitz,S., & Urban,S.** The Pre-S2 Domain of the Hepatitis B Virus Is Dispensable for Infectivity but Serves a Spacer Function for L-Protein-Connected Virus Assembly. *J. Virol.* **84**, (2010).

41. **Le Seyec,J., Chouteau,P., Cannie,I., Guguen-Guillouzo,C., & Gripon,P.** Role of the Pre-S2 Domain of the Large Envelope Protein in Hepatitis B Virus Assembly and Infectivity. *J. Virol.* **72**, (1998).

42. **Gripon,P., Le Seyec,J., Rumin,S., & Guguen-Guillouzo,C.** Myristylation of the Hepatitis B Virus Large Surface Protein Is Essential for Viral Infectivity. *Virology* **213**, (1995).

43. **Neurath,A.R., Strick,N., & Sproul,P.** Search for hepatitis B virus cell receptors reveals binding sites for interleukin 6 on the virus envelope protein. *The Journal of Experimental Medicine* **175**, (1992).

44. **De Falco,S. *et al.*** Cloning and Expression of a Novel Hepatitis B Virus-binding Protein from HepG2 Cells. *Journal of Biological Chemistry* **276**, (2001).

45. **Zhang,X. *et al.*** Asialoglycoprotein receptor interacts with the preS1 domain of hepatitis B virus *Archives of Virology*.(2011).

46. **Breiner,K.M., Urban,S., & Schaller,H.** Carboxypeptidase D (gp180), a Golgi-Resident Protein, Functions in the Attachment and Entry of Avian Hepatitis B Viruses. *J. Virol.* **72**, (1998).

47. **Urban,S. *et al.*** Receptor recognition by a hepatitis B virus reveals a novel mode of high affinity virus-receptor interaction. *Embo J* **19**, (2000).

48. **Kann,M., Sodeik,B., Vlachou,A., Gerlich,W.H., & Helenius,A.** Phosphorylation-dependent Binding of Hepatitis B Virus Core Particles to the Nuclear Pore Complex. *The Journal of Cell Biology* **145**, (1999).

49. **Rabe,B., Glebe,D., & Kann,M.** Lipid-Mediated Introduction of Hepatitis B Virus Capsids into Nonsusceptible Cells Allows Highly Efficient Replication and Facilitates the Study of Early Infection Events. *J. Virol.* **80**, (2006).

50. **Kock,J. & Schlicht,H.J.** Analysis of the earliest steps of hepadnavirus replication: genome repair after infectious entry into hepatocytes does not depend on viral polymerase activity. *J. Virol.* **67**, (1993).

51. **Hirsch,R.C., Lavine,J.E., Chang,L., Varmus,H.E., & Ganem,D.** Polymerase gene products of hepatitis B viruses are required for genomic RNA packaging as well as for reverse transcription. *Nature* **344**, (1990).

52. **Bartenschlager, R.** Hepadnaviral assembly is initiated by polymerase binding to the encapsidation signal in the viral RNA genome. *Embo J* **11**, (1992).

53. **Bartenschlager, R.** The amino-terminal domain of the hepadnaviral P-gene encodes the terminal protein (genome-linked protein) believed to prime reverse transcription. *Embo J* **7**, (1988).

54. **Radziwill,G., Tucker,W., & Schaller,H.** Mutational analysis of the hepatitis B virus P gene product: domain structure and RNase H activity. *J. Virol.* **64**, (1990).

55. **Lien,J.M., Aldrich,C.E., & Mason,W.S.** Evidence that a capped oligoribonucleotide is the primer for duck hepatitis B virus plus-strand DNA synthesis. *J. Virol.* **57**, (1986).

56. **Tuttleman,J.S., Pourcel,C., & Summers,J.** Formation of the pool of covalently closed circular viral DNA in hepadnavirus-infected cells. *Cell* **47**, (1986).

57. **Huovila,A.P., Eder,A.M., & Fuller,S.D.** Hepatitis B surface antigen assembles in a post-ER, pre-Golgi compartment. *The Journal of Cell Biology* **118**, (1992).

58. **Wei,Y., Tavis,J.E., & Ganem,D.** Relationship between viral DNA synthesis and virion envelopment in hepatitis B viruses. *J. Virol.* **70**, (1996).

59. **Gripon,P., Cannie,I., & Urban,S.** Efficient Inhibition of Hepatitis B Virus Infection by Acylated Peptides Derived from the Large Viral Surface Protein. *J. Virol.* **79**, (2005).

60. **Glebe,D. *et al.*** Mapping of the hepatitis B virus attachment site by use of infection-inhibiting preS1 lipopeptides and tupaia hepatocytes. *Gastroenterology* **129**, (2005).

61. **Petersen,J. *et al.*** Prevention of hepatitis B virus infection in vivo by entry inhibitors derived from the large envelope protein. *Nat Biotech* **26**, (2008).

62. **Schulze,A., Schieck,A., Ni,Y., Mier,W., & Urban,S.** Fine Mapping of Pre-S Sequence Requirements for Hepatitis B Virus Large Envelope Protein-Mediated Receptor Interaction. *J. Virol.* **84,** (2010).

63. Schieck,A. Festphasensynthese und pharmakokinetische in vivo-Charakterisierung von Lipopeptiden: Untersuchung des Lebertropismus von Hepatitis B-Viren. 2008.

64. Meier,A. Visualization and Characterization of HBV-Receptor Interactions. 2010.

65. **Martens,S. & McMahon,H.T.** Mechanisms of membrane fusion: disparate players and common principles. *Nature Reviews Molecular Cell Biology* **9**, (2008).

66. **Colman,P.M. & Lawrence,M.C.** The structural biology of type I viral membrane fusion. *Nat. Rev. Mol. Cell Biol.* **4**, 309-319 (2003).

67. **Backovic,M. & Jardetzky,T.S.** Class III viral membrane fusion proteins. *Curr. Opin. Struct. Biol.* **19**, 189-196 (2009).

68. **Steinhauer,D.A.** Role of hemagglutinin cleavage for the pathogenicity of influenza virus. *Virology* **258**, 1-20 (1999).

69. **Bottcher,E. *et al.*** Proteolytic activation of influenza viruses by serine proteases TMPRSS2 and HAT from human airway epithelium. *J Virol.* **80**, 9896-9898 (2006).

70. **Harrison,S.C.** Viral membrane fusion. *Nat. Struct. Mol. Biol.* **15**, 690-698 (2008).

71. **Lakadamyali,M., Rust,M.J., & Zhuang,X.** Endocytosis of influenza viruses. *Microbes. Infect.* **6**, 929-936 (2004).

72. **Skehel,J.J. & Wiley,D.C.** Receptor binding and membrane fusion in virus entry: the influenza hemagglutinin. *Annu. Rev. Biochem.* **69**, 531-569 (2000).

73. **Han,X., Bushweller,J.H., Cafiso,D.S., & Tamm,L.K.** Membrane structure and fusion-triggering conformational change of the fusion domain from influenza hemagglutinin. *Nat Struct Mol Biol* **8**, (2001).

74. **Luneberg,J., Martin,I., Nüssler,F., Ruysschaert,J.-M., & Herrmann,A.** Structure and Topology of the Influenza Virus Fusion Peptide in Lipid Bilayers. *Journal of Biological Chemistry* **270**, (1995).

75. **Cross,K.J., Burleigh,L.M., & Steinhauer,D.A.** Mechanisms of cell entry by influenza virus. *Expert. Rev. Mol. Med.* **3**, 1-18 (2001).

76. **Brasseur,R. *et al.*** The mode of insertion of the paramyxovirus F1 N-terminus into lipid matrix, an initial step in host cell/virus fusion. *Virus Genes* **1**, (1988).

77. **Moreno,M.R. *et al.*** Characterization of the Interaction of Two Peptides from the N Terminus of the NHR Domain of HIV-1 gp41 with Phospholipid Membranesâ€ . *Biochemistry* **46**, (2007).

78. **Galdiero,S. *et al.*** Role of membranotropic sequences from herpes simplex virus type I glycoproteins B and H in the fusion process. *Biochimica et Biophysica Acta (BBA) - Biomembranes* **1798**.

79. **Liao,M. & Kielian,M.** Domain III from class II fusion proteins functions as a dominant-negative inhibitor of virus membrane fusion. *The Journal of Cell Biology* **171**, (2005).

80. **Weise,K. & Reed,J.** Fusion Peptides and Transmembrane Domains of Fusion Proteins are Characterized by Different but Specific Structural Properties. *ChemBioChem* **9**, (2008).

81. **Hofmann,M.W. *et al.*** De novo design of conformationally flexible transmembrane peptides driving membrane fusion. *Proceedings of the National Academy of Sciences of the United States of America* **101**, (2004).

82. **Lu,X., Block,T.M., & Gerlich,W.H.** Protease-induced infectivity of hepatitis B virus for a human hepatoblastoma cell line. *J Virol* **70**, (1996).

83. **Chojnacki,J., Anderson,D.A., & Grgacic,E.V.** A hydrophobic domain in the large envelope protein is essential for fusion of duck hepatitis B virus at the late endosome. *J Virol* **79**, (2005).

84. **Grgacic,E.V. & Schaller,H.** A metastable form of the large envelope protein of duck hepatitis B virus: low-pH release results in a transition to a hydrophobic, potentially fusogenic conformation. *J Virol* **74**, (2000).

85. **Núñez,E. *et al.*** Interaction of preS domains of hepatitis B virus with phospholipid vesicles. *Biochimica et Biophysica Acta (BBA) - Biomembranes* **1788**, (2009).

86. **Rizzetto,M. *et al.*** Immunofluorescence detection of new antigen-antibody system (delta/anti-delta) associated to hepatitis B virus in liver and in serum of HBsAg carriers. *Gut* **18**, (1977).

87. **Rizzetto,M. *et al.*** delta Agent: association of delta antigen with hepatitis B surface antigen and RNA in serum of delta-infected chimpanzees. *Proceedings of the National Academy of Sciences of the United States of America* **77**, (1980).

88. **Le Gal F, Gault E,Ripault M-P,Serpaggi J,Trinchet J-C,Gordien E,et al** Eighth major clade for hepatitis delta virus. *Emerg Infect Dis* **12**, (2006).

89. **Dienes,H.P., Purcell,R.H., Popper,H., & Ponzetto,A.** The significance of infections with two types of viral hepatitis demonstrated by histologic features in chimpanzees. *Journal of hepatology* **10**, (1990).

90. **Farci,P. *et al.*** Acute and chronic hepatitis delta virus infection: Direct or indirect effect on hepatitis B virus replication? *Journal of Medical Virology* **26**, (1988).

91. **Weiner,A.J. *et al.*** A single antigenomic open reading frame of the hepatitis delta virus encodes the epitope(s) of both hepatitis delta antigen polypeptides p24 delta and p27 delta. *J. Virol.* **62**, (1988).

92. **Alves,C., Freitas,N., & Cunha,C.** Characterization of the nuclear localization signal of the hepatitis delta virus antigen. *Virology* **370**, (2008).

93. **Lee,C.-H., Chang,S.C., Chen,C.-J., & Chang,M.-F.** The Nucleolin Binding Activity of Hepatitis Delta Antigen Is Associated with Nucleolus Targeting. *Journal of Biological Chemistry* **273**, (1998).

94. **Chao,M., Hsieh,S.Y., & Taylor,J.** The antigen of hepatitis delta virus: examination of in vitro RNA-binding specificity. *J. Virol.* **65**, (1991).

95. **Lee,C.-H., Chang,S.C., Wu,C.H.H., & Chang,M.-F.** A Novel Chromosome Region Maintenance 1-independent Nuclear Export Signal of the Large Form of Hepatitis Delta Antigen That Is Required for the Viral Assembly. *Journal of Biological Chemistry* **276**, (2001).

96. **Glenn,J.S., Watson,J.A., Havel,C.M., & White,J.M.** Identification of a prenylation site in delta virus large antigen. *Science* **256**, (1992).

97. **Sureau,C., Guerra,B., & Lanford,R.E.** Role of the large hepatitis B virus envelope protein in infectivity of the hepatitis delta virion. *J. Virol.* **67**, (1993).

98. **Blanchet,M. & Sureau,C.** Infectivity Determinants of the Hepatitis B Virus Pre-S Domain Are Confined to the N-Terminal 75 Amino Acid Residues. *J. Virol.* **81**, (2007).

99. **Abou-Jaoude,G. & Sureau,C.** Entry of Hepatitis Delta Virus Requires the Conserved Cysteine Residues of the Hepatitis B Virus Envelope Protein Antigenic Loop and Is Blocked by Inhibitors of Thiol-Disulfide Exchange. *J. Virol.* **81**, (2007).

100. **Engelke,M. *et al.*** Characterization of a hepatitis B and hepatitis delta virus receptor binding site. *Hepatology* **43**, (2006).

101. **Sureau,C., Fournier-Wirth,C., & Maurel,P.** Role of N Glycosylation of Hepatitis B Virus Envelope Proteins in Morphogenesis and Infectivity of Hepatitis Delta Virus. *J. Virol.* **77**, (2003).

102. **Jaoude,G.A. & Sureau,C.** Role of the Antigenic Loop of the Hepatitis B Virus Envelope Proteins in Infectivity of Hepatitis Delta Virus. *J. Virol.* **79**, (2005).

103. **Le Duff,Y., Blanchet,M., & Sureau,C.** The Pre-S1 and Antigenic Loop Infectivity Determinants of the Hepatitis B Virus Envelope Proteins Are Functionally Independent. *J. Virol.* **83**, (2009).

104. **Chen,P.J. *et al.*** Structure and replication of the genome of the hepatitis delta virus. *Proceedings of the National Academy of Sciences of the United States of America* **83**, (1986).

105. **Denniston,K.J. *et al.*** Cloned fragment of the hepatitis delta virus RNA genome: sequence and diagnostic application. *Science* **232**, (1986).

106. **Wang,K.-S. *et al.*** Structure, sequence and expression of the hepatitis delta ([delta]) viral genome. *Nature* **323**, (1986).

107. **Kuo,M.Y., Sharmeen,L., Dinter-Gottlieb,G., & Taylor,J.** Characterization of self-cleaving RNA sequences on the genome and antigenome of human hepatitis delta virus. *J. Virol.* **62**, (1988).

108. **Sharmeen,L., Kuo,M.Y., Dinter-Gottlieb,G., & Taylor,J.** Antigenomic RNA of human hepatitis delta virus can undergo self-cleavage. *J. Virol.* **62**, (1988).

109. **Chang,J., Nie,X., Chang,H.E., Han,Z., & Taylor,J.** Transcription of Hepatitis Delta Virus RNA by RNA Polymerase II. *J. Virol.* **82**, (2008).

110. **Branch,A.D. & Robertson,H.D.** A replication cycle for viroids and other small infectious RNA's. *Science* **223**, (1984).

111. **Reid,C.E. & Lazinski,D.W.** A host-specific function is required for ligation of a wide variety of ribozyme-processed RNAs. *Proceedings of the National Academy of Sciences of the United States of America* **97**, (2000).

112. **Wong,S.K. & Lazinski,D.W.** Replicating hepatitis delta virus RNA is edited in the nucleus by the small form of ADAR1. *Proceedings of the National Academy of Sciences of the United States of America* **99**, (2002).

113. **Glenn,J.S. & White,J.M.** trans-dominant inhibition of human hepatitis delta virus genome replication. *J. Virol.* **65**, (1991).

114. **Wang,C.J., Chen,P.J., Wu,J.C., Patel,D., & Chen,D.S.** Small-form hepatitis B surface antigen is sufficient to help in the assembly of hepatitis delta virus-like particles. *J. Virol.* **65**, (1991).

115. **Hwang,S.B. & Lai,M.M.** Isoprenylation mediates direct protein-protein interactions between hepatitis large delta antigen and hepatitis B virus surface antigen. *J. Virol.* **67**, (1993).

116. Modrow,S., Falke,D., & Truyen,U. *Molekulare Virologie* Heidelberg, Berlin, 2003).

117. Nelson,D. & Cox,M. *Lehninger Biochemie* (Springer Verlag, **Berlin Heidelberg** , 2001).

118. **Nielsen,S.U. *et al.*** Association between Hepatitis C Virus and Very-Low-Density Lipoprotein (VLDL)/LDL Analyzed in Iodixanol Density Gradients. *J. Virol.* **80**, (2006).

119. **Kendall,F.E.** STUDIES ON HUMAN SERUM PROTEINS. *Journal of Biological Chemistry* **138**, (1941).

120. **Fredrickson,D.S. & Gordon,R.S.** The Metabolism of Albumin Bound C14-Labeled Unesterified Fatty Acids in Normal Human Subjects. *The Journal of Clinical Investigation* **37**, (1958).

121. **Bhattacharya,A.A., Grüne,T., & Curry,S.** Crystallographic analysis reveals common modes of binding of medium and long-chain fatty acids to human serum albumin. *Journal of Molecular Biology* **303**, (2000).

122. **Sudlow,G., Birkett,D.J., & Wade,D.N.** The Characterization of Two Specific Drug Binding Sites on Human Serum Albumin. *Molecular Pharmacology* **11**, (1975).

123. **Zhu,L., Yang,F., Chen,L., Meehan,E.J., & Huang,M.** A new drug binding subsite on human serum albumin and drug-drug interaction studied by X-ray crystallography. *Journal of Structural Biology* **162**, (2008).

124. **Chuang,V.T.G. & Otagiri,M.** How Do Fatty Acids Cause Allosteric Binding of Drugs to Human Serum Albumin? *Pharmaceutical Research* **19**, (2002).

125. **Quinlan,G.J., Martin,G.S., & Evans,T.W.** Albumin: biochemical properties and therapeutic potential. *Hepatology* **41**, 1211-1219 (2005).

126. **Demant,E.J.F., Richieri,G.V., & Kleinfeld,A.M.** Stopped-flow kinetic analysis of long-chain fatty acid dissociation from bovine serum albumin. *Biochem. J.* **363**, (2002).

127. **Ghuman,J. *et al.*** Structural basis of the drug-binding specificity of human serum albumin. *J Mol. Biol.* **353**, 38-52 (2005).

128. **Netter,H.J., Gerin,J.L., Tennant,B.C., & Taylor,J.M.** Apparent helper-independent infection of woodchucks by hepatitis delta virus and subsequent rescue with woodchuck hepatitis virus. *J. Virol.* **68**, (1994).

129. **Zunszain,P., Ghuman,J., Komatsu,T., Tsuchida,E., & Curry,S.** Crystal structural analysis of human serum albumin complexed with hemin and fatty acid. *BMC Structural Biology* **3**, (2003).

130. **Svenson,J., Brandsdal,B.B.-O., Stensen,W., & Svendsen,J.S.** Albumin Binding of Short Cationic Antimicrobial Micropeptides and Its Influence on the in Vitro Bactericidal Effect. *Journal of Medicinal Chemistry* **50**, (2007).

131. **He,X.M. & Carter,D.C.** Atomic structure and chemistry of human serum albumin. *Nature* **358**, (1992).

132. **Birkett,D.J., Myers,S.P., & Sudlow,G.** Effects of Fatty Acids on Two Specific Drug Binding Sites on Human Serum Albumin. *Molecular Pharmacology* **13**, (1977).

133. **Rifici,V.A. & Eder,H.A.** A hepatocyte receptor for high-density lipoproteins specific for apolipoprotein A-I. *Journal of Biological Chemistry* **259**, (1984).

134. **Taniguchi,H.** Protein myristoylation in protein-lipid and protein-protein interactions. *Biophysical Chemistry* **82**, (1999).

135. **Resh,M.D.** Fatty acylation of proteins: new insights into membrane targeting of myristoylated and palmitoylated proteins. *Biochimica et Biophysica Acta (BBA) - Molecular Cell Research* **1451**, (1999).

136. **Rodríguez-Fariñas,N., Gomez-Gomez,M., & Camara-Rica,C.** Study of tungstate–protein interaction in human serum by LC–ICP-MS and MALDI-TOF. *Analytical and Bioanalytical Chemistry* **390**, (2008).

137. **High,S. *et al.*** Site-specific photocross-linking reveals that Sec61p and TRAM contact different regions of a membrane-inserted signal sequence. *Journal of Biological Chemistry* **268**, (1993).

138. **Ridder,A.N.J.A. *et al.*** Photo-Crosslinking Analysis of Preferential Interactions between a Transmembrane Peptide and Matching Lipidsâ€ . *Biochemistry* **43**, (2004).

139. **Kragh-Hansen,U.** Octanoate binding to the indole- and benzodiazepine-binding region of human serum albumin. *Biochem. J.* **273**, (1991).

140. **Liu,P., He,M., Chen,F., Li,X., & Zhang,C.** The Interaction Between Cholesterol and Human Serum Albumin. *Protein & Peptide Letters* **15**, (2008).

141. **Wang,X.-J., Hodgkinson,C., Wright,M., & Paine,A.** Temperature-sensitive mRNA degradation is an early event in hepatocyte de-differentiation. *Biochemical Journal* **328**, 937-944 (1997).

142. **Weisiger,R., Gollan,J., & Ockner,R.** Receptor for albumin on the liver cell surface may mediate uptake of fatty acids and other albumin-bound substances. *Science* **211**, (1981).

143. **Stollman,Y.R., GÃ¤rtner,U., Theilmann,L., Ohmi,N., & Wolkoff,A.W.** Hepatic bilirubin uptake in the isolated perfused rat liver is not facilitated by albumin binding. *The Journal of Clinical Investigation* **72**, (1983).

144. **Stremmel W,P.B.B.P.** Studies of albumin binding to rat liver plasma membranes. Implications for the albumin receptor hypothesis. *Biochim Biophys Acta.* **756**, (1983).

145. **Nunes,R., Kiang,C.L., Sorrentino,D., & Berk,P.D.** [`]Albumin-receptor' uptake kinetics do not require an intact lobular architecture and are not specific for albumin. *Journal of hepatology* **7**, (1988).

146. **Ockner,R.K., Weisiger,R.A., & Gollan,J.L.** Hepatic uptake of albumin-bound substances: albumin receptor concept. *American Journal of Physiology - Gastrointestinal and Liver Physiology* **245**, (1983).

147. **Wright,T.L., Lysenko,N., Ockner,R.K., & Weisiger,R.A.** Interaction of natural and synthetic albumin polymers with hepatocytes. *Hepatology* **7**, (1987).

148. **Takami,M., Kasuya,I., & Tsunoo,H.** Polymerized Albumin Receptor on Rat Liver Cells. *Journal of Biochemistry* **111**, (1992).

149. **Reed,R.G. & Burrington,C.M.** The albumin receptor effect may be due to a surface-induced conformational change in albumin. *J Biol. Chem.* **264**, 9867-9872 (1989).

150. **Forker,E.L. & Luxon,B.A.** Albumin helps mediate removal of taurocholate by rat liver. *J Clin. Invest* **67**, 1517-1522 (1981).

151. **Weisiger,R.A., Pond,S., & Bass,L.** Hepatic uptake of protein-bound ligands: extended sinusoidal perfusion model. *American Journal of Physiology - Gastrointestinal and Liver Physiology* **261**, (1991).

152. **Hansson,B.G. & Purcell,R.H.** Sites that bind polymerized albumin on hepatitis B surface antigen particles: detection by radioimmunoassay. *Infect. Immun.* **26**, 125-130 (1979).

153. **Machida,A. *et al.*** A polypeptide containing 55 amino acid residues coded by the pre-S region of hepatitis B virus deoxyribonucleic acid bears the receptor for

polymerized human as well as chimpanzee albumins. *Gastroenterology* **86**, (1984).

154. **Krone,B. *et al.*** Interaction between hepatitis B surface proteins and monomeric human serum albumin. *Hepatology* **11**, (1990).

155. **Pontisso,P., Petit,M.A., Bankowski,M.J., & Peeples,M.E.** Human liver plasma membranes contain receptors for the hepatitis B virus pre-S1 region and, via polymerized human serum albumin, for the pre-S2 region. *J. Virol.* **63**, (1989).

156. **Merz,A. *et al.*** Biochemical and Morphological Properties of Hepatitis C Virus Particles and Determination of Their Lipidome. *Journal of Biological Chemistry* **286,** (2011).

157. **Huang,H. *et al.*** Hepatitis C virus production by human hepatocytes dependent on assembly and secretion of very low-density lipoproteins. *Proceedings of the National Academy of Sciences* **104**, (2007).

158. **Chouteau,P. *et al.*** A Short N-Proximal Region in the Large Envelope Protein Harbors a Determinant That Contributes to the Species Specificity of Human Hepatitis B Virus. *J. Virol.* **75**, (2001).

159. **Scarselli,E. *et al.*** The human scavenger receptor class B type I is a novel candidate receptor for the hepatitis C virus. *Embo J* **21**, (2002).

160. Gähler,C. Charakterisierung des bindeverhaltens von Hepatitis B Viren an Heparin in Abhängigkeit von Partikeltyp und Hüllproteinen sowie Funktionsanalyse der identifizierten Bindetypen. 2007.

161. **Mehdi,H. *et al.*** Hepatitis B virus surface antigen binds to apolipoprotein H. *J. Virol.* **68**, (1994).

162. **Mehdi,H., Yang,X.U., & Peeples,M.E.** An Altered Form of Apolipoprotein H Binds Hepatitis B Virus Surface Antigen Most Efficiently. *Virology* **217**, (1996).

163. **Acton,S. *et al.*** Identification of Scavenger Receptor SR-BI as a High Density Lipoprotein Receptor. *Science* **271**, (1996).

164. **Parac-Vogt,T.N. *et al.*** Synthesis, Characterization, and Pharmacokinetic Evaluation of a Potential MRI Contrast Agent Containing Two Paramagnetic Centers with Albumin Binding Affinity. *Chemistry – A European Journal* **11**, (2005).

165. **Chi,S.W., Kim,D.H., Lee,S.H., Chang,I., & Han,K.H.** Pre-structured motifs in the natively unstructured preS1 surface antigen of hepatitis B virus. *Protein Sci.* **16**, 2108-2117 (2007).

166. **Yang,P.L., Althage,A., Chung,J., & Chisari,F.V.** Hydrodynamic injection of viral DNA: A mouse model of acute hepatitis B virus infection. *Proceedings of the National Academy of Sciences of the United States of America* **99**, (2002).

167. **Guidotti,L.G., Matzke,B., Schaller,H., & Chisari,F.V.** High-level hepatitis B virus replication in transgenic mice. *J. Virol.* **69**, (1995).

168. **Yan,R.Q. *et al.*** Human hepatitis B virus and hepatocellular carcinoma I. Experimental infection of tree shrews with hepatitis B virus. *Journal of Cancer Research and Clinical Oncology* **122**, (1996).

169. **Li Q,D.M.W.H.** The infection of hepatitis D virus in adult tupaia. *Chinese Journal of medical genetics* **75**, (1995).

170. **Tyler,G.V., Summers,J.W., & Synder,R.L.** Woodchuck hepatitis virus in natural woodchuck populations. *J Wildl Dis* **17**, (1981).

171. **Gudima,S. *et al.*** Primary Human Hepatocytes Are Susceptible to Infection by Hepatitis Delta Virus Assembled with Envelope Proteins of Woodchuck Hepatitis Virus. *J. Virol.* **82**, (2008).

6. Acknowledgements

An erster Stelle möchte ich mich bei Prof. Dr. Stephan Urban bedanken. Er gab mir die Möglichkeit, diese Doktorarbeit in seinem Labor anzufertigen und unterstützte mich stets mit Vorschlägen, Anregungen und Diskussionen. Sein anhaltendes Bemühen um selbstständiges Arbeiten aller Mitarbeiter und die häufigen Möglichkeiten, Ergebnisse auf Kongressen selbst zu präsentieren, habe ich sehr geschätzt.
Auch möchte ich Prof. Dr. Ralf Bartenschlager für die wissenschaftliche und finanzielle Unterstützung danken.
Großer Dank gilt meiner Familie. Meiner Mutter danke ich für die stete Begleitung, meinem Vater und Kathy Mampe für die liebevolle Unterstützung gerade während der Anfangszeit meines Studiums. Ihr habt einen wesentlichen Anteil daran gehabt, dass ich auch schwierige Zeiten überwunden habe. Meinen Geschwistern Jonas, Marit und Anne danke ich für den großartigen Zusammenhalt während der letzten dreißig Jahre.
Mircea Iancu möchte ich einen besonderen Dank aussprechen. Er gibt mir nicht nur ein Zuhause hier und in Timişoara, sondern auch ein mutiges und fröhliches Zusammenleben an jedem Tag.
Nicht zuletzt danke ich meinen Laborkollegen, von denen mir viele zu Freunden geworden sind, insbesondere Martina für die Kaffepausen und Anja für die Etablierung, sowie Berit, Jessika, Christina, Andreas, Stefan Mehrle und Yi. Stefan Seitz gilt besonderer Dank für wertvolle Ideen und Diskussionen.
Yvette Schollmeier danke ich für die gute Zusammenarbeit, Begleitung bei diversem Sport und eine gute Freundschaft.